THE MUNICIPAL UNIVERSITY OF WICHITA

PERFORMANCE TESTS OF A SIDE-INLET, STEAM-TO-AIR JET PUMP WITH AN INBOARD NOZZLE

by A.M. Heinrich

Engineering Report No. 131

for the Office of Naval Research
Contract N-onr 201(01)

February 1954
University of Wichita
School of Engineering
Wichita, Kansas

PERFORMANCE TEST OF A SIDE-INLET,
STEAM-TO-AIR JET PUMP WITH AN INBOARD NOZZLE

by A.M. Heinrich

Engineering Report No. 131

for the Office of Naval Research
Contract N-onr 201(01)

February 1954
University of Wichita
School of Engineering
Wichita, Kansas

TABLE OF CONTENTS

	Page
LIST OF FIGURES	ii
SUMMARY	1
INTRODUCTION	1
SYMBOLS AND SUBSCRIPTS	2
APPARATUS	3
TESTS	
Measurements	4
Data Recorded	5
PERFORMANCE ANALYSIS	5
RESULTS AND DISCUSSION	7
CONCLUSIONS	8
REFERENCES	8
APPENDICES	
A.- Steam Nozzle Design and Calibration	9
B.- Steam Generator and Superheater	16
C.- Test Log of SISA-1 Jet Pump	19
FIGURES	26

LIST OF FIGURES

Figures	Page
1.- Planform outline; side-inlet, steam-air jet pump.	26
2.- Cross section of SISA-1 jet-pump at nozzle exit.	27
3.- Side-inlet, steam jet pump with an inboard nozzle.	28
4.- Arrangement of mixing-tube pressure taps and throat-adjustment bolts.	29
5.- Exit orifice installation.	29
6.- Arrangement of mixing-tube static pressure taps.	30
7.- Arrangement of suction-slot pressure taps.	30
8.- Suction slot, static-pressure taps and cascaded mixing-tube throat.	31
9.- Multitube manometer with static pressures of suction slot on left and mixing-tube throat on right.	31
10.- Multitube manometer with mixing-tube static pressures on right and inboard suction-slot static pressures on left.	32
11.- Instrumentation schematic.	33
12.- Mixing-tube temperature survey probe.	34
13.- Mixing-tube, total-pressure survey probe.	35
14.- Variation of pressure ratio with mass ratio.	36
15.- Variation of efficiency with mass ratio.	37
16.- Distribution of available energy efficiency.	38
17.- Variation of suction-duct, total-pressure loss with flow quantity.	39
18.- Influence of jet total pressure and pressure ratio on suction-slot quantity distribution.	40
19.- Suction-duct flow pattern with slot and throat throttling.	47
20.- Suction-slot width variation.	48
21.- Mixing-tube entrance throat widths.	50

Figures Page

22.- Influence of jet total pressure and pressure ratio on throat static-pressure distribution. 51

23.- Influence of jet total pressure and slot throttling on mixing-tube, static-pressure distribution. 53

24.- Influence of jet total pressure and pressure ratio on mixing-tube, total-pressure distribution. 55

25.- Influence of jet total pressure and pressure ratio on temperature distribution. 66

PERFORMANCE TEST OF A SIDE-INLET, STEAM-TO-AIR JET PUMP WITH AN INBOARD NOZZLE

SUMMARY

An experimental investigation was conducted to determine the performance of a side-inlet, steam-to-air jet pump with an inboard nozzle. A jet pump with a cylindrical mixing tube was tested for mass ratio, pressure ratio, and efficiency. The transfer of the available energy in the primary flow to the secondary flow and the influence on performance of controlling the direction of secondary air flow into the mixing tube were also investigated.

Performance curves are presented together with curves showing mixing-tube, cross-sectional distributions of temperature and total pressure taken at several survey stations. This report is the first in a series on jet pumps with different taper ratio mixing tubes.

INTRODUCTION

The application of circulation control to an airplane wing has been proved practical and advantageous. A typical form of application consists of combined sucking and blowing air through slots adjacent to trailing-edge flaps and ailerons (the 'Arado' system). Since the basic structural components of an airplane wing are generally located in the forward area of the wing a pumping system for circulation control may conveniently fit within the area between flaps and ailerons, and the rear span.

The pumping unit for such a circulation control system may take the form of a jet-pump, which is light in weight and simple in operation. The suction section, or intake of the pumping unit, requires a compact arrangement of suction slot and jet-pump mixing tube; this led to the concept of the side-inlet-flow jet pump. A short, direct flow path is thereby provided for the secondary air to the mixing tube. It is the suction duct and mixing tube of such a system that is the subject of this report (see fig. 1). The particular arrangement (SISA-1) involved a cylindrical mixing tube.

A primary fluid with known thermodynamic properties was desirable. This fluid had to have a variable energy level and it was desirable that it be produced by an easily controlled generator. The energy level and characteristics of the primary fluid were to be comparable to those of an actual installation. Superheated steam, since it conveniently simulated products of combustion (of hydrogen peroxide), was selected as the primary fluid.

The purpose of this report was to organize the data and present the test results in a manner usable for subsequent comparative evaluation. Also, the experimental procedures have been explained. The design, construction and tests of the jet pump were performed by the University of Wichita, School of Engineering under the authority of Contract N-onr 201(01) from the Air Branch of the Office of Naval Research.

SYMBOLS

D	diameter of mixing tube or orifice, inches
L	length of mixing tube, inches
m	mass, slugs
ρ	mass density, slugs/ft^3
Q	heat quantity, BTU
h	enthalpy, BTU/lb
T	absolute temperature, °R
t	temperature °F
p_t	total pressure, lbs/ft^2
p	static pressure, lbs/ft^2
P	power, ft-lb/sec
W	work, ft-lb
J	mechanical equivalent of heat, 778 ft-lb/BTU
V	velocity, ft/sec
v	local velocity, ft/sec
g	gravitational acceleration, ft/sec^2
q	volumetric flow rate, ft^3/sec
w	weight flow rate, lbs/sec
α	pressure ratio = p_{t_3}/p_{t_0}
μ	mass ratio = w_s/w_j
η	efficiency = P_{eff}/P_{in}

SUBSCRIPTS

0	free-stream or ambient conditions
1	suction-slot condition
2	mixing-tube-entrance throat condition
3	mixing-tube exit condition
AE	available energy
e	nozzle exit
f	friction
j	primary or jet flow
s	secondary flow
m	mixture of primary and secondary flow
x	axial position from the inboard end of mixing tube
in	input
eff	effective

APPARATUS

Figures 1 through 8 show the constructional details and arrangement of the side-inlet, stream-to-air jet pump. The principle parts of the model were fabricated from sheet metal and supported by a plywood framework. This assembly was mounted on and held in position with respect to the jet nozzle by an adjustable metal stand attached to the floor.

Schematics of the side-inlet steam jet pumps are shown as figures 1 and 2. The secondary air enters the suction slot, traverses the suction duct and enters the mixing tube through the throat cascade. Within the mixing tube the secondary air mixes with the higher velocity primary jet. Energy of the primary jet is transferred to the secondary air during the mixing process and the mixture is then ejected through the diffuser and blowing tube.

The model physical variables included suction-slot width, mixing-tube entrance throat width, and exit throttle diameter. Width of the suction slot was controlled by adjustmentment of the intake throttle shown in figure 2. The throat width was controlled by adjustment of the bolts attached to the suction duct at the throat as shown in figures 2 and 4. Figure 5 shows the installation of an orifice-type exit throttle, and figures 6 and 7 show typical test setups.

For the pressure measurements a variety of manometers were used as shown in figures 9 and 10. An instrumentation schematic is given as figure 11. Alcohol was used as the manometer fluid, except in the few cases where mercury was necessary. Ambient air and liquid temperatures were taken with mercury thermometers, while iron-constantan thermocouples were used to measure steam temperatures with an indicating potentiometer.

A total-pressure survey tube and a temperature survey probe were constructed to give approximately the stagnation conditions (i.e., turbulence effects and recovery factor were neglected). It was found necessary to insulate the temperature probe tip from the brass body to reduce heat transfer. Phenolic fiber was satisfactory for this purpose.

The primary fluid (superheated steam) was supplied by a Besler Corporation steam-generator-superheater system. These units supplied steam at pressures from 225 to 325 psig with temperatures from saturation to 650°F. A description of this equipment is given in Appendix B and reference 2. The steam nozzles were designed, fabricated and calibrated as described in Appendix A.

TESTS

The test procedures and data recording were in accordance with the pre-test report (Ref. 1). Initial adjustments of the throat and slot widths were accomplished in a series of short runs to obtain the desired suction-slot flow-quantity distribution. The maximum mass ratio was obtained by adjustments of the suction-slot throttle rather than the entrance throat. Suction-slot throttling was used for all tests subsequent to this initial investigation, even though secondary-flow-quantity distribution was more difficult to obtain with suction-slot throttling, and large spanwise slot-width variations were required.

The following measurements and variations to the model configuration were then performed.

<u>Measurements</u>.-
1. Suction slot area.
2. Mixing-tube-entrance throat area.
3. Suction slot static-pressure distribution.
4. Mixing-tube entrance throat static-pressure distribution.
5. Mixing-tube cross-sectional, total-pressure distribution.
6. Configuration changes:
   Repetition of the above measurements in successive steps from the condition of an open exit tube to a condition of restricted exit producing incipient reverse flow in the suction slot.

<u>Data Recorded</u>.- All data listed under 'Measurements' were recorded, together with the following:

1. Suction-slot air temperature.
2. Throat air temperature.
3. Mixing-tube-flow temperature distribution at each survey station.
4. Steam temperature.
5. Steam pressure.
6. Barometric pressure.

PERFORMANCE ANALYSIS

The jet-pump performance parameters were detailed in the pretest report (Ref. 1). The influence of specific impulse on performance will be evaluated later. Total-pressure losses in the suction duct were determined from average velocities and pressures found by integrating the flow-quantity distribution curves. The throat flow distribution was not similar to the slot distribution because of cross flow in the suction duct (Fig. 25). Therefore, the spanwise variation of the losses was not determined.

The average suction-duct losses were determined by the following procedure-

a) Bernoulli's equation at the suction slot is

$$p_{t_0} = p_{t_0} + p_1 + \frac{\rho_1 V_1^2}{2}\text{ , or, } -p_1 = \frac{\rho_1 V_1^2}{2} .$$

This relation was used to calculate the suction slot velocities which then gave the secondary flow quantity by integration across the slot.

b) The suction-slot quantity was temperature corrected for conductive heating effects by

$$q_2 = q_1 \frac{T_2}{T_1}$$, since the flow was essentially incompressible.

c) Then an average throat velocity was calculated from

$$V_2 = \frac{q_2}{A_2} .$$

d) Finally, the approximate total-pressure loss in the suction duct resulted from the relation

$$\Delta p_t = p_{t_1} - p_{t_2} = p_{t_0} - \left[(p_{t_0} + p_2) + \tfrac{1}{2}\rho_2 V_2^2 \right] = -p_2 - \tfrac{1}{2}\rho_2 V_2^2$$

The efficiency of the jet pump was determined from the ratio of effective power output to power input. The effective power output was defined as the summation of the products of the primary and secondary flow quantities and their respective adiabatic pressure changes (Ref. 1):

$$P_{eff} = q_s\,(p_{t_3} - p_{t_1}) + q_j\,(p_{t_3} - p_{t_0}).$$

The power input (Ref. 1) was defined as the product of the primary weight flow rate and the enthalpy change through the nozzle, where the enthalpy change included the effects of friction:

$$P_{in} = w_j \Delta h J.$$

The efficiency was therefore-

$$\eta = \frac{P_{eff}}{P_{in}} = \frac{q_s(p_{t_3}-p_{t_1})+q_j(p_{t_3}-p_{t_0})}{w_j \Delta h J}.$$

The mass ratio was expressed by the secondary to primary weight flow ratio,

$$\mu = \frac{w_s}{w_j}.$$

The available-energy efficiency at any point in the mixing tube was the ratio of the local available energy of the mixture to the available energy of the primary flow at the nozzle. This efficiency varied through the mixing tube as the primary-flow energy was transferred and dissipated by the mixing process. At any point the available energy was the sum of the kinetic energy and pressure. The energy ratio was

$$\eta_{AE_x} = \frac{\frac{1}{2}\,\rho_{m_x} V_{m_x}^2 + p_{m_x}}{\frac{1}{2}\,\rho_j V_j^2}.$$

The change of available energy through the mixing tube indicated the amount of energy transferred from the primary flow by adiabatic compression minus that dissipated by turbulence.

The jet-pump pressure ratio was defined as the ratio of the mixed-flow total pressure to the ambient total pressure

$$\alpha = \frac{p_{t_3}}{p_{t_0}}.$$

RESULTS AND DISCUSSION

Figures 14 through 17 show the performance of the side-inlet jet pump tested. The secondary mass flow increased as a function of the primary mass flow (fig. 18), but the mass ratio decreased due to the increase in pressure ratio (fig. 14). The pressure ratio increase resulted from forcing larger quantities of mixture through the same blowing-tube exit area. The effects of greater pressure ratios are given by figures 14 and 15. The highest pressure ratio was measured at the point of incipient reverse flow in the suction slot. Higher pressure ratios would have resulted in a rapid decrease in mass ratio.

Figure 18 shows the influence of the variables of primary pressure, pressure ratio, slot throttling, throat throttling, and cascades on suction-slot quantity distributions. Comparison of secondary-flow distributions secured by adjustments of the throat and/or the slot showed that slot adjustment for desired quantity distribution with constant throat produced the most secondary flow quantity, and therefore the largest mass ratio. This may not be true for a tapered mixing tube since the mixing-tube flow conditions control the suction-duct flow.

Cascades in the inboard 12 inches of throat critically influenced the performance while the remainder had only a slight influence on the performance. Removal of all the cascades caused intermittent reverse flow in the outboard throat area and a strong ring-vortex in the mixing tube at the inboard end around the nozzle flow.

Figure 19 shows the influence of slot throttling on the direction of air flow in the suction duct. The variations of the slot and throat widths to obtain the desired quantity distributions are shown in figures 20 and 21.

The throat and mixing-tube static pressure distributions, figures 22 and 23, showed that most of the mixing took place within the inboard 16 inches of the mixing tube. Available-energy efficiency distribution also showed this to be true (Fig. 16). This 'effective' mixing zone appears in all jet-pumps (Refs. 4 and 5). Although pressure surveys were not taken inboard of station 16 the mixing-tube surface temperatures indicated that the effective mixing zone extended 12 inches downstream from the nozzle. The end of the effective mixing zone is usually considered as the point where the mixed flow first fills the entire tube cross section.

Cross-section survey profiles of total pressure and temperature in the mixing tube are shown in figures 24 and 25. Average values of the integrated horizontal and vertical profiles of the total pressure distribution combined with the static pressure were used to roughly calculate the local available energy of the mixing tube flow. The temperature surveys were taken to supplement the total pressure surveys for the study of mixing characteristics. In figure 25 the temperature profiles indicate by their magnitude the areas of mixed and unmixed flow. The areas of unmixed flow, indicated by low temperatures, were adjacent to the mixing-tube entrance throat.

The performance of the steam-to-air jet pump tested was not considered optimum because of rough surfaces, sharp corners, etc. However, the performance analysis for a tapered mixing-tube jet-pump of similar construction will show comparatively the importance of mixing-tube shape. Also, these analyses will show the relative merits of secondary flow guidance and distribution methods.

CONCLUSIONS

Tests of a side-inlet, steam-to-air jet pump with an inboard nozzle and a cylindrical mixing-tube have shown this arrangement to have high losses and poor suction-slot, quantity- distribution properties. The high losses were ascribed to the extreme suction-slot throttling required for intake flow-quantity distribution and to the uncontrolled dissipation of the primary flow in the first part of the mixing-tube.

Further tests should be conducted with various taper-ratio mixing-tubes to determine the influence of this factor on the control of the mixing process and secondary flow-quantity distribution.

REFERENCES

1.- Heinrich, A.M.: Pre-Test Report on the Performance Study of a Side-Inlet Jet Pump with an Inboard Nozzle. University of Wichita Engineering Study No. 117, October 1953.

2.- Wagner, Friedrich; McCune, Charles J.: A Progress Report on Jet Pump Research. University of Wichita Engineering Report No. 085, October 1952.

3.- Everett, H.A.: Thermodynamics. D. Van Nostrand Co., Inc., New York, 1948.

4.- Wagner, F.: A Contribution to the Development of Jet Pumps. ATI No. 20253, July 1944.

5.- Helmbold, H.B.: Contributions to Jet Pump Theory, III. Simplified Theory of Mixing-Zone Spreading. University of Wichita Engineering Report No. 107, July 1953.

APPENDIX A

STEAM NOZZLE DESIGN AND CALIBRATION

STEAM NOZZLE DESIGN AND CALIBRATION

The design of the supersonic steam nozzle was based on the adiabatic expansion of superheated steam through a convergent-divergent passage. The flow was corrected for the entropy increase due to wall friction. Since very little of the expansion was to take place in the saturated or supersaturated region, the losses for droplet lag and supersaturation were considered negligible. The upstream velocity was also negligible since it was small compared to the nozzle velocity.

Given: Nozzle as shown in figure A1 and,

1. Quantity - 810 lbs/hr
2. Initial state pressure - 300 psia
3. Initial state temp. - 650°F
4. Final state pressure - 14.7 psia
5. Nozzle efficiency 96 percent (4 percent friction loss).

From steam tables or Mollier diagram:

s_1 = 1.652 Btu/lb = initial state entropy

h_1 = 1342 Btu/lb = initial state enthalpy

for superheated steam with k = 1.3

$$p_{th}/p_{t1} = 0.545$$

where p_{th} = throat pressure

p_{t1} = initial state pressure

$$p_{th} = .545 \times 300 = 163.5 \text{ psia}$$

$$s_{th} = s_1 = 1.652 \text{ Btu/lb °F}$$

$$t_{th} = 504°F$$

$$v_{th} = 3.382 \text{ ft}^3/\text{lb} = \text{throat specific volume}$$

$$h_{th} = 1274.87$$

$$V_{th} = \sqrt{2gJ\,(h_1 - h_{th})} \quad \text{when } h_2 = h_{th}$$

$$V_{th} = 224\sqrt{1342 - 1274.87} = 1840 \text{ ft/sec}$$

$$A_{th} = \frac{810 \times 3.382 \times 144}{3600 \times 1840} = .0596 \text{ in}^2$$

$$dia_{th} = \sqrt{\frac{.0596 \times 4}{\pi}} = .2755 \text{ inches}$$

$$h_e = 1080 \text{ Btu/lb}$$

$V_e = 224\sqrt{1342 - 1080} = 3620$ ft/sec

quality $x_e = \frac{s_1 - s_{f2}}{s_{fg_2}} \times 100 = 92.75$ percent

$v_e = v_{f_e} + x_e v_{fg_e}$

$v_e = .02 + (.9275)(26.8) = 24.87$ ft³/lb

$A_e = \frac{810 \times 24.87 \times 144}{3600 \times 3620} = .223$ in²

$dia_e = \sqrt{\frac{.223 \times 4}{\pi}} = .533$ in

THROAT AREA CORRECTION FOR FRICTION

$p_{th} = 163.5$ psia

$V_{th} = 224\sqrt{.96 \times 67.13} = 1800$ ft/sec

Reheat to throat = .04 x 67.13 = 2.685 Btu/lb

$h_{th} = 1274.87 + 2.685 = 1277.56$ Btu/lb

$t_{th} = 510°F$

$v_{th} = 3.416$ ft³/lb

$A_{th} = \frac{810 \times 3.416 \times 144}{3600 \times 1800} = .0615$ in²

$dia_{th} = \sqrt{\frac{.0615 \times 4}{\pi}} = .280$ in

EXIT AREA CORRECTION FOR FRICTION

$V_e = 224\sqrt{.96 \times 262} = 3550$ ft/sec

Reheat to exit = .04 x 262 = 10.5 Btu/lb

$h_e = 1080 + 10.5 = 1090.5$

$x_e = 100 - 6.5 = 93.5$ percent

$v_e = .02 + (.935)(26.8) = 25$ ft³/lb

$A_e = \frac{810 \times 25 \times 144}{3600 \times 3550} = .229$ in²

$dia_e = \sqrt{\frac{.229 \times 4}{\pi}} = .54$ in

The nozzle layout was arbitrarily selected to give a smooth round entrance to the throat and a straight taper from the throat to the exit. Figure A1 shows the cross-section of the nozzle. The nozzle was machined from stainless steel with extreme internal dimensional control and then polished.

A nozzle calibration was performed through timed measurement of inlet and waste flow of water to the stream generating unit. These flow rates were determined at various pressures and temperatures and plotted as figures A2 and A3.

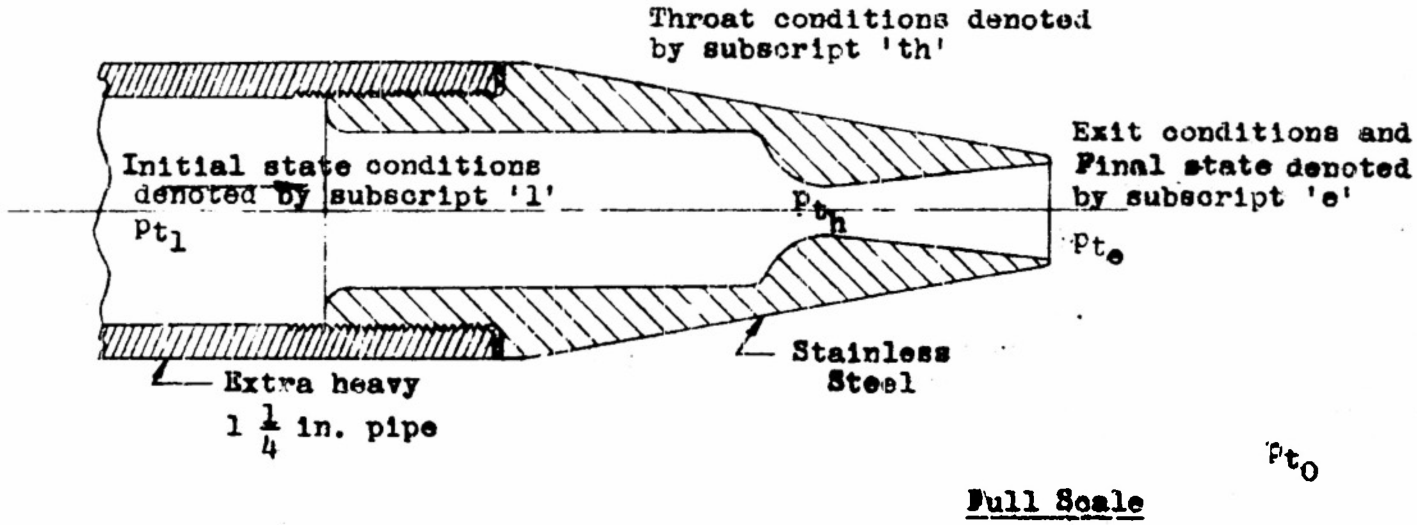

Figure A1.- Cross section, convergent-divergent steam nozzle.

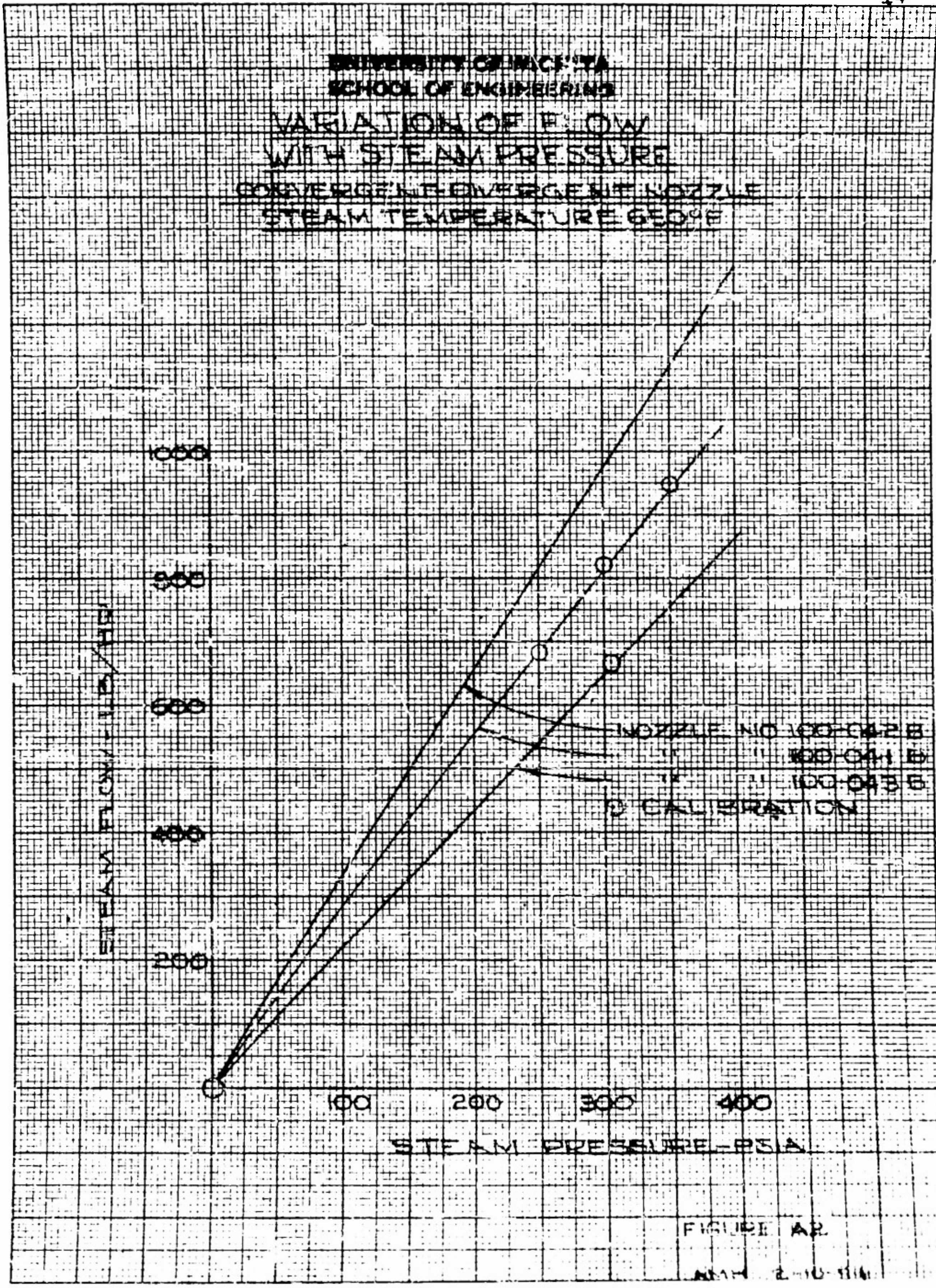
UNIVERSITY OF WICHITA
SCHOOL OF ENGINEERING
VARIATION OF FLOW
WITH STEAM PRESSURE
CONVERGENT-DIVERGENT NOZZLE
STEAM TEMPERATURE 650°F
1000
800
600
400
200
STEAM FLOW - LBS/HR
100
200
300
400
STEAM PRESSURE-PSIA
NOZZLE NO 100-042 B
" " 100-041 B
" " 100-043 B
⊙ CALIBRATION
FIGURE A2

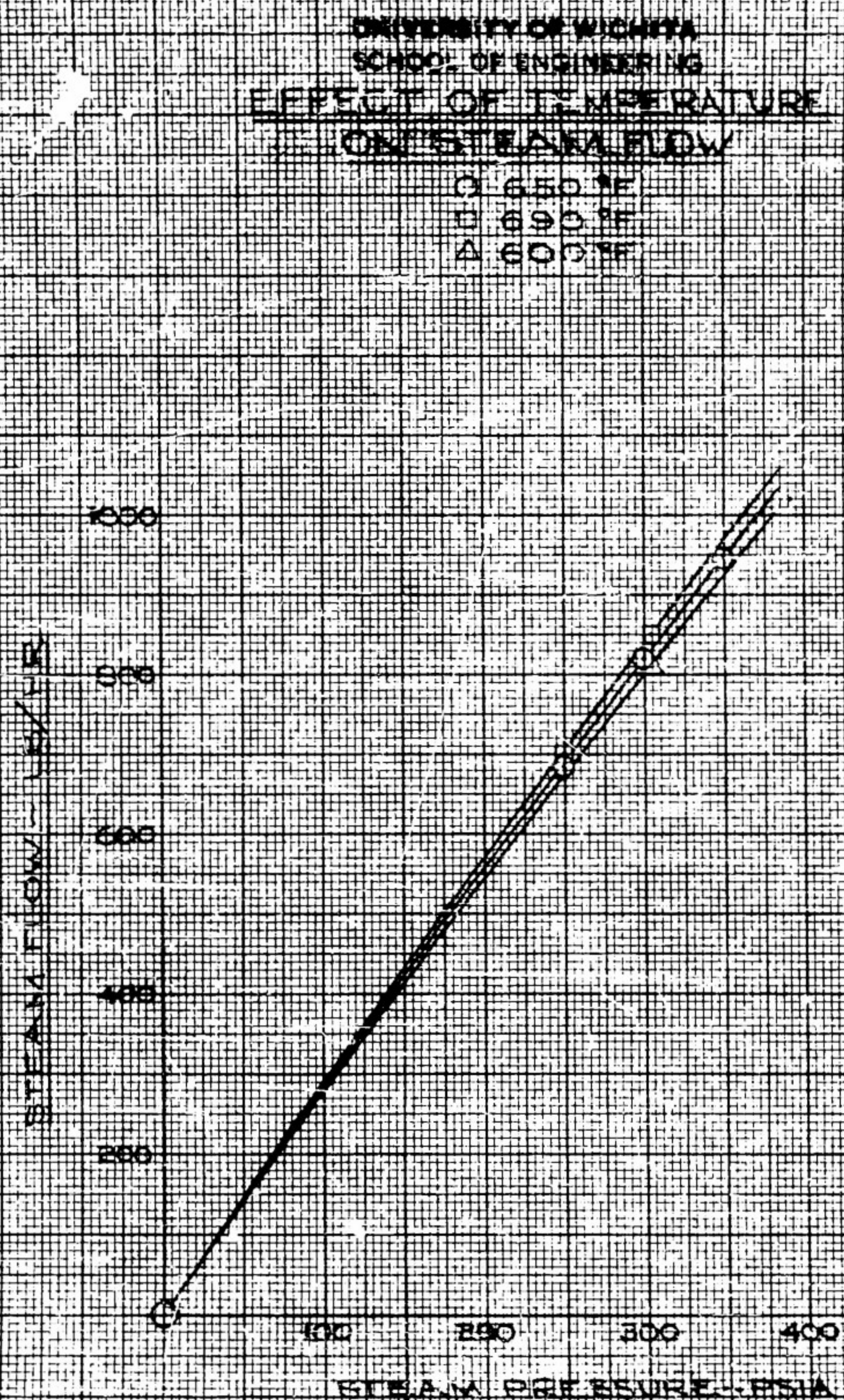

FIGURE A2

K+E KEUFFEL & ESSER CO. 10 X 10 TO THE ½ INCH 359-11

APPENDIX B

STEAM GENERATOR AND SUPERHEATER

STEAM GENERATOR AND SUPERHEATER

Steam for the primary fluid was produced by a Besler Model 85 generator (Fig. B1). This generator is a package unit containing the boiler, auxiliaries, and auxiliary drive motor incorporporated within a single framework. The unit is regulated by an air-operated, modulation control system. The control system will maintain a constant-pressure supply of steam at a given flow rate up to a maximum of 2500 pounds per hour. A change in either the pressure and/or the flow rate requires readjustment of the control system.

A Besler superheater (Fig. B2) was used to superheat the steam. It is a small, compact unit that burns diesel fuel and uses 110-volt single-phase power for operation. An electric motor drives the blower and fuel pump and the 110 volt power is transformed to 10,000 volts and imposed across a set of electrodes for combustion-chamber ignition. Temperature control is obtained by a thermostatically actuated fuel bleed control. Manual adjustment of the spring tension in this device regulates the fuel flow. The unit with its integral fuel tank is portable and requires only the availability of 110-volt, single-phase power for operation.

The rectangular manifold over the waste steam line shown in figure B1 is a condenser used to facilitate measurement of the generator waste flow for nozzle calibration purposes.

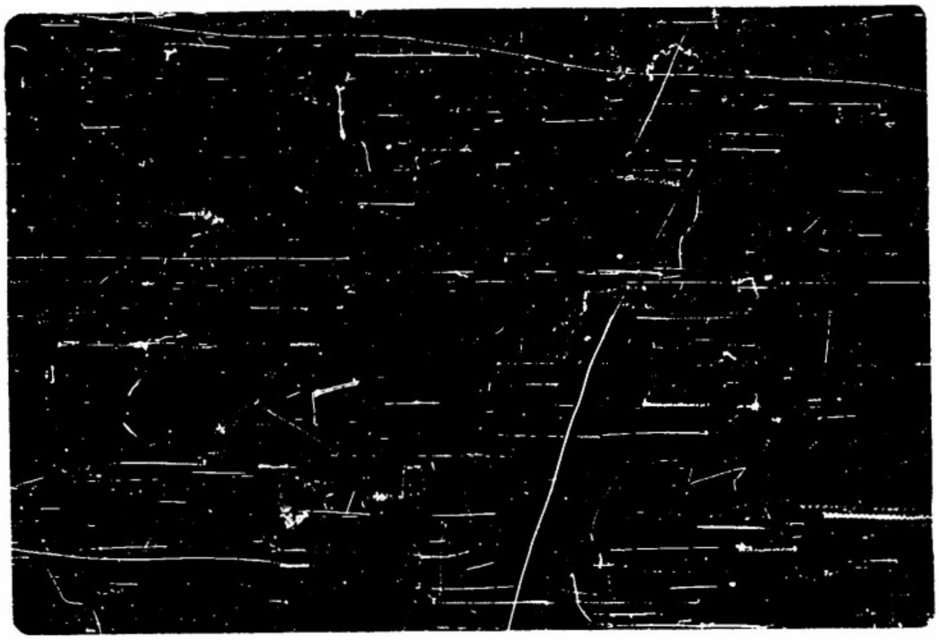

Figure B1.- Steam generator.

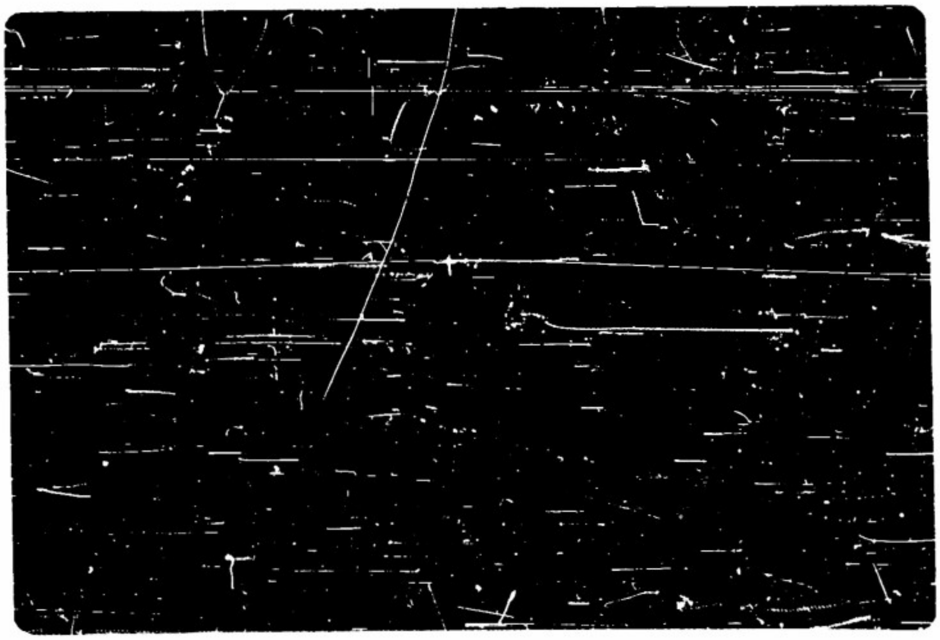

Figure B2.- Steam superheater and generator.

APPENDIX C

TEST LOG OF SISA-1 JET PUMP

Runs SISA-1-1 through SISA-1 27

TEST LOG, SISA-1 JET PUMP

Run No.	Configuration	Remarks
1	Throat width A. Slot width 1.6 inches, constant.	Outboard suction slot flow too small to measure.
2	Throat width B. Slot width 1.6 inches, constant.	Entire suction slot flow too small to measure.
3	Throat width B. Slot width 0.8 inches, constant.	Suction slot flow distribution measured. Distribution fairly constant over inboard half of suction slot and diminishing to negligible flow at outboard end of slot.
4	Throat width C. Slot shape throttle A.	Suction slot flow distribution measured.
5	Throat width C. Slot shape throttle B.	Suction slot flow distribution recorded. Mixing tube static pressure gradient recorded.
6	Throat width C. Slot shape throttle B. Sonic nozzle this run only.	Suction slot flow. Distribution recorded. Mixing tube static pressure gradient recorded. Nozzle flow case of extreme under-expansion.
7	Throat width C. Slot shape throttle C.	Suction duct outboard of station 42.3 blocked off. Measurements: a. Suction slot flow b. Mixing tube static pressure c. Total pressure survey at mixing tube station A (vertical only).
8	Throat width C. Slot shape throttle D.	Measurements: a. Suction slot flow b. Mixing tube static pressure distribution.
9	Throat width C. Slot shape throttle E.	Measurements: a. Suction slot flow b. Mixing tube static pressure distribution.

Run No.	Configuration	Remarks
10	Throat width C. Slot shape throttle F.	Total pressure probe tube diameter increased to prevent moisture clogging. Measurements: a. Suction slot flow b. Mixing-tube static pressure c. Mixing-tube total pressure distribution at stations A and D.
11	Throat width C. Slot shape throttle F.	Measurements: Same as 10 except total pressure taken at stations A through D.
12	Throat width C. Slot shape throttle F.	Temperature probe tried and found to have intolerable heat transfer from body to tip. Measurements: a. Mixing-tube total pressure distribution taken at stations E and F. b. Mixing-tube temperature distribution taken at stations A through F.
13	Throat width C. Slot shape throttle F.	Temperature probe with phenolic insulated tip proved satisfactory. Measurements: Temperature survey taken at mixing-tube stations A through F.
14	Throat width C. Slot shape throttle F.	Suction duct flow direction studied with a wool tuft. Measurements: a. Temperature and total pressure survey taken at mixing tube station F. b. Suction slot flow c. Mixing-tube static pressure distribution d. Suction slot temperature distribution.

Run No.	Configuration	Remarks
15	Throat width C. Slot shape throttle F. Cascaded turning vanes removed from throat.	Intermittent reverse flow at outboard end of suction slot. Surface temperature and static pressure of mixing tube at inboard end showed evidence of a strong vortex within first 6 inches of mixing tube length. Measurements: a. Suction slot flow b. Mixing tube static pressure distribution. c. Suction slot average temperature.
16	Throat width C. Slot shape throttle F. Cascaded turning vanes in inboard 12 inches of throat only.	No reverse flow in suction slot. No evidence of the vortex as found in Run 15. Suction duct flow was studied with a wool tuft. Measurements: a. Suction slot flow b. Mixing tube static pressure distribution c. Suction slot average temperature.
17	Throat width C. Slot shape throttle F. Cascaded turning vanes in inboard 20 inches of throat only	Similar characteristics of Run 16. Suction duct flow was studied with a wool tuft. Measurements: a. Suction slot flow b. Mixing tube static pressure distribution c. Suction slot average temperature.
18	Throat width C. Slot shape throttle F. Cascaded turning vanes in inboard 12 inches of throat only.	Verification of Run 16.
19	Throat width C. Slot shape throttle F. All cascaded turning vanes installed.	Performance run. Measurements: Steam p_{t_j} = 224 psig, t_j = 653°F a. Suction slot flow b. Mixing tube entrance throat static pressure distribution

Run No.	Configuration	Remarks
		c. Mixing tube static pressure distribution. d. Mixing tube temperature and total pressure survey at stations A through F.
20	Throat width C. Slot shape throttle F. All cascaded turning vanes installed.	Performance run. Measurements: Same as for Run 19. Steam pt_j=253 psig, t = 660°F.
21	Throat width C. Slot shape throttle F. All cascaded turning vanes installed.	Performance run. Measurements: Same as for Run 19. Steam pt_j=275 psig, t=653°F.
22	Throat width C. Slot shape throttle F. All cascaded turning vanes installed.	Performance run. Measurements: Same as for Run 19. Steam pt_j=300 psig, t=657°F.
23	Throat width C. Slot shape throttle F. All cascaded turning vanes installed.	Performance run. Measurements: Same as for Run 19. Steam pt_j=327 psig, t=660°F.
24	Throat width C. Slot shape throttle F. All cascaded turning vanes installed. Two different sizes of exit orifices were installed.	Test to establish maximum pressure ratio for incipient reverse flow in section slot. Measurements: a. Suction slot flow b. Mixing tube static pressure distribution
25	Throat width C. Slot shape throttle F. All cascaded turning vanes installed. Exit orifice diameter ratio = 1.0.	Reference run for Runs 26 and 27. Measurements: Steam pt_j=303 psig, t =653°F a. Suction slot flow b. Mixing tube entrance throat static pressure distribution c. Mixing tube static pressure distribution d. Mixing tube temperature and total pressure survey at station F.

Run No.	Configuration	Remarks
26	Same as Run 25 except exit orifice diameter ratio = .908	Performance test with additional pressure ratio. Measurements same as for Run 25.
27	Same as Run 25 except orifice diameter ratio = .824	Performance test with additional pressure ratio. Measurements same as for Run 25.

TABLE C1.- SISA-1 JET PUMP PERFORMANCE

Run No.	pt_j (psia)	t_j (°F)	w_s (lb/sec)	w_j (lb/sec)	w_s/w_j	p_{t3}/p_{t_o}	η
1	300	650					
2	300	650					
3	300	650					
4	315	650					
5	315	650					
6	314	650					
7	314	650	1.765	0.235	7.51		
8	314	650	1.740	0.235	7.40		
9	314	650	1.710	0.235	7.28		
10	314	650	1.77	0.235	7.53		
11	314	650	1.74	0.235	7.40		
12	314	650	----	0.235	----		
13	314	650	----	0.235	----		
14	314	650	1.765	0.235	7.51		
15	314	650	1.140	0.235	4.85		
16	314	650	1.80	0.235	7.66		
17	314	650	1.72	0.235	7.32		
18	314	650	1.75	0.235	7.45		
19	238	653	1.315	0.179	7.35	1.0045	0.625
20	266.9	660	1.44	0.200	7.20	1.0055	0.788
21	289	653	1.46	0.2165	6.74	1.0055	0.751
22	314.2	657	1.65	0.235	7.02	1.0059	0.871
23	341.7	660	1.765	0.2555	6.9	1.0062	0.905
24	300	415	-----	------	---	------	-----
25	316.9	653	1.645	0.228	7.2	1.005	0.915
26	315.9	652	1.498	0.228	6.56	1.01	1.42
27	315.9	651	1.345	0.228	5.9	1.014	1.88

Approximate values ± 5°F and ± 5 psi
Runs No. 1 through 18

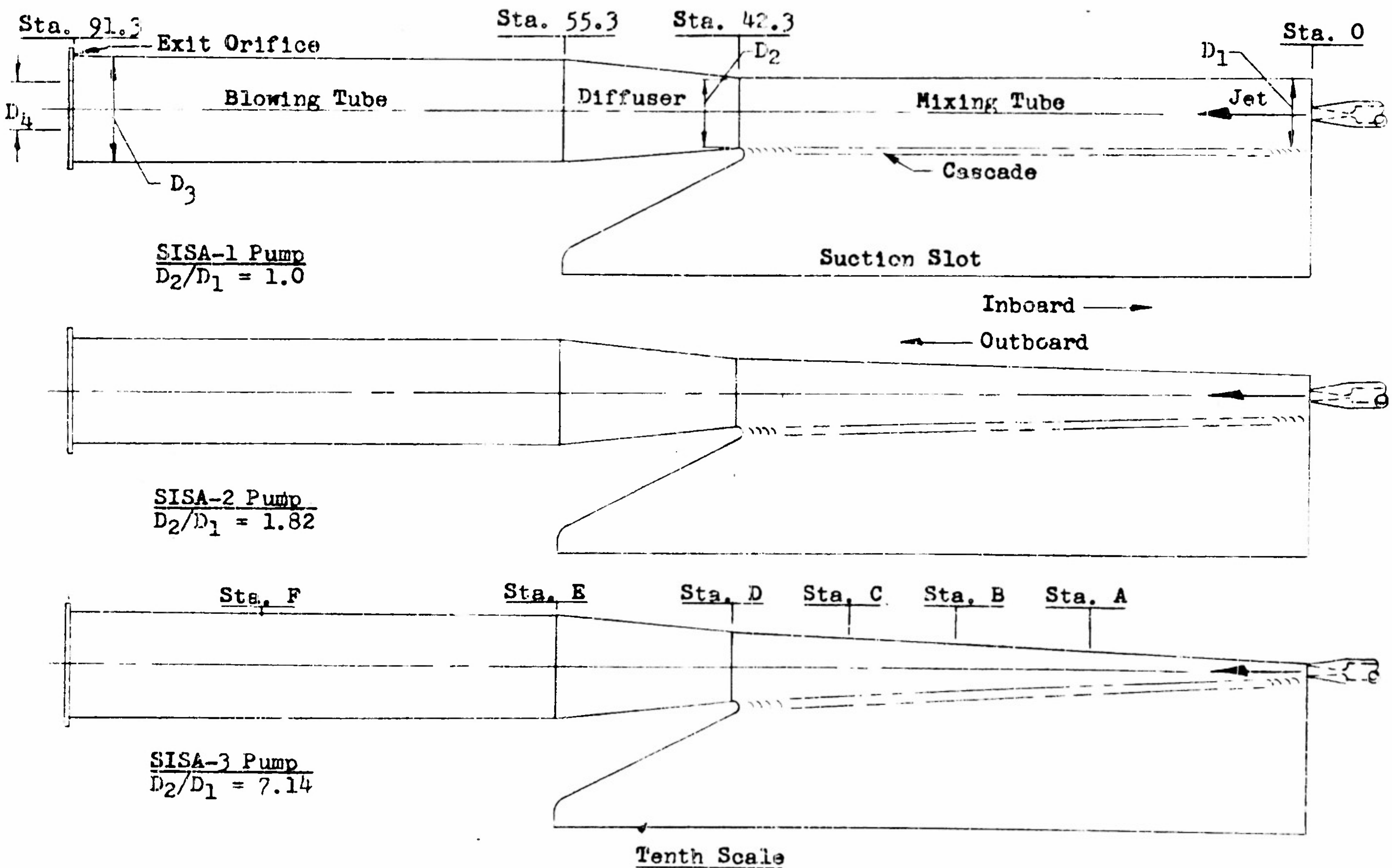

Figure 1.- Planform outline, side inlet, steam-air jet-pump.

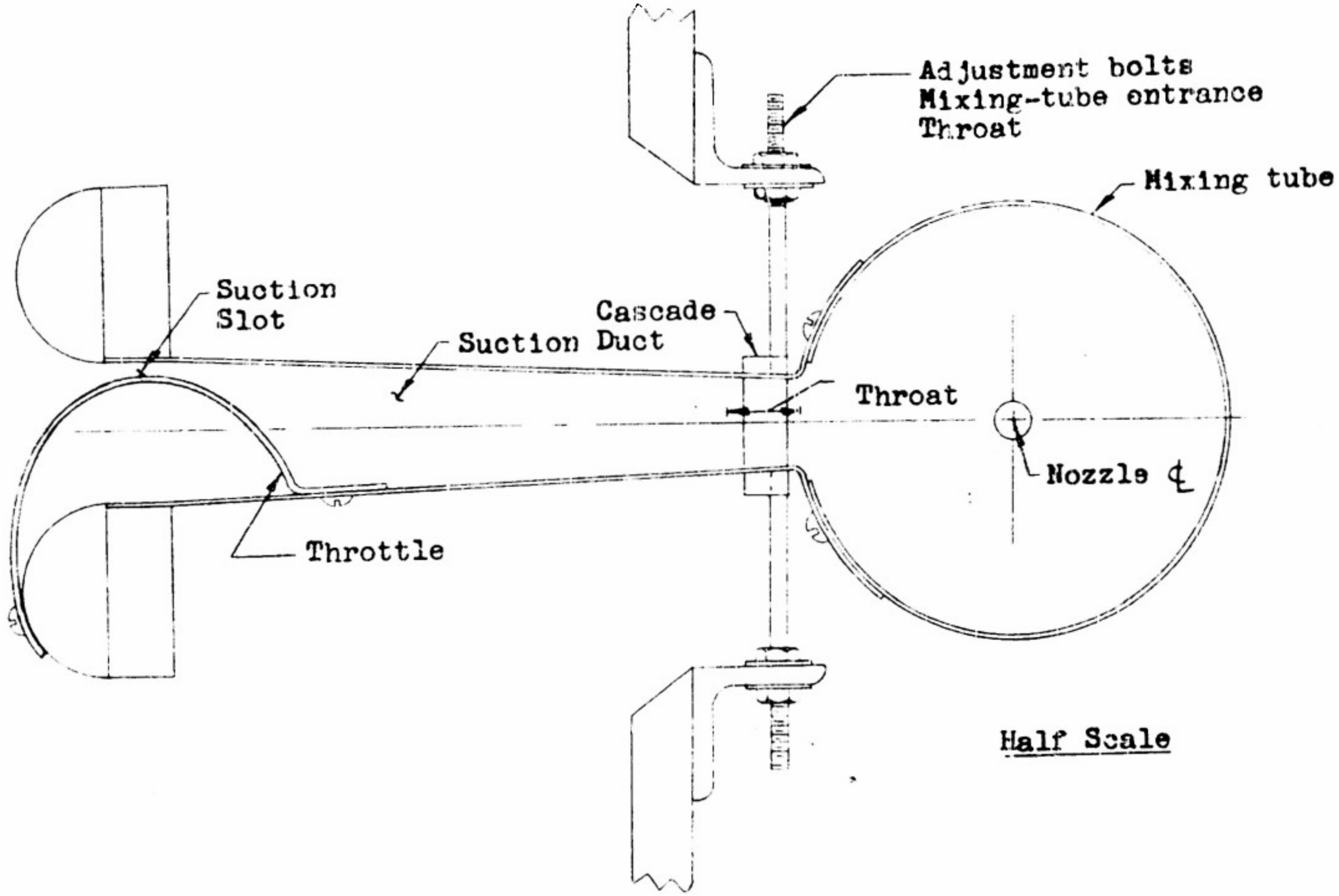

Figure 2.- Cross section of SIMA-1 jet-pump at nozzle exit.

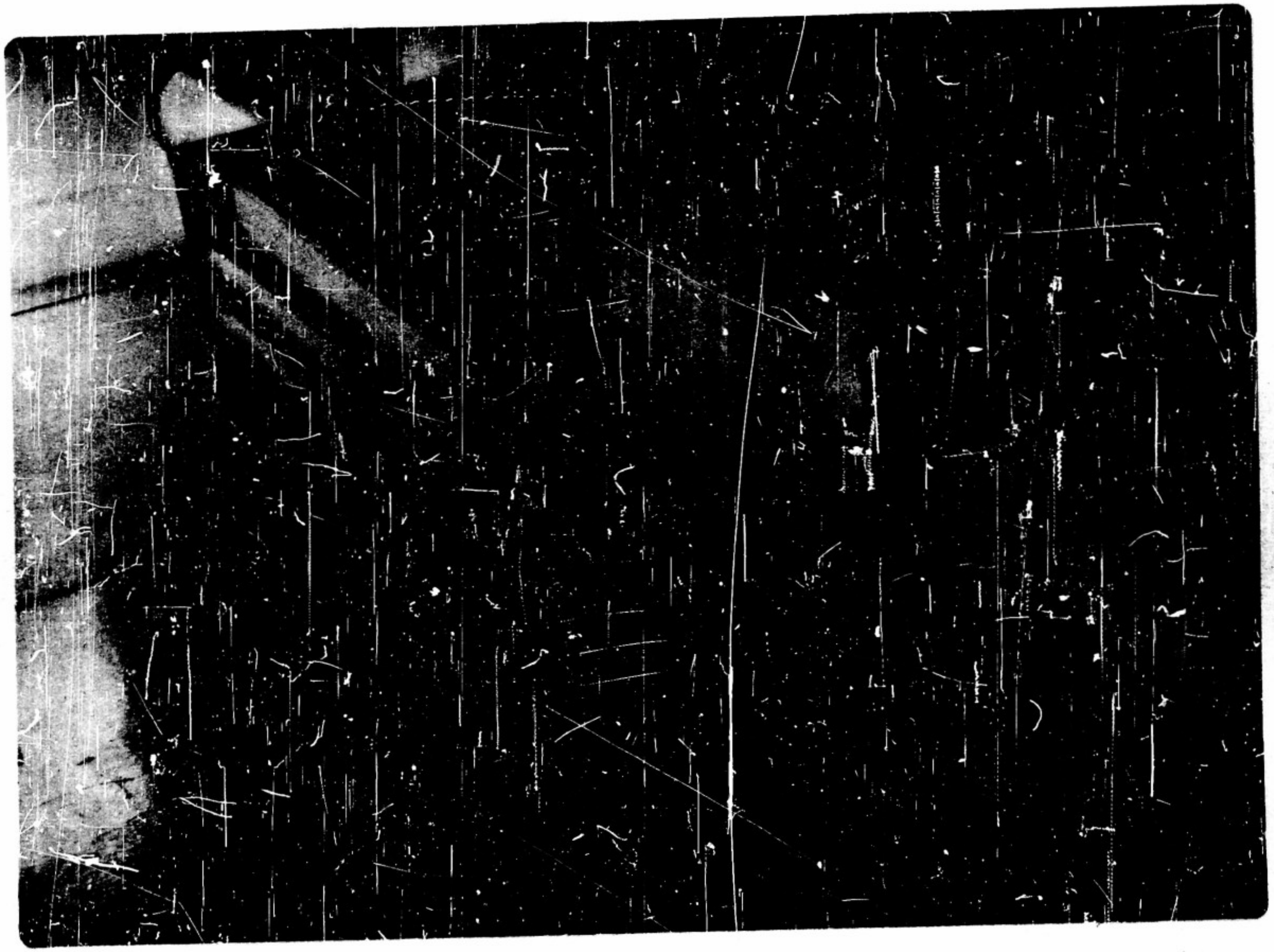

Figure 3.- Side-inlet, steam jet pump with an inboard nozzle.

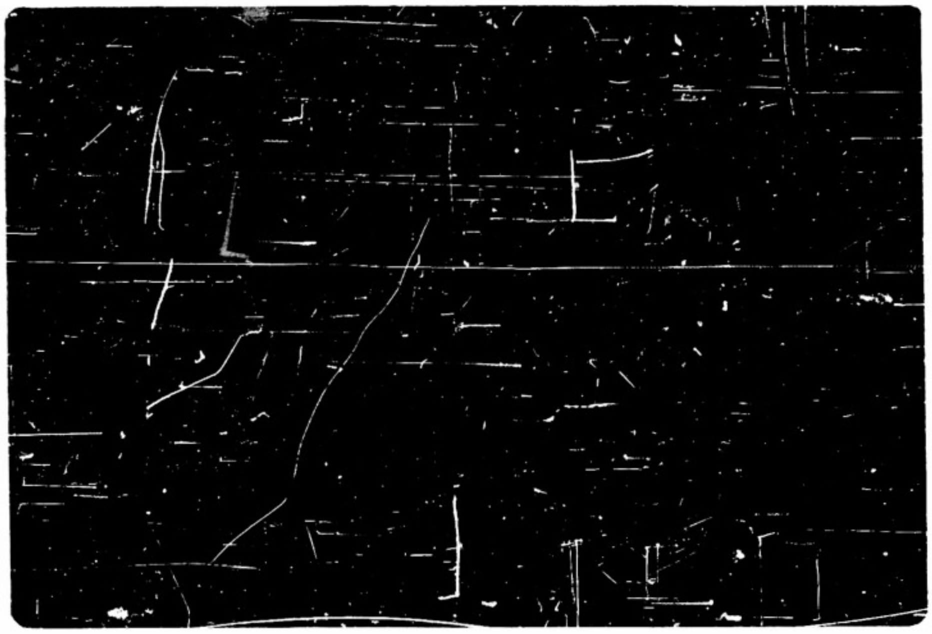

Figure 4.- Arrangement of mixing-tube pressure taps and throat-adjustment bolts.

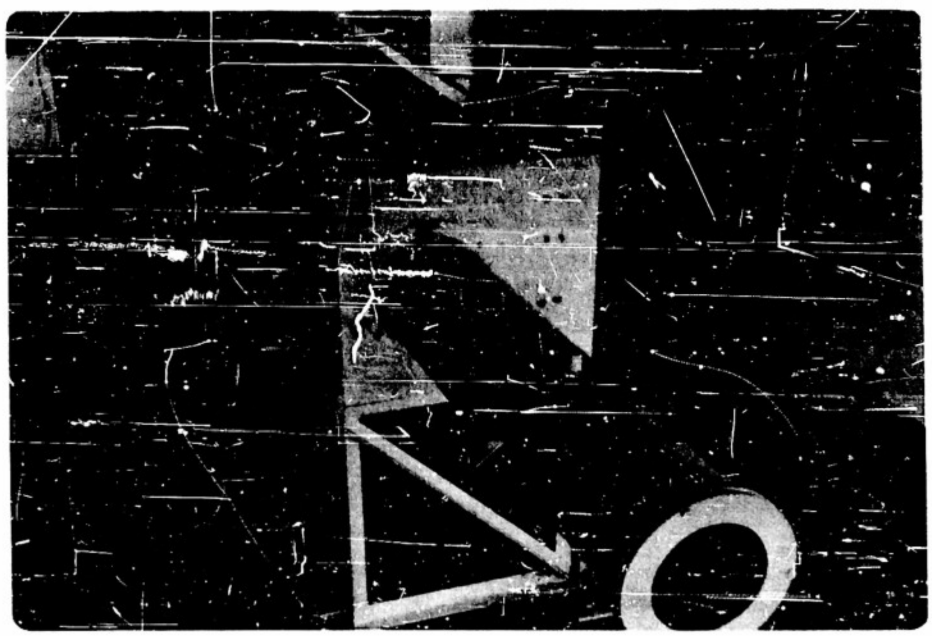

Figure 5.- Exit orifice installation.

Figure 6.- Arrangement of mixing-tube static pressure taps.

Figure 7.- Arrangement of suction-slot pressure taps.

on right.

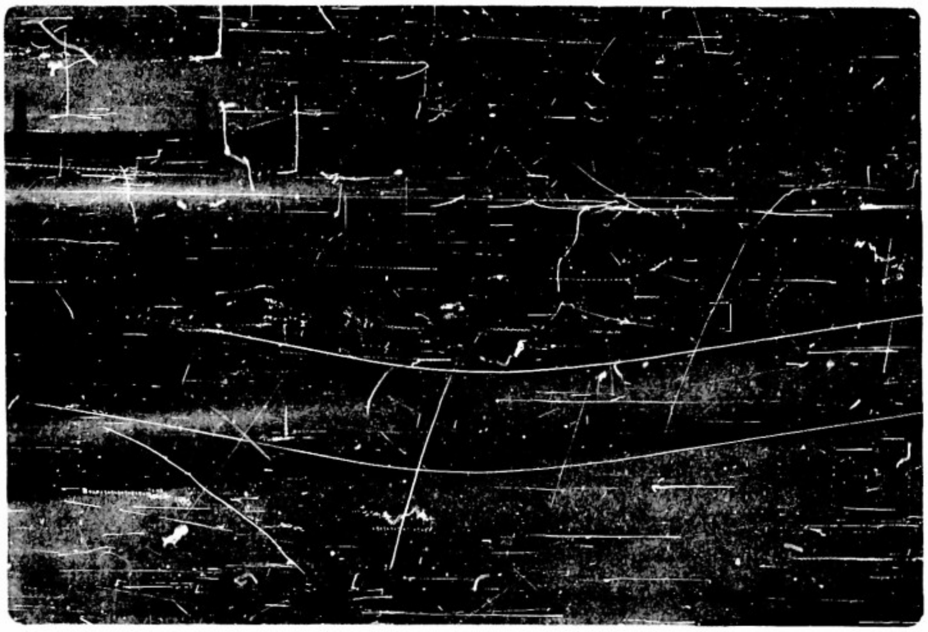

Figure 8.- Suction slot, static-pressure taps, and cascaded mixing-tube throat.

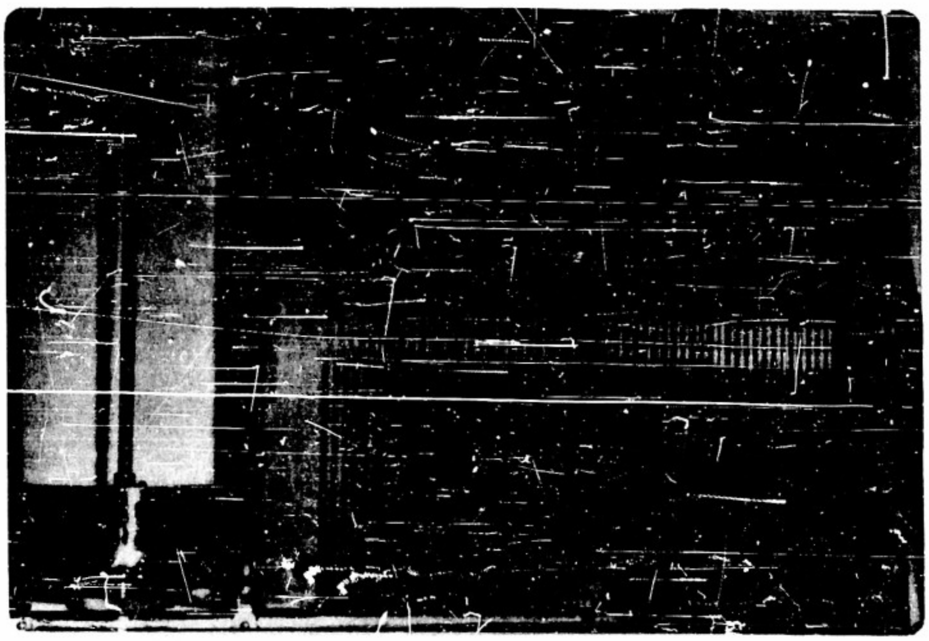

Figure 9.- Multitube manometer with static pressures of suction slot on left and mixing-tube throat on right.

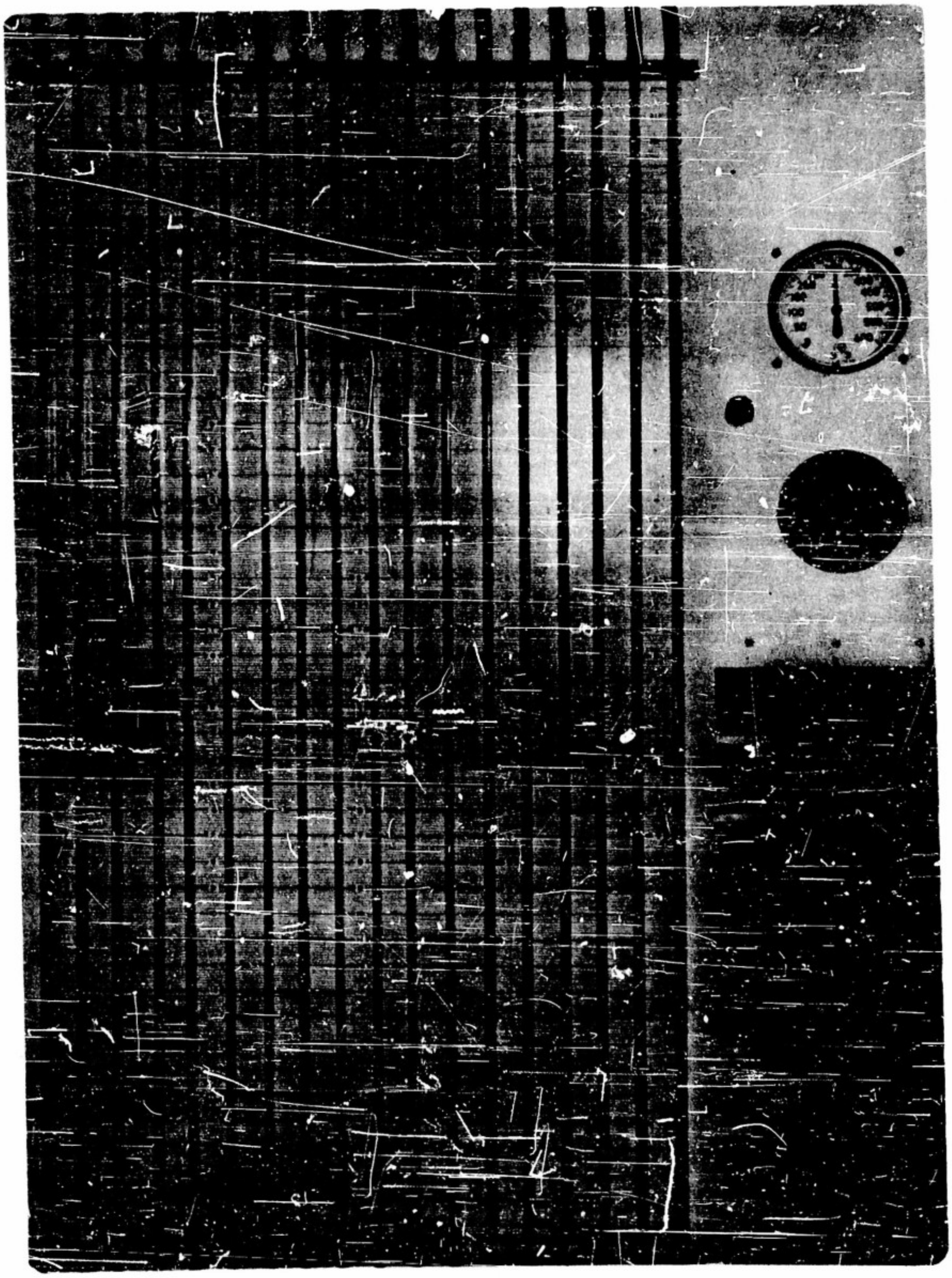

Figure 10.- Multitube manometer with mixing-tube static pressures on right and inboard suction-slot static pressures on left.

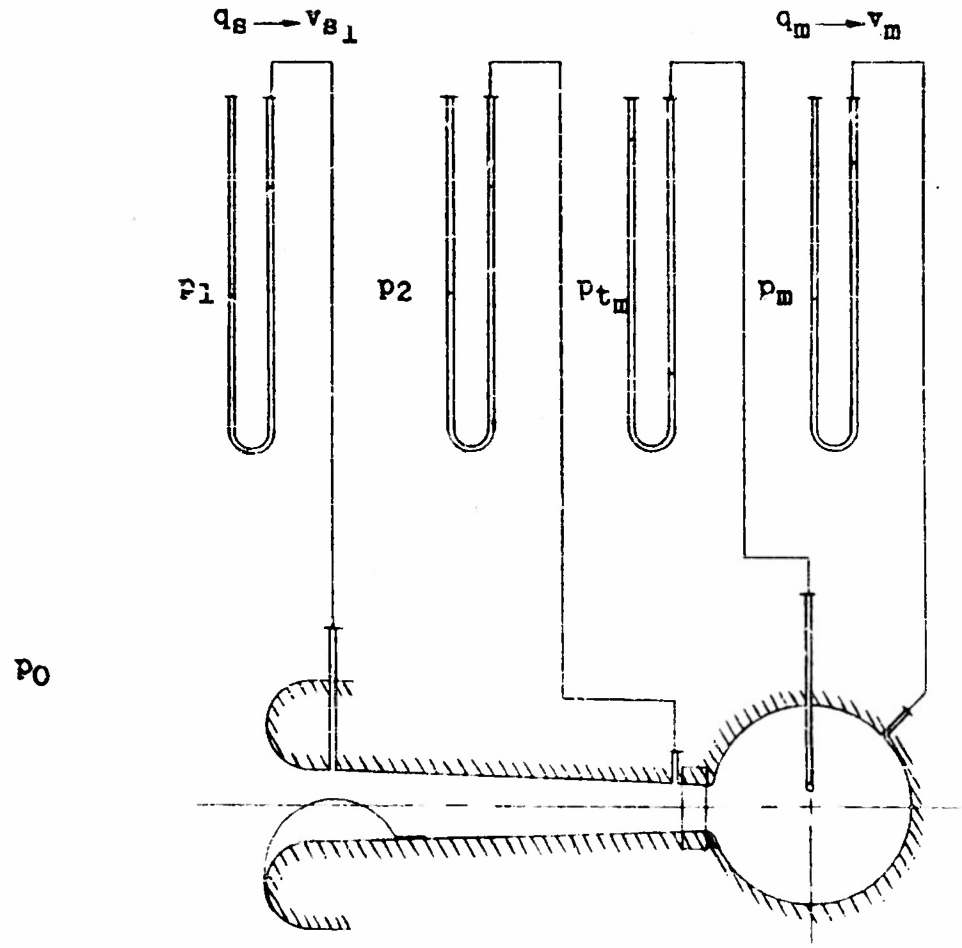

Figure 11.- Instrumentation schematic

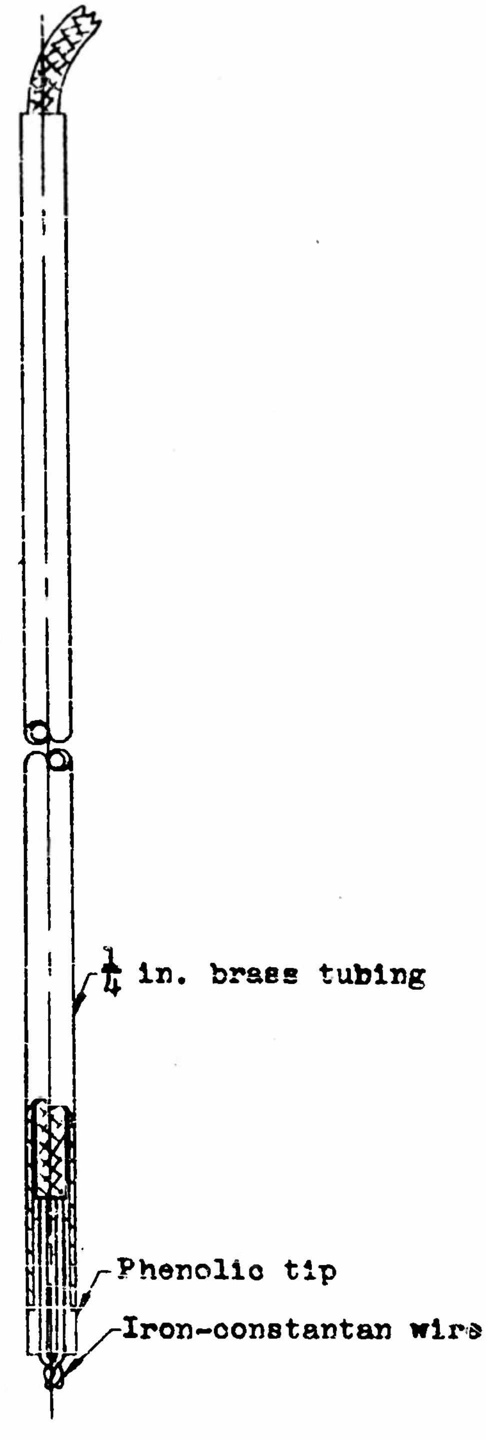

Full Scale

Figure 12.- Mixing-tube temperature survey probe

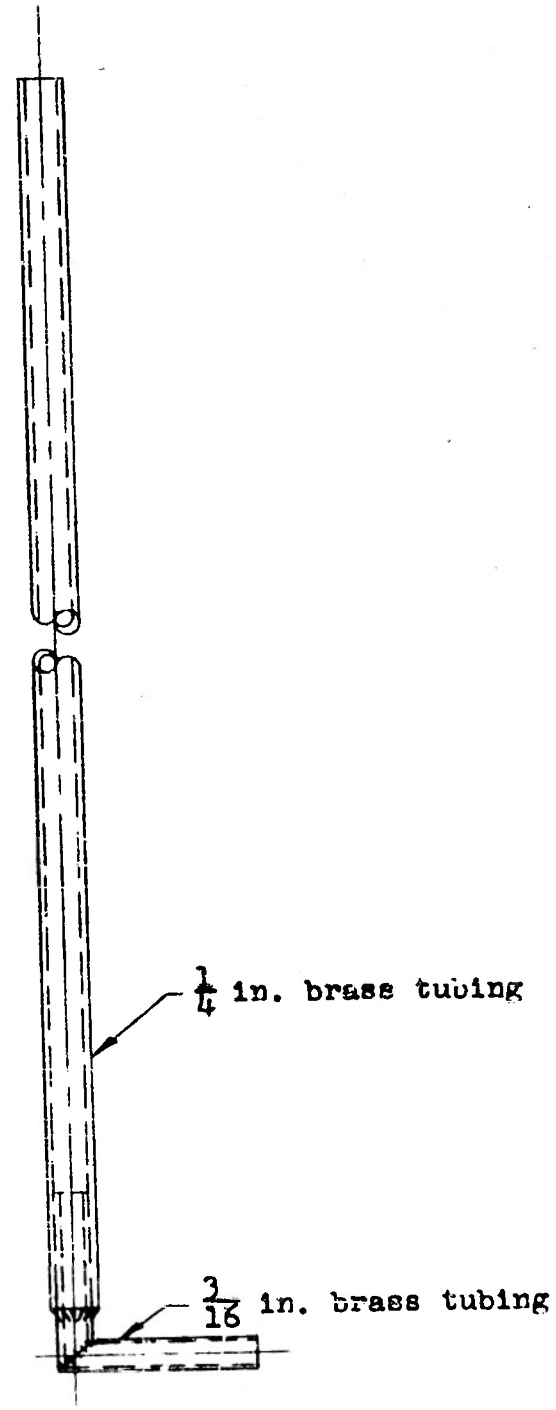

Full Scale

Figure 13.- Mixing-tube total-pressure survey probe.

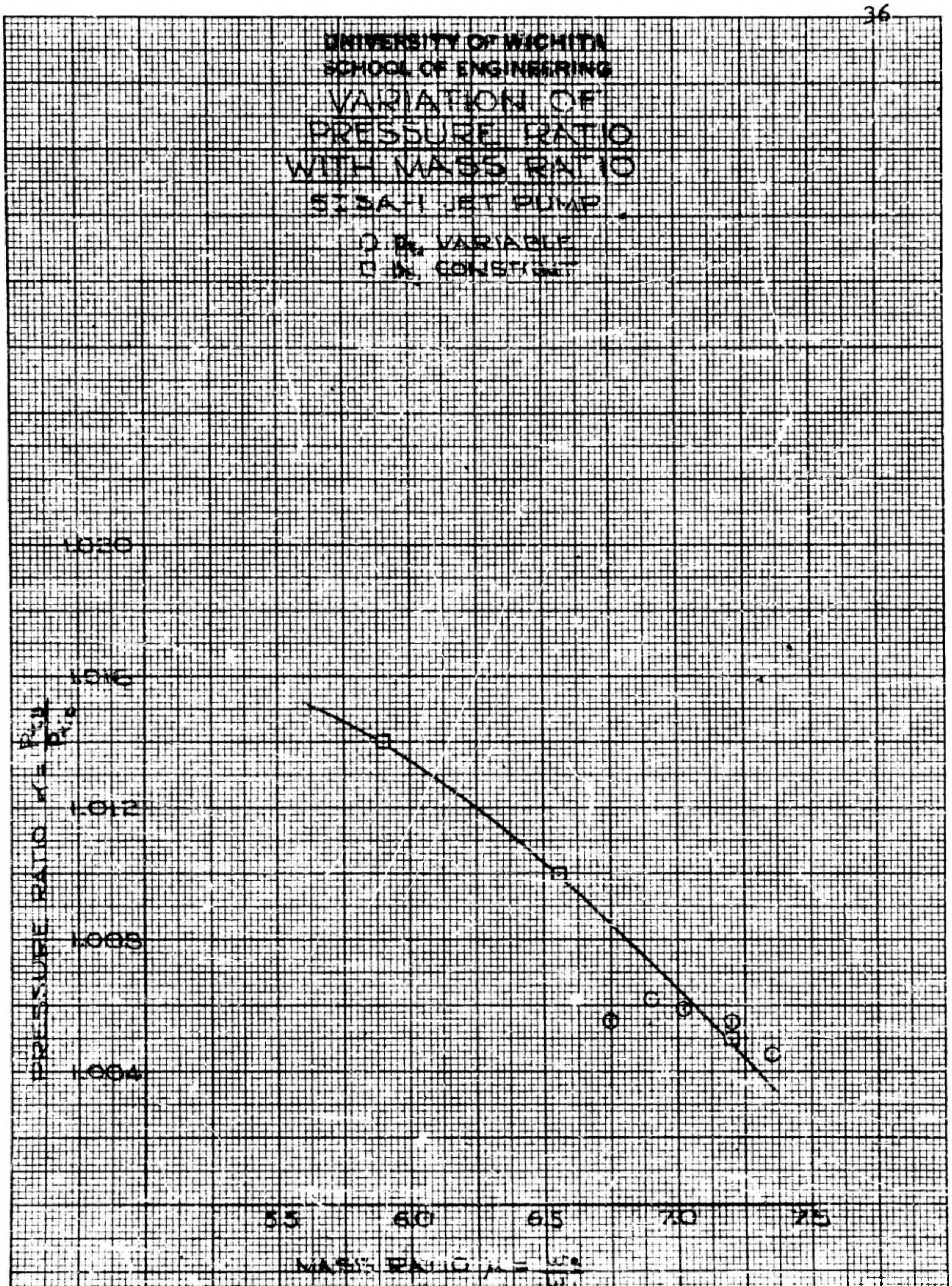
UNIVERSITY OF WICHITA
SCHOOL OF ENGINEERING
VARIATION OF
PRESSURE RATIO
WITH MASS RATIO
5I3A-1 JET PUMP
VARIABLE
CONSTANT
1.020
1.016
1.012
1.008
1.004
PRESSURE RATIO
.55
.60
.65
.70
.75
MASS RATIO
AMH 3-9-54

FIGURE 14

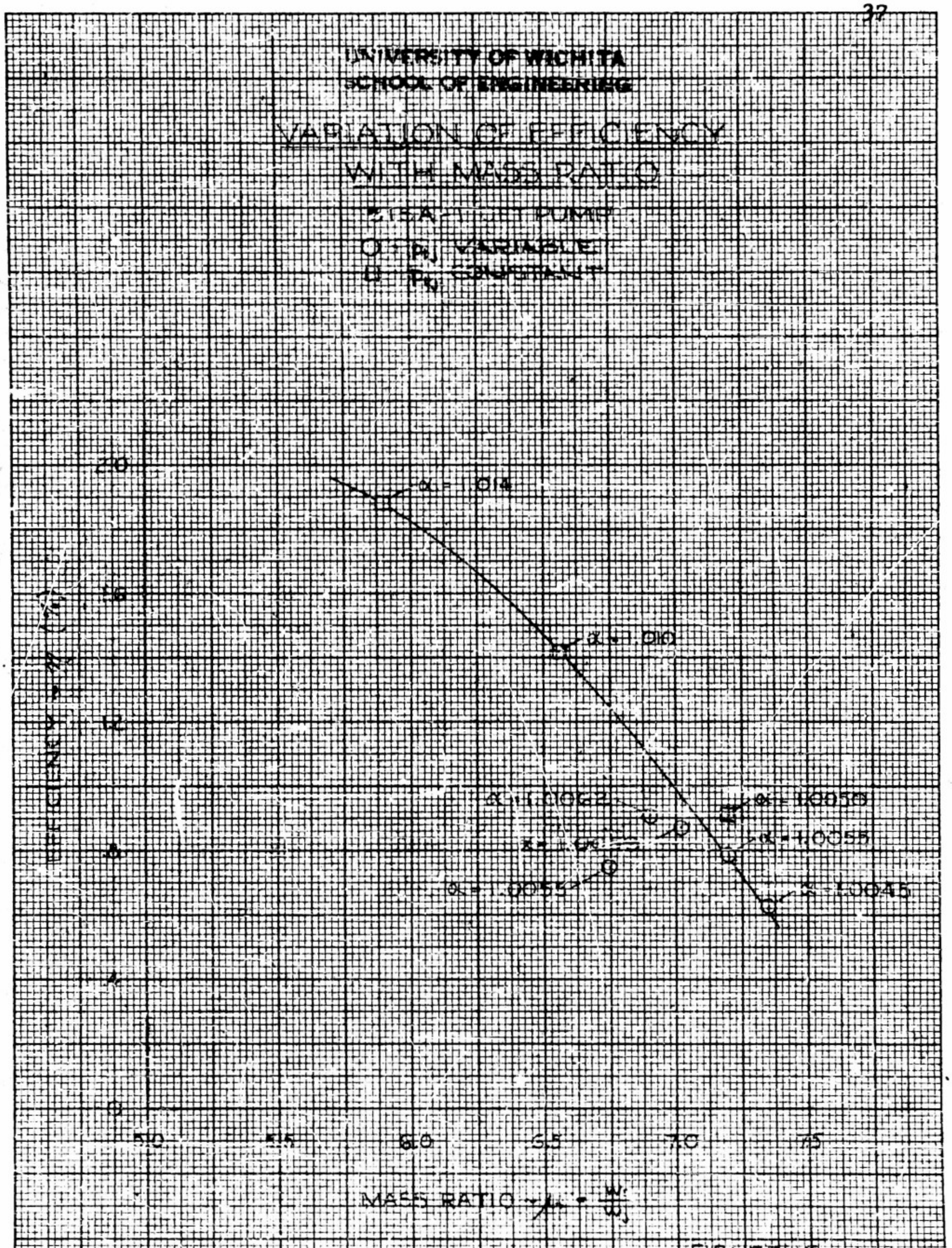
UNIVERSITY OF WICHITA
SCHOOL OF ENGINEERING
VARIATION OF EFFICIENCY
WITH MASS RATIO
PUMP
VARIABLE
CONSTANT
α = 1.014
α = 1.010
α = 1.0062
α = 1.0050
α = 1.0055
α = 1.0055
α = 1.0045
20
16
12
8
4
0
5.0
5.5
6.0
6.5
7.0
7.5
MASS RATIO
EFFICIENCY

FIGURE 5

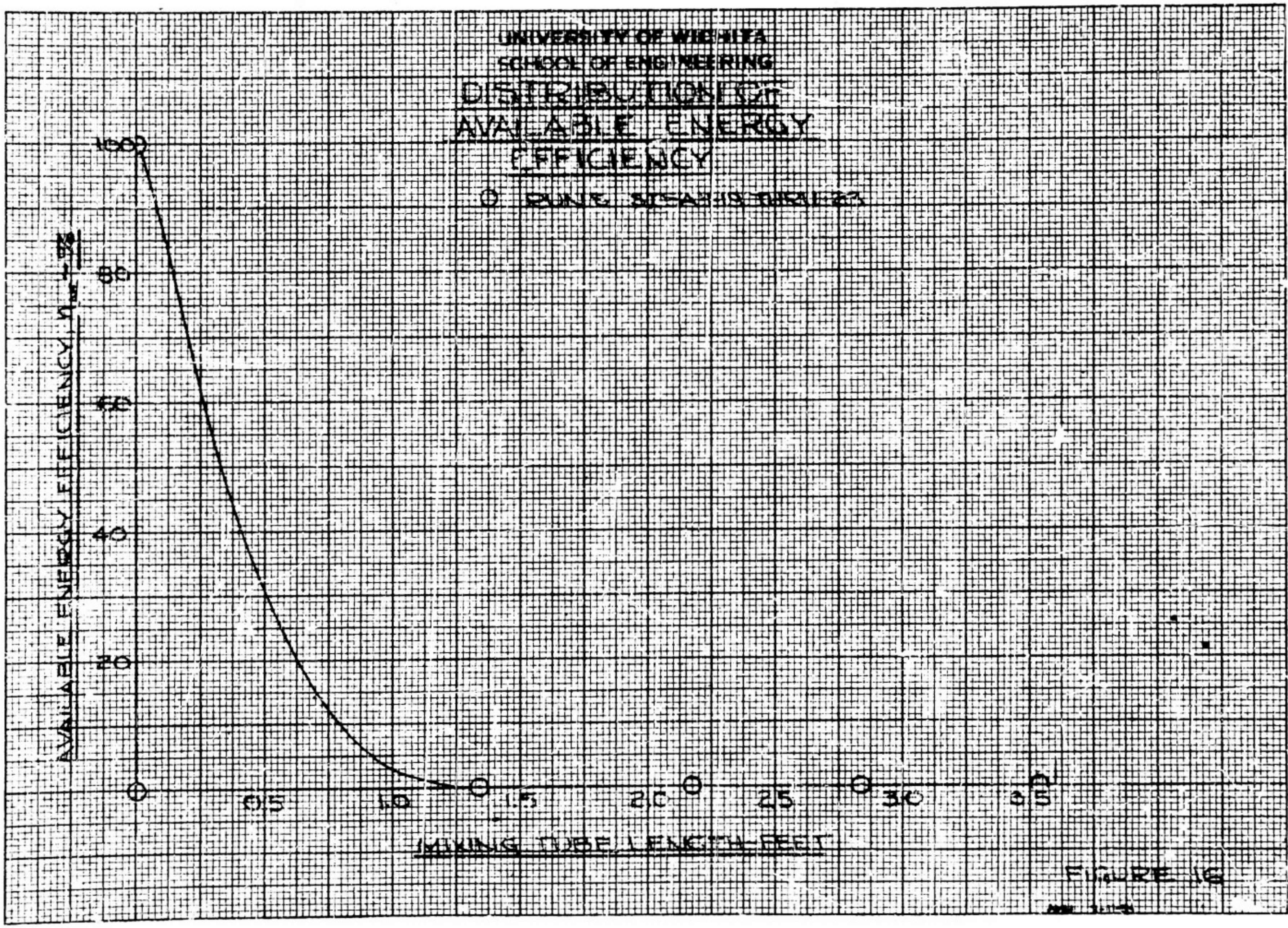
UNIVERSITY OF WICHITA
SCHOOL OF ENGINEERING
DISTRIBUTION OF
AVAILABLE ENERGY
EFFICIENCY
100
80
60
40
20
0.5
1.0
1.5
2.0
2.5
3.0
3.5
AVAILABLE ENERGY EFFICIENCY
MIXING TUBE LENGTH-FEET

FIGURE 16

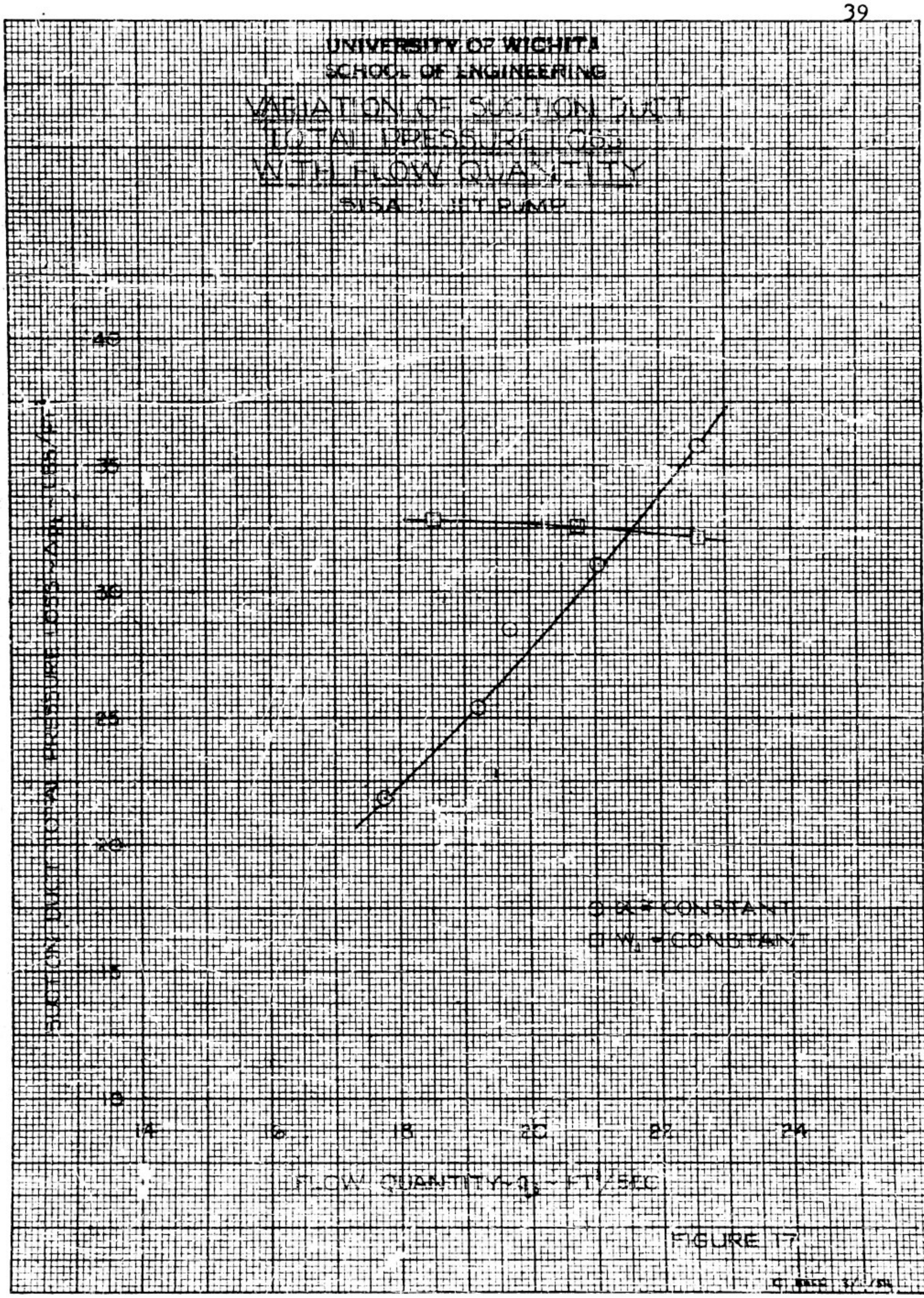
UNIVERSITY OF WICHITA
SCHOOL OF ENGINEERING
VARIATION OF SUCTION DUCT
TOTAL PRESSURE LOSS
WITH FLOW QUANTITY
SUCTION DUCT TOTAL PRESSURE LOSS
40
35
30
25
20
15
10
14
16
18
20
22
24
FLOW QUANTITY
CONSTANT
CONSTANT
FIGURE 17

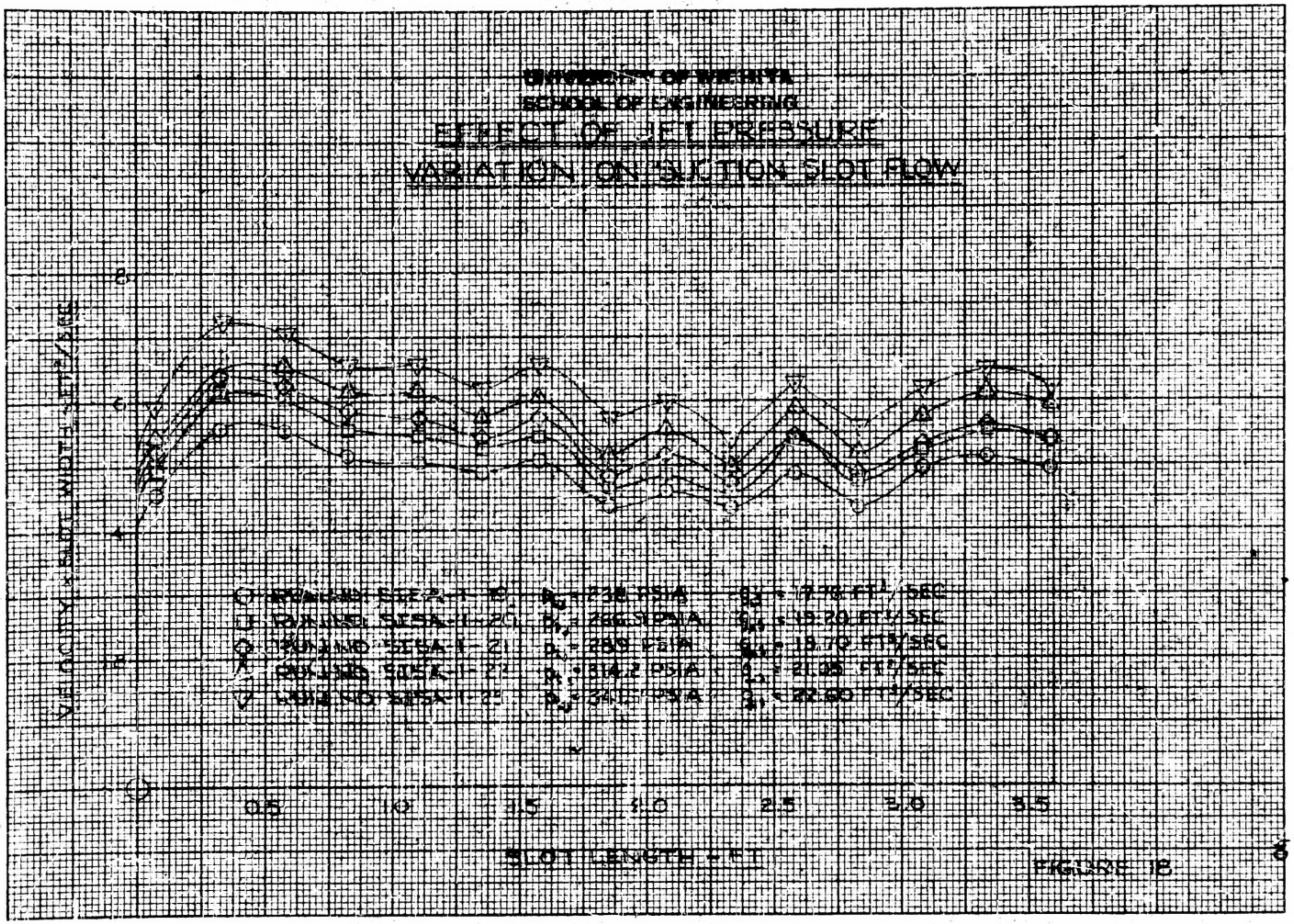

SCHOOL OF ENGINEERING
EFFECT OF JET PRESSURE
VARIATION ON SUCTION SLOT FLOW
VELOCITY x SLOT WIDTH - FT²/SEC
8
6
4
0.5
1.0
1.5
2.0
2.5
3.0
3.5
SLOT LENGTH - FT

FIGURE 18

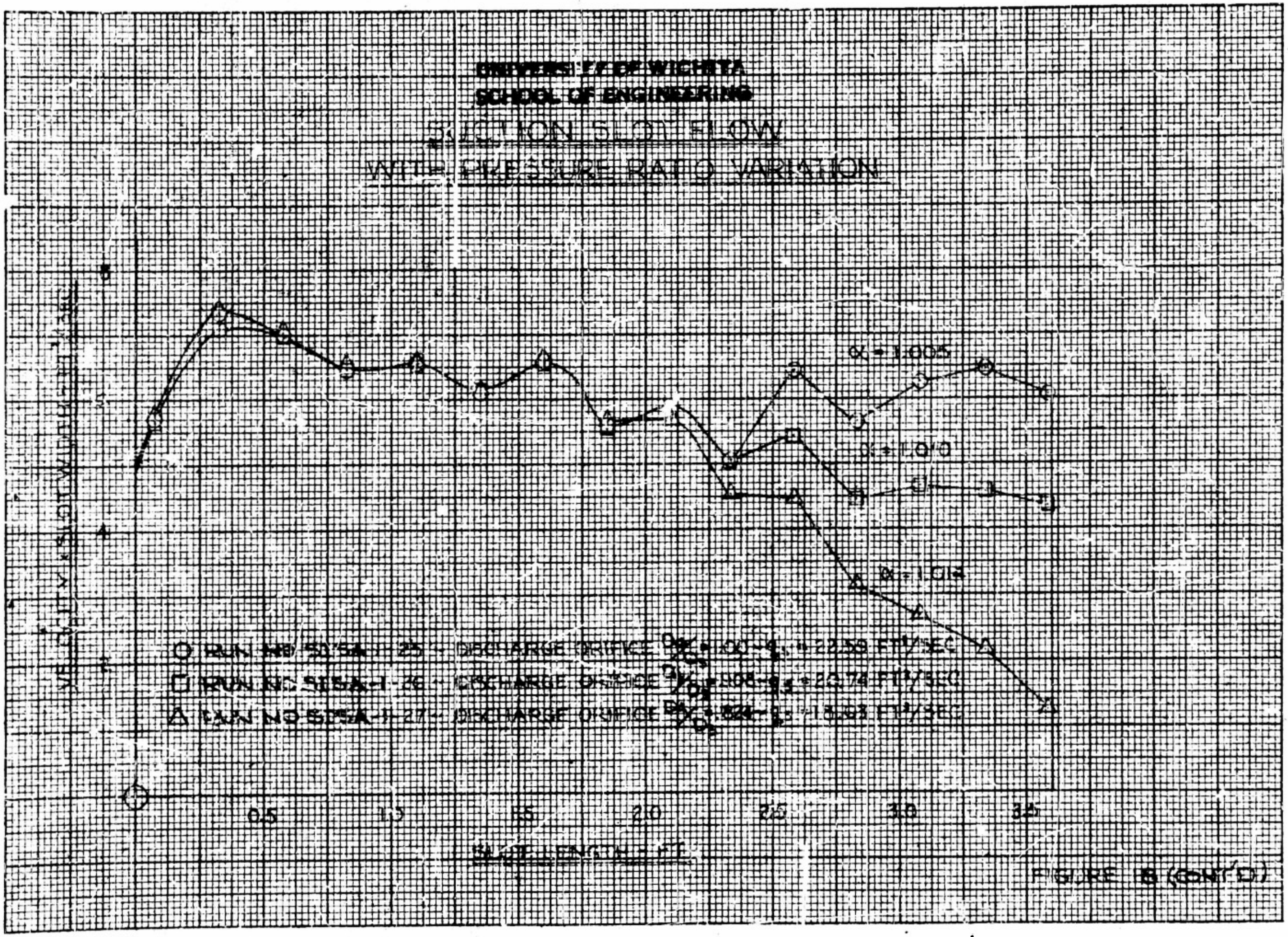

FIGURE 15 (CONT'D)

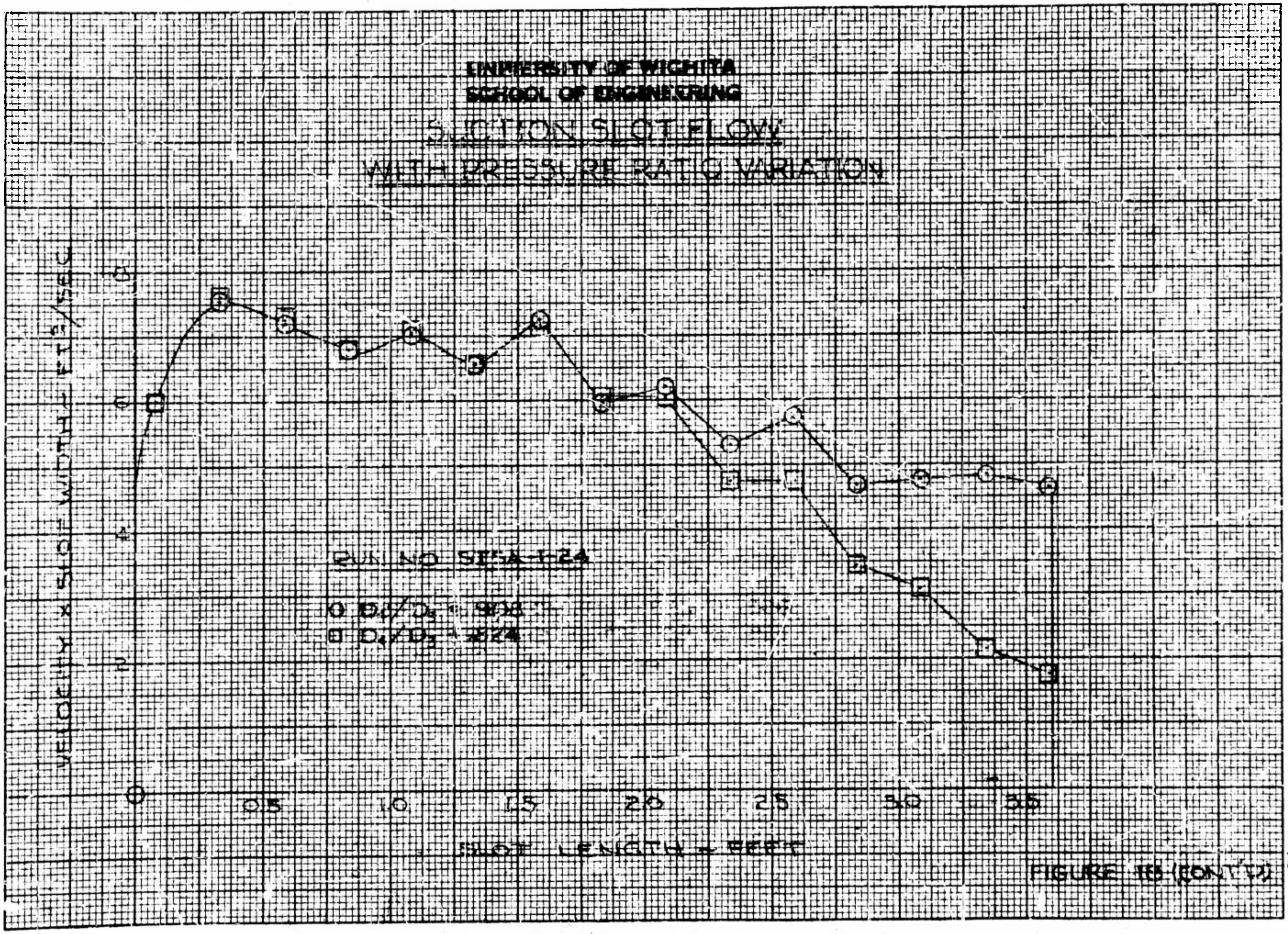

FIGURE 18 (CONT'D)

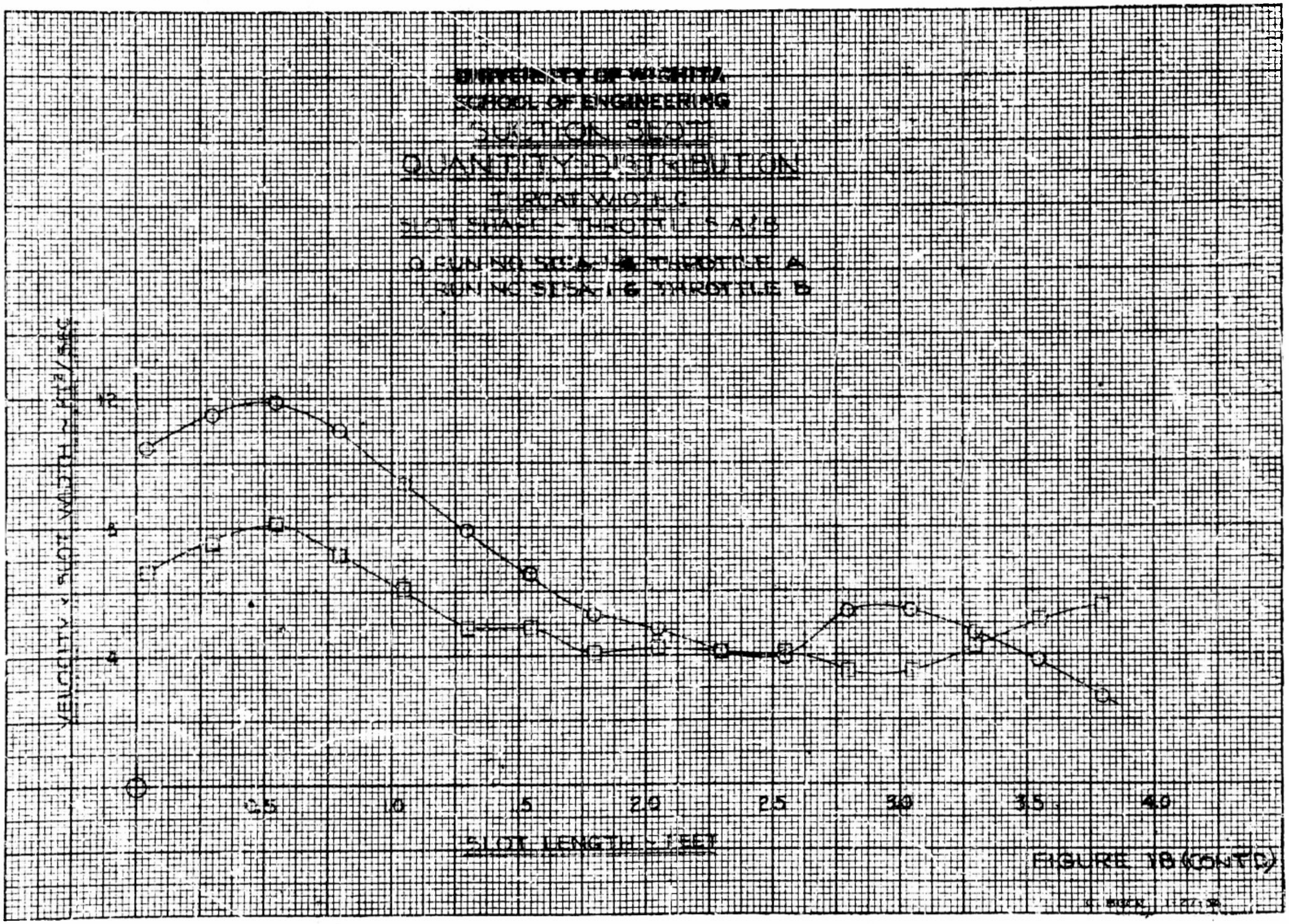

FIGURE 18 (CONT'D)

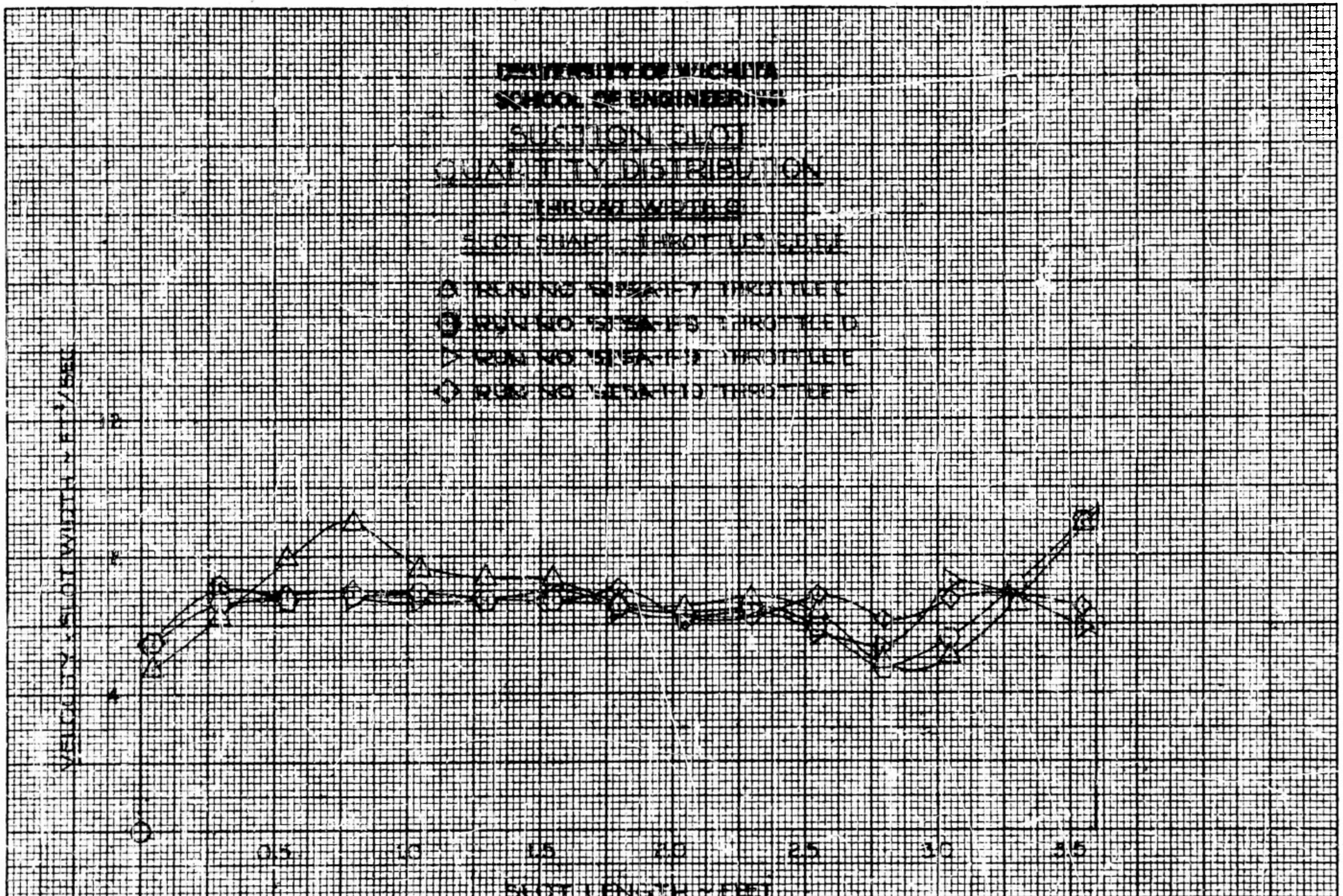

FIGURE 13 (CONT'D)

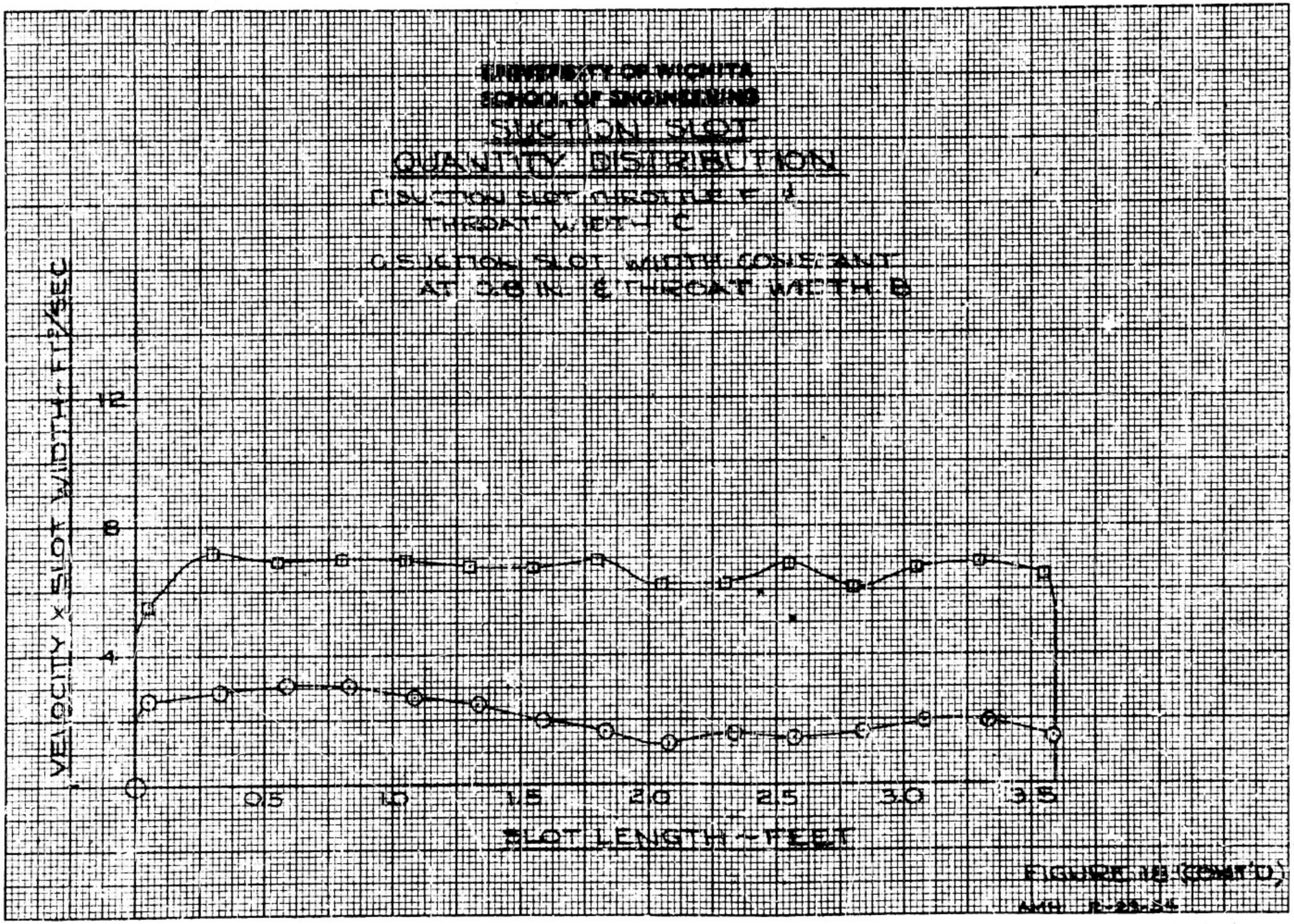

FIGURE [illegible] (CONT'D)

AMH [illegible]

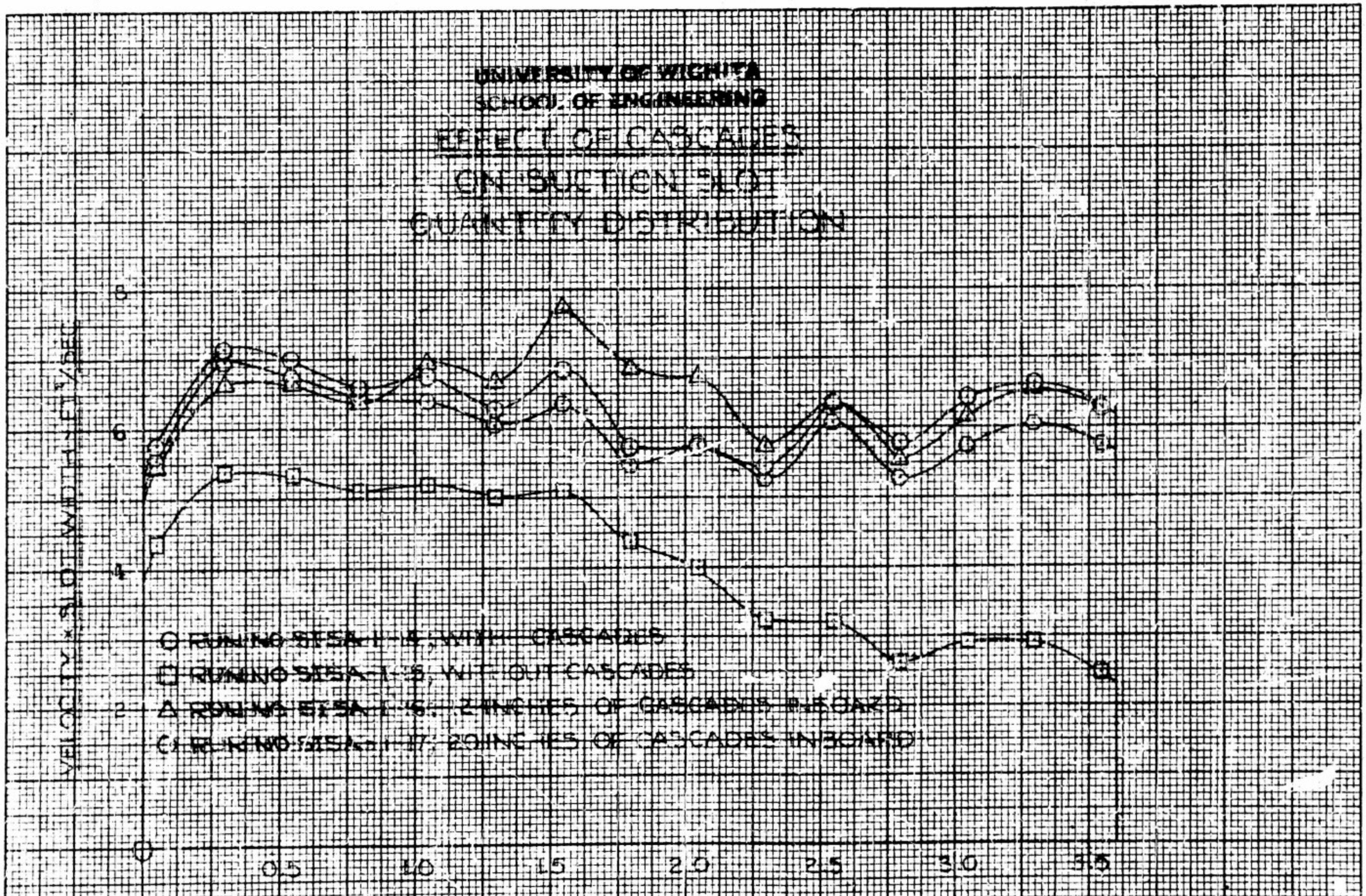

FIGURE 18 (CONC'D)

C. SECT. 2-1-58

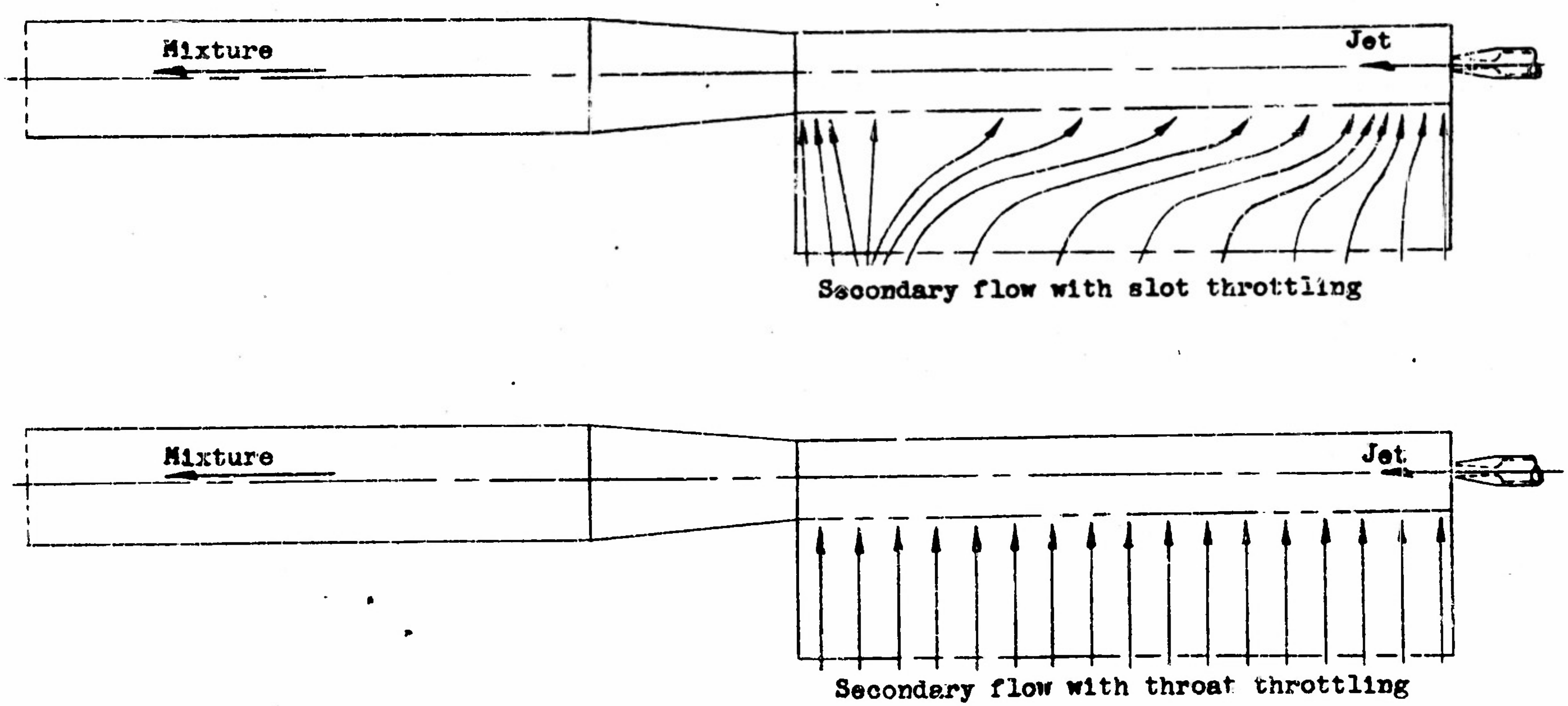

Figure 19.-- Suction-duct flow pattern with slot and throat throttling.

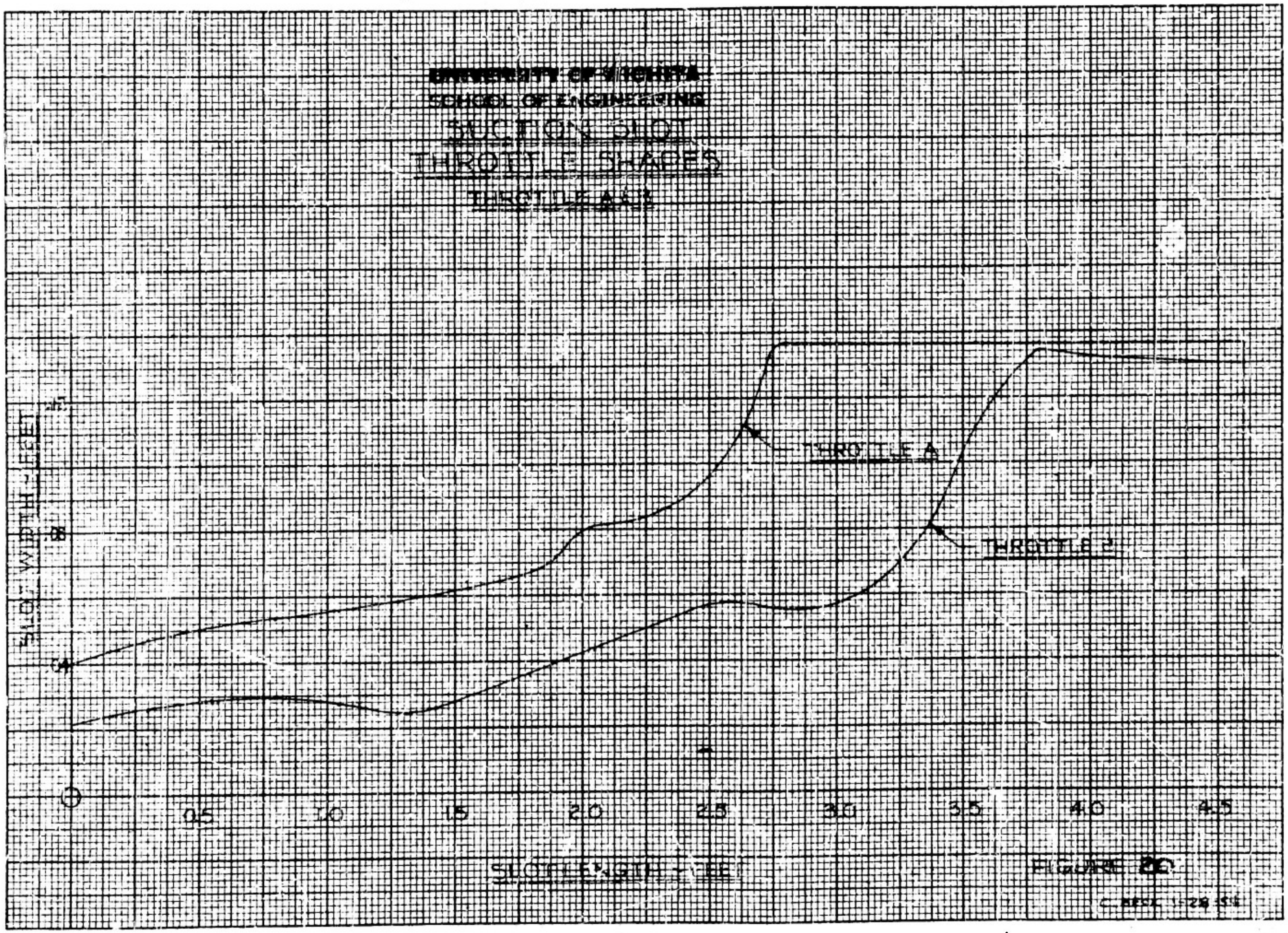
UNIVERSITY OF WICHITA
SCHOOL OF ENGINEERING
SUCTION SLOT
THROTTLE SHAPES
THROTTLE A & B
THROTTLE A
THROTTLE B
SLOT WIDTH - FEET
SLOT LENGTH - FEET
0
.04
.08
.12
0.5
1.0
1.5
2.0
2.5
3.0
3.5
4.0
4.5
C. BECK 1-28-55

FIGURE 20

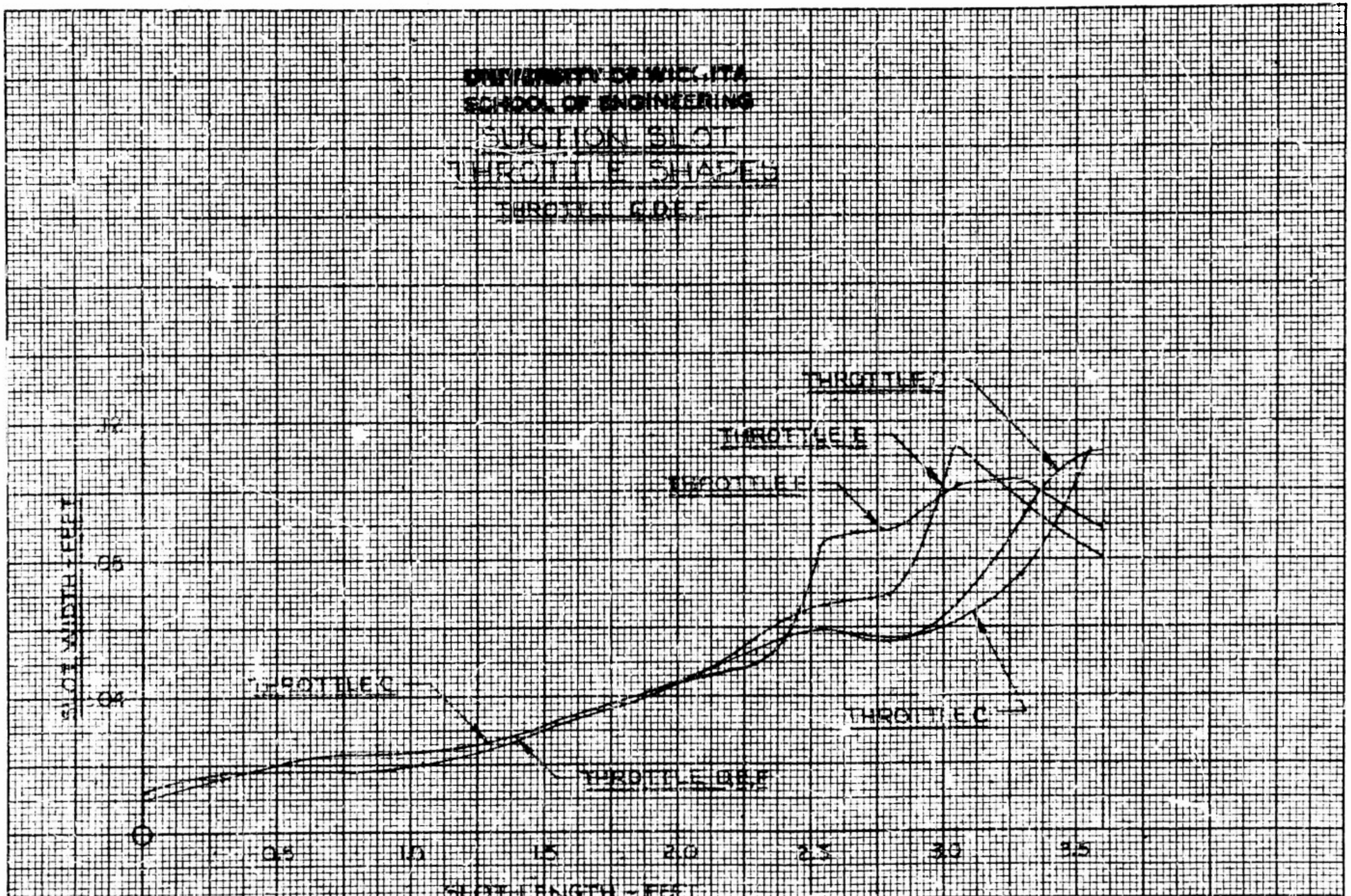

FIGURE 20 (CONC'D)

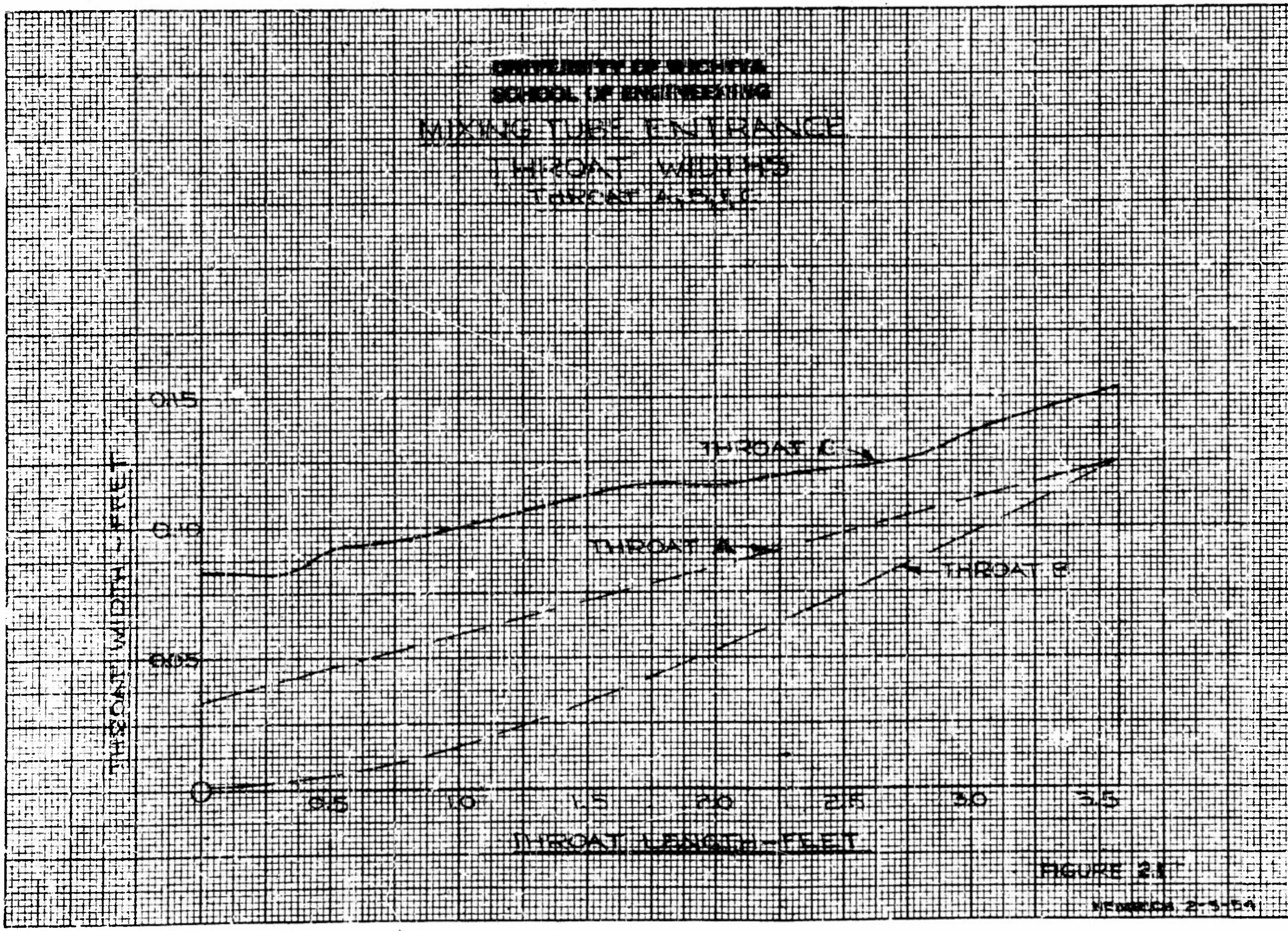
UNIVERSITY OF WICHITA
SCHOOL OF ENGINEERING
MIXING TUBE ENTRANCE
THROAT WIDTHS
THROAT A, B, & C
0.15
0.10
0.05
0
0.5
1.0
1.5
2.0
2.5
3.0
3.5
THROAT C
THROAT A
THROAT B
THROAT WIDTH - FEET
THROAT LENGTH - FEET

FIGURE 2.1

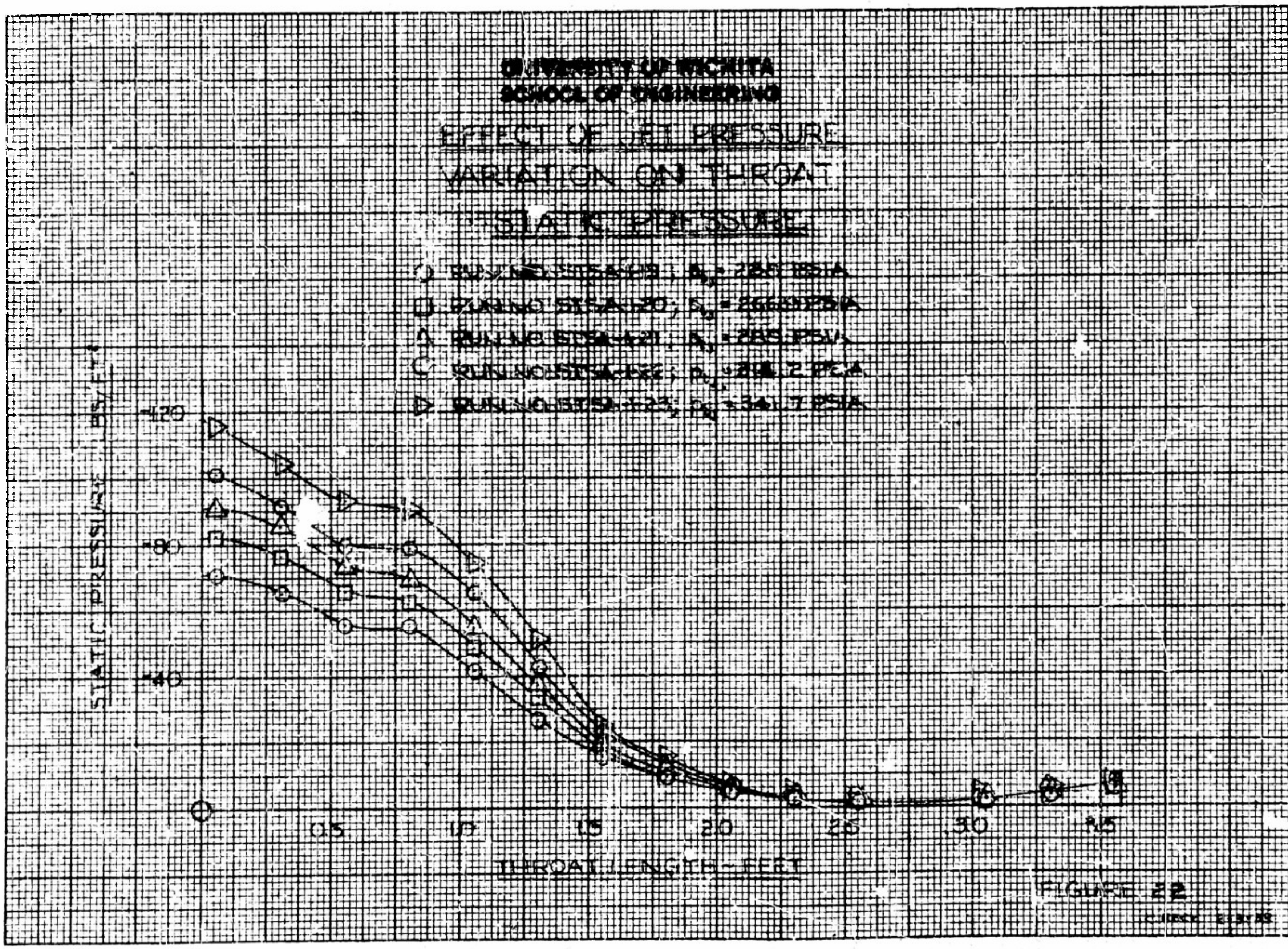
UNIVERSITY OF WICHITA
SCHOOL OF ENGINEERING
EFFECT OF JET PRESSURE
VARIATION ON THROAT
STATIC PRESSURE
STATIC PRESSURE
120
80
40
0.5
1.0
1.5
2.0
2.5
3.0
3.5
THROAT LENGTH - FEET

FIGURE 22

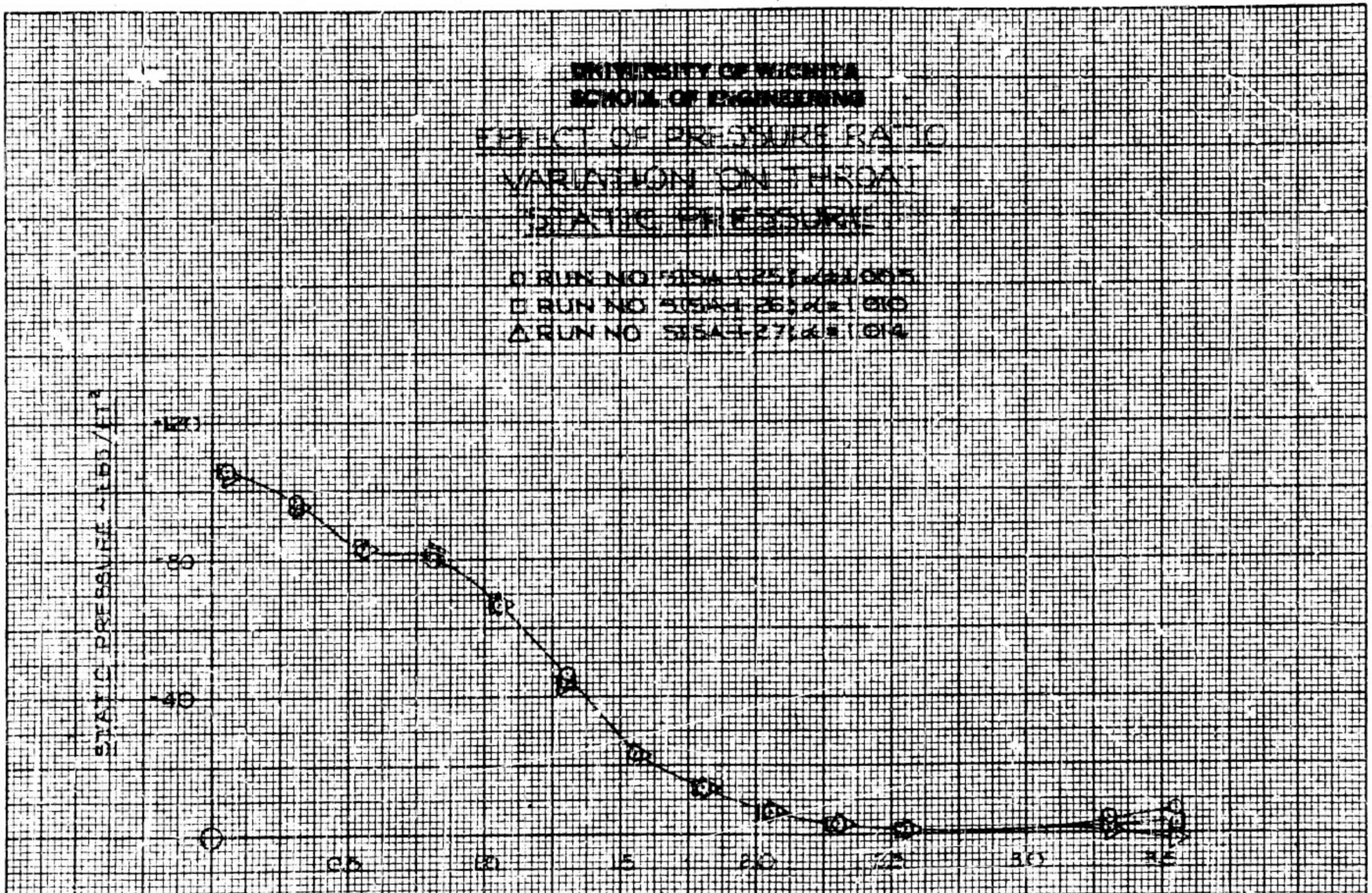

FIGURE 22 (CONC'D)

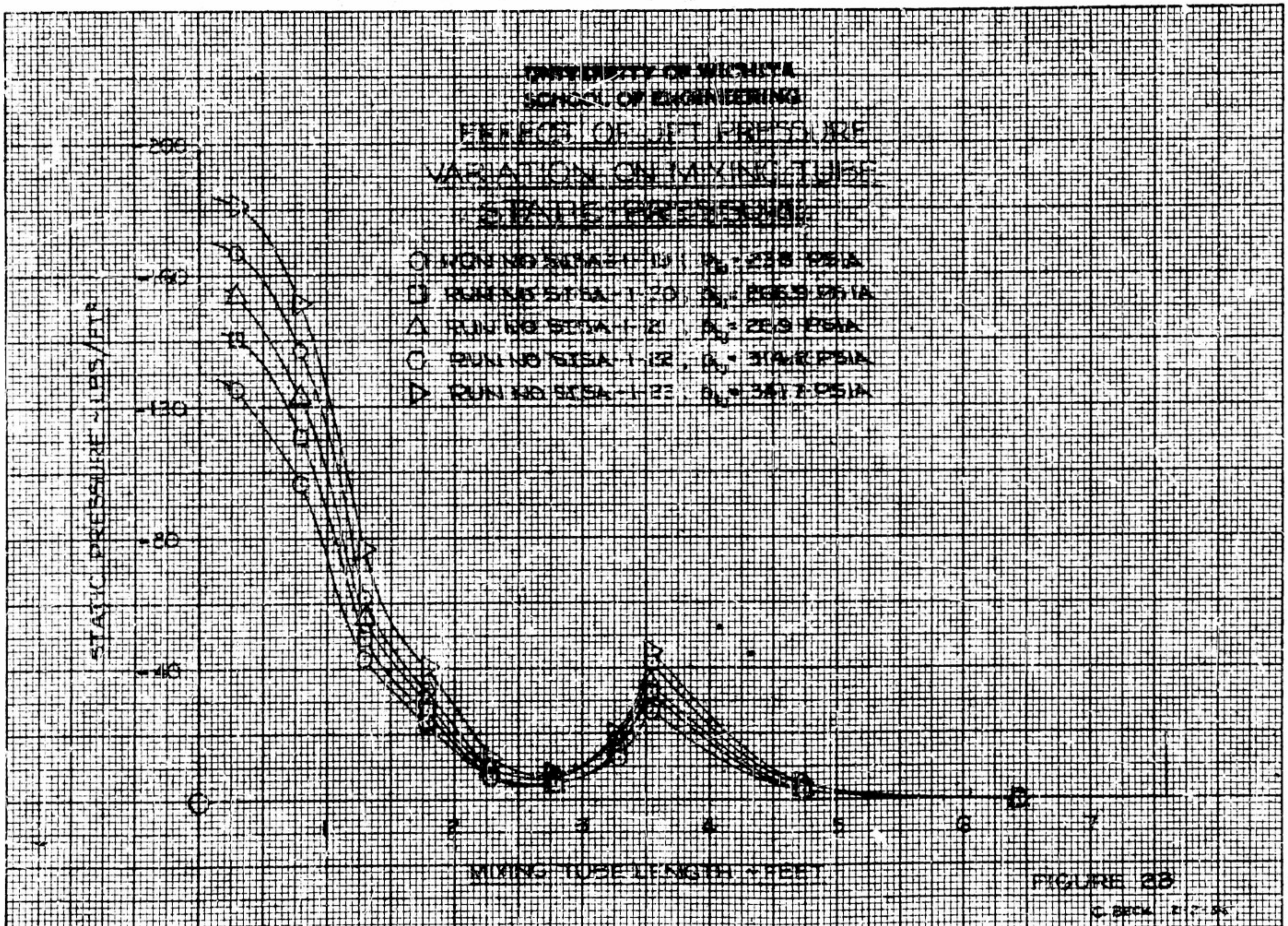
UNIVERSITY OF WICHITA
SCHOOL OF ENGINEERING
EFFECT OF JET PRESSURE
VARIATION ON MIXING TUBE
STATIC PRESSURE
STATIC PRESSURE ~ LBS/FT²
-200
-160
-120
-80
-40
1
2
3
4
5
6
7
MIXING TUBE LENGTH ~ FEET
C. BECK

FIGURE 28

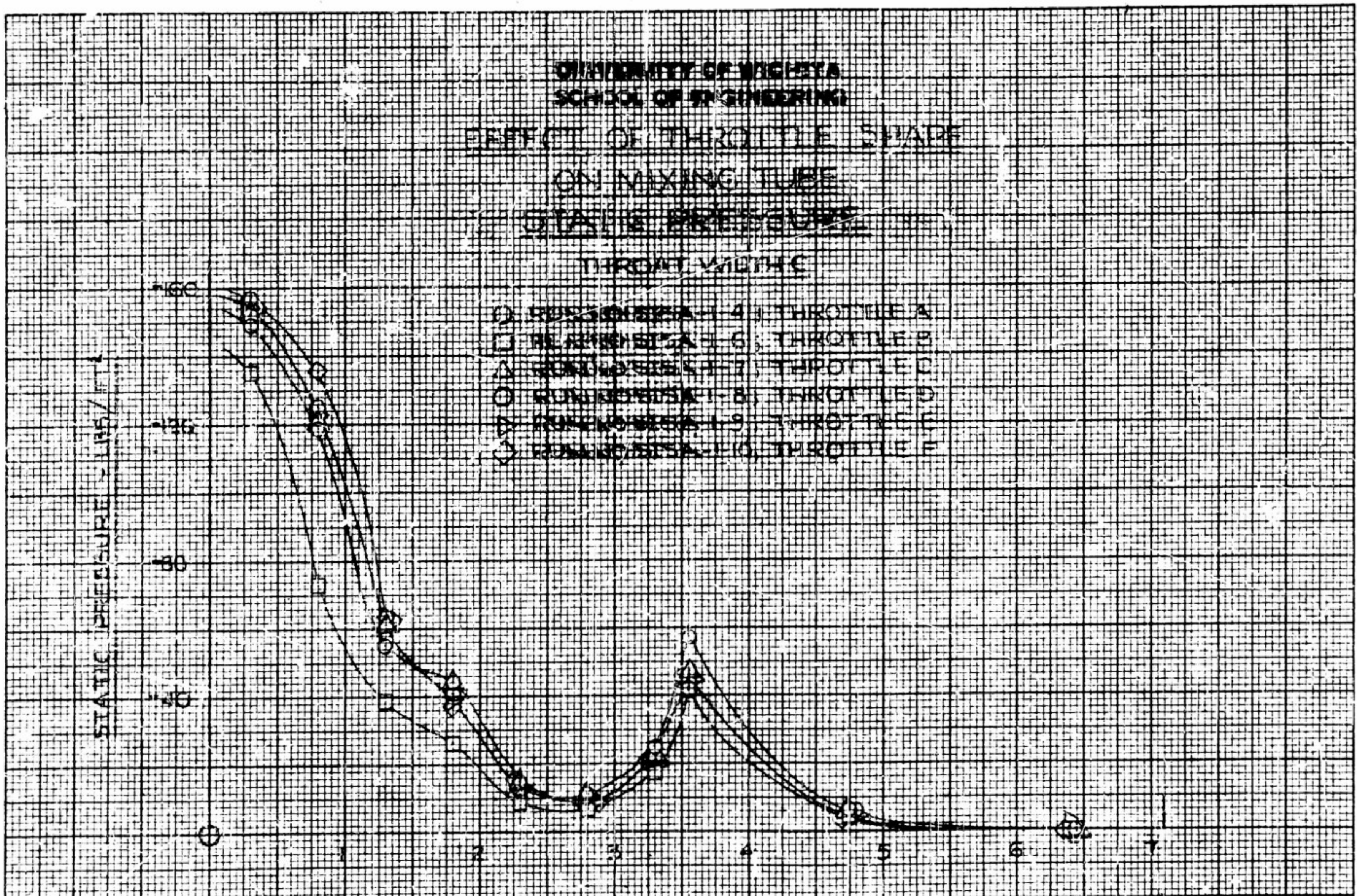

FIGURE 23 (CONC'D)

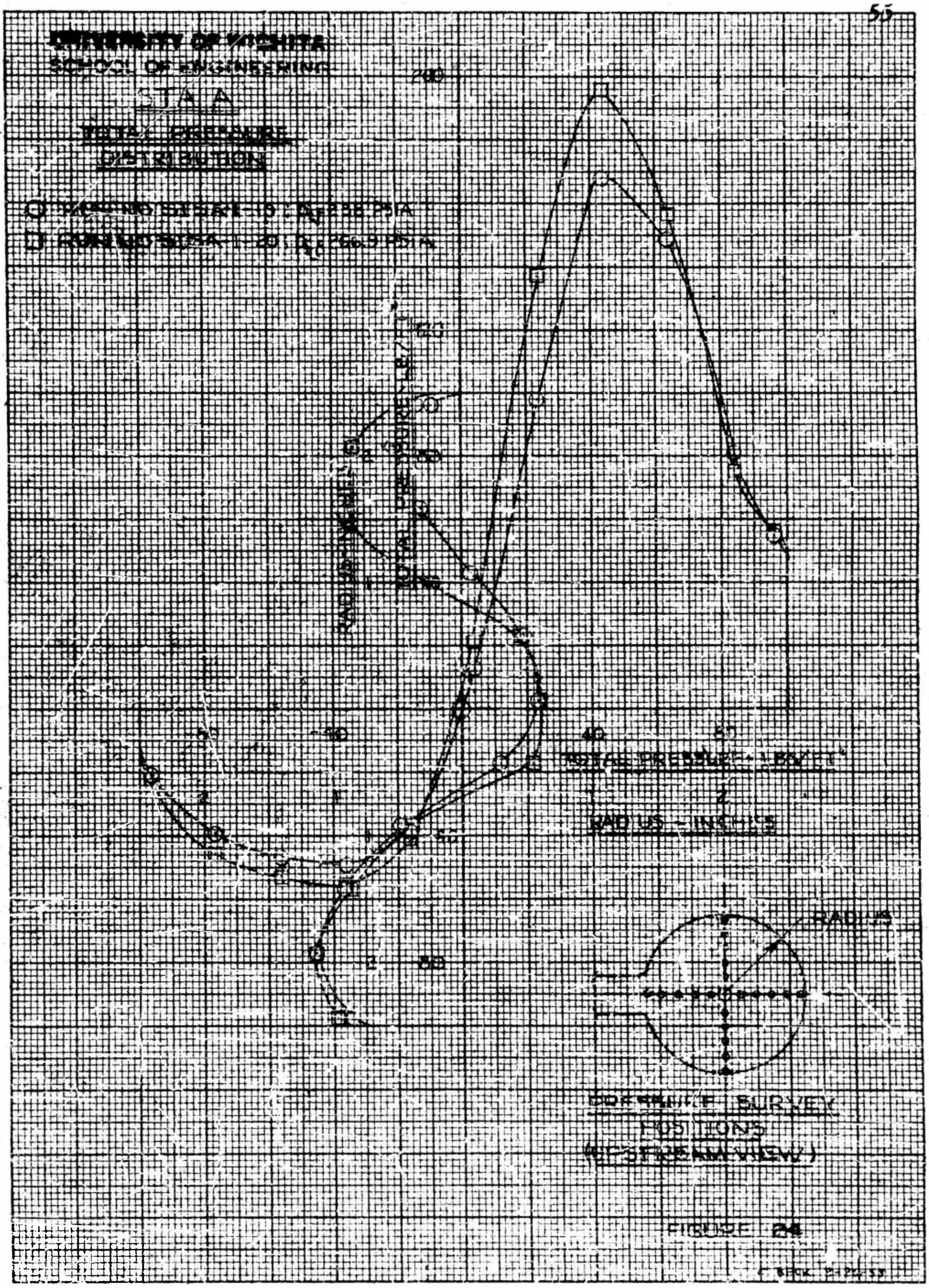
UNIVERSITY OF WICHITA
SCHOOL OF ENGINEERING
STA A
TOTAL PRESSURE
DISTRIBUTION
200
120
40
50
TOTAL PRESSURE - LB/FT²
RADIUS - INCHES
RADIUS
PRESSURE SURVEY
POSITIONS
(UPSTREAM VIEW)
FIGURE 24

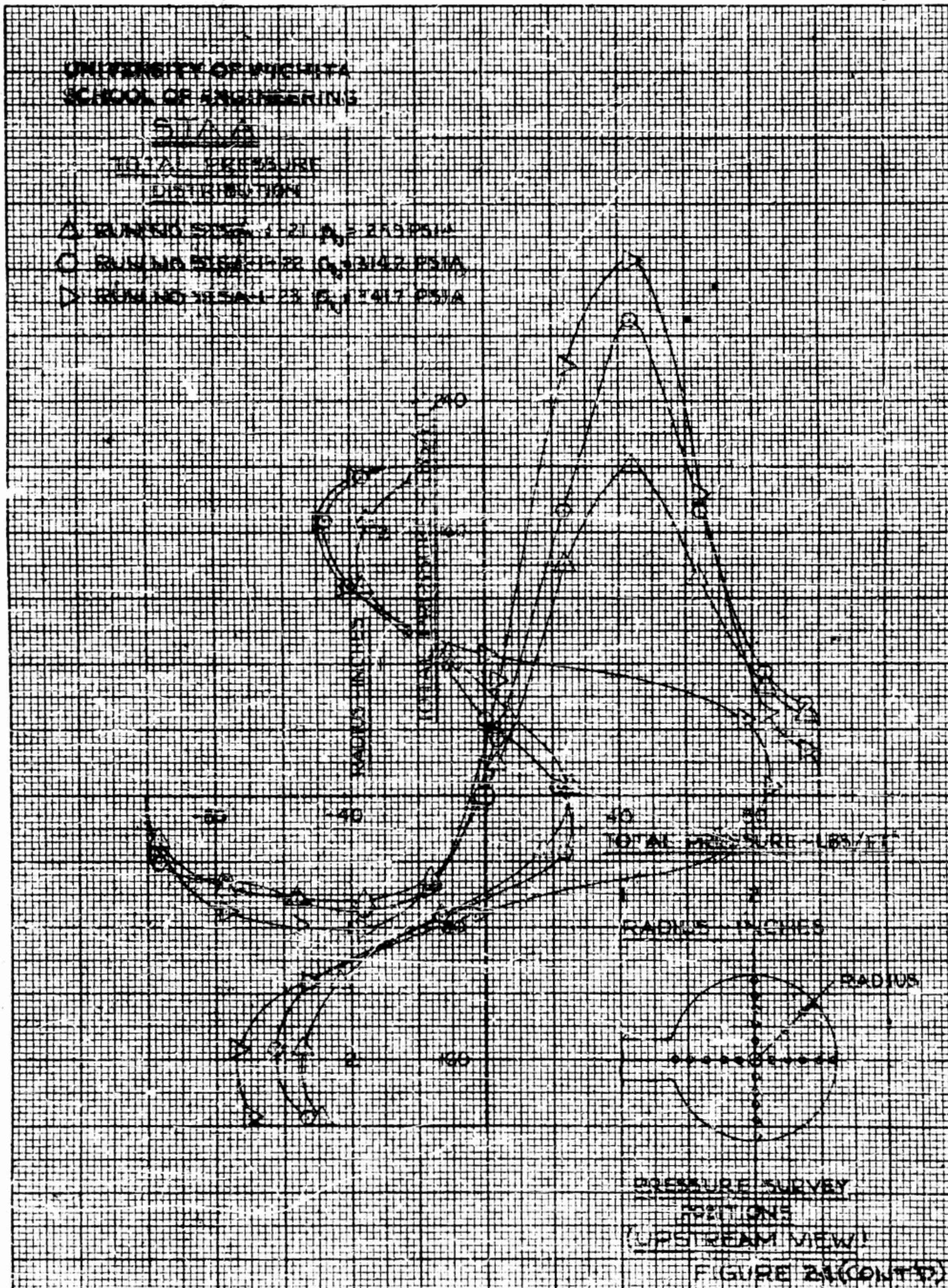

FIGURE 21 (CONT'D)

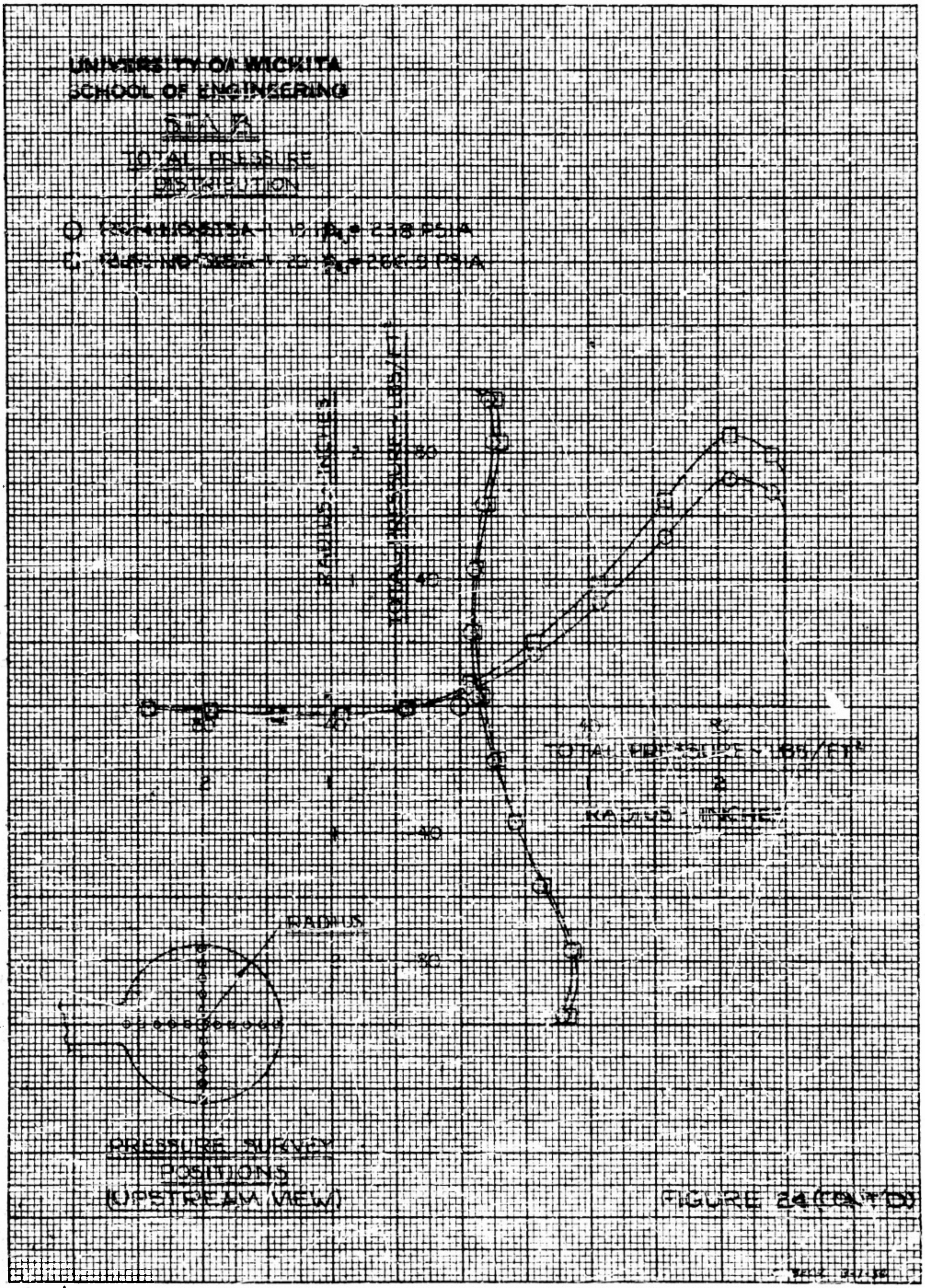

FIGURE 24 (CON'T'D)

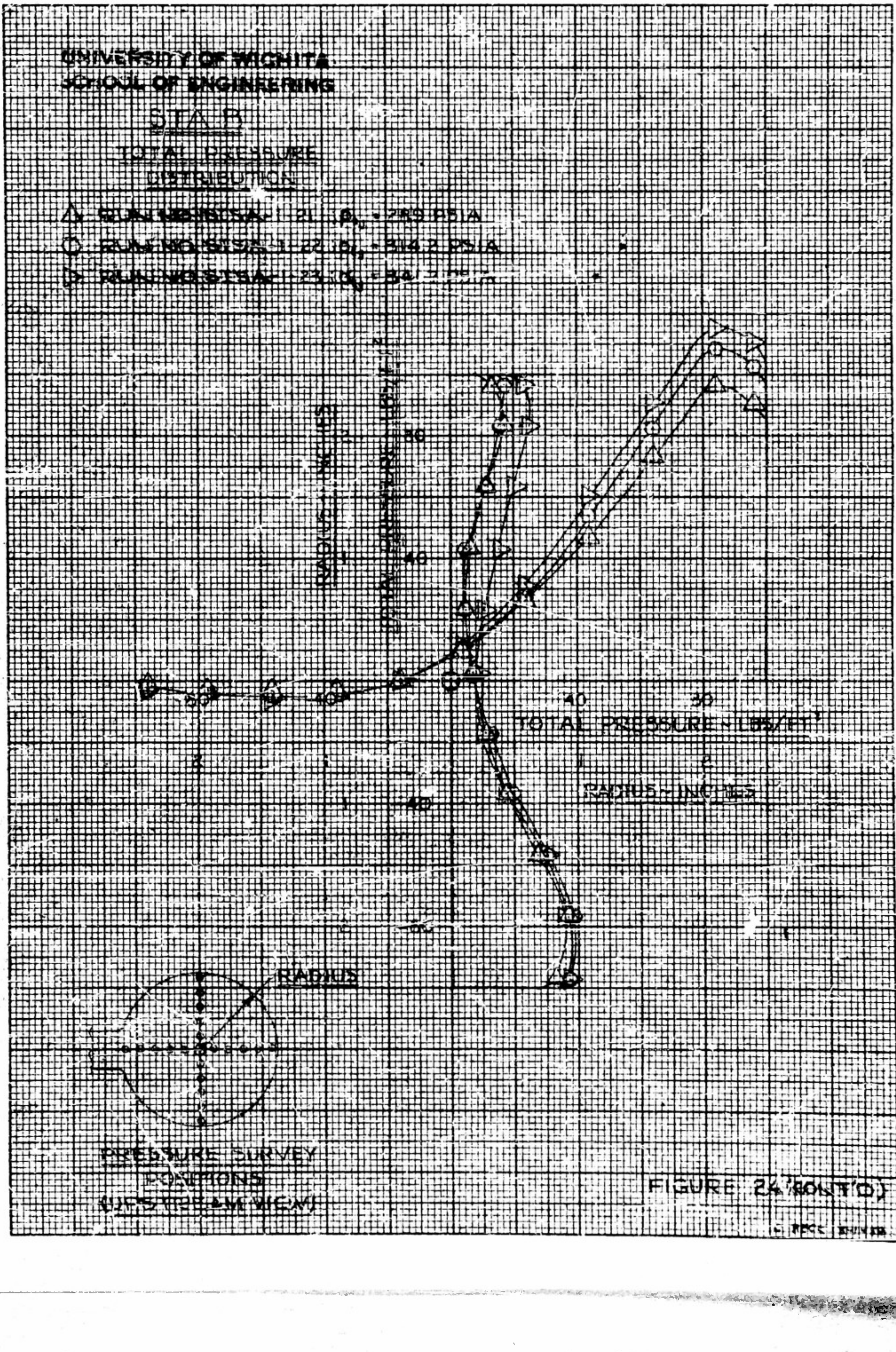

FIGURE 24 (CONT'D)

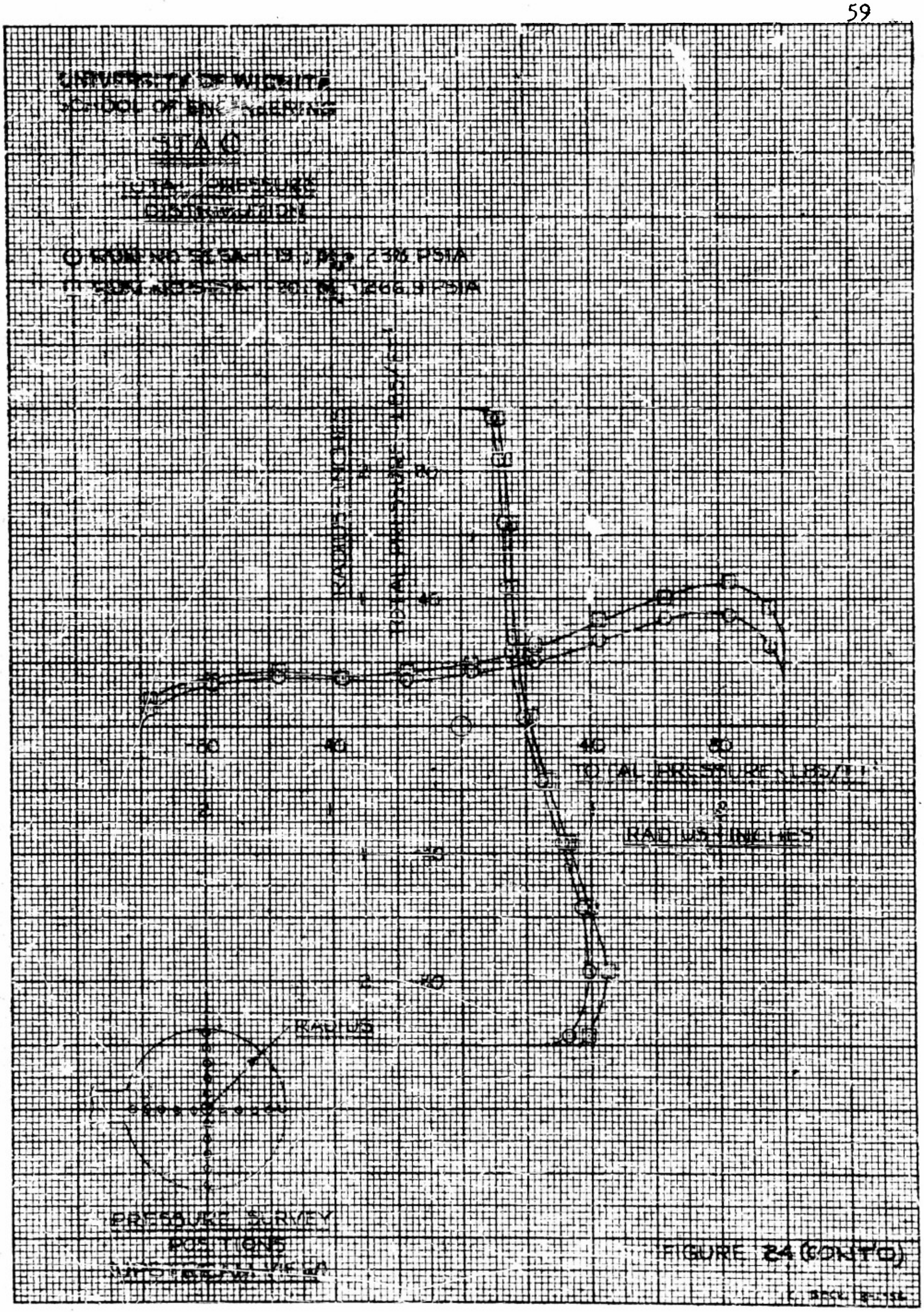

FIGURE 24 (CONT'D)

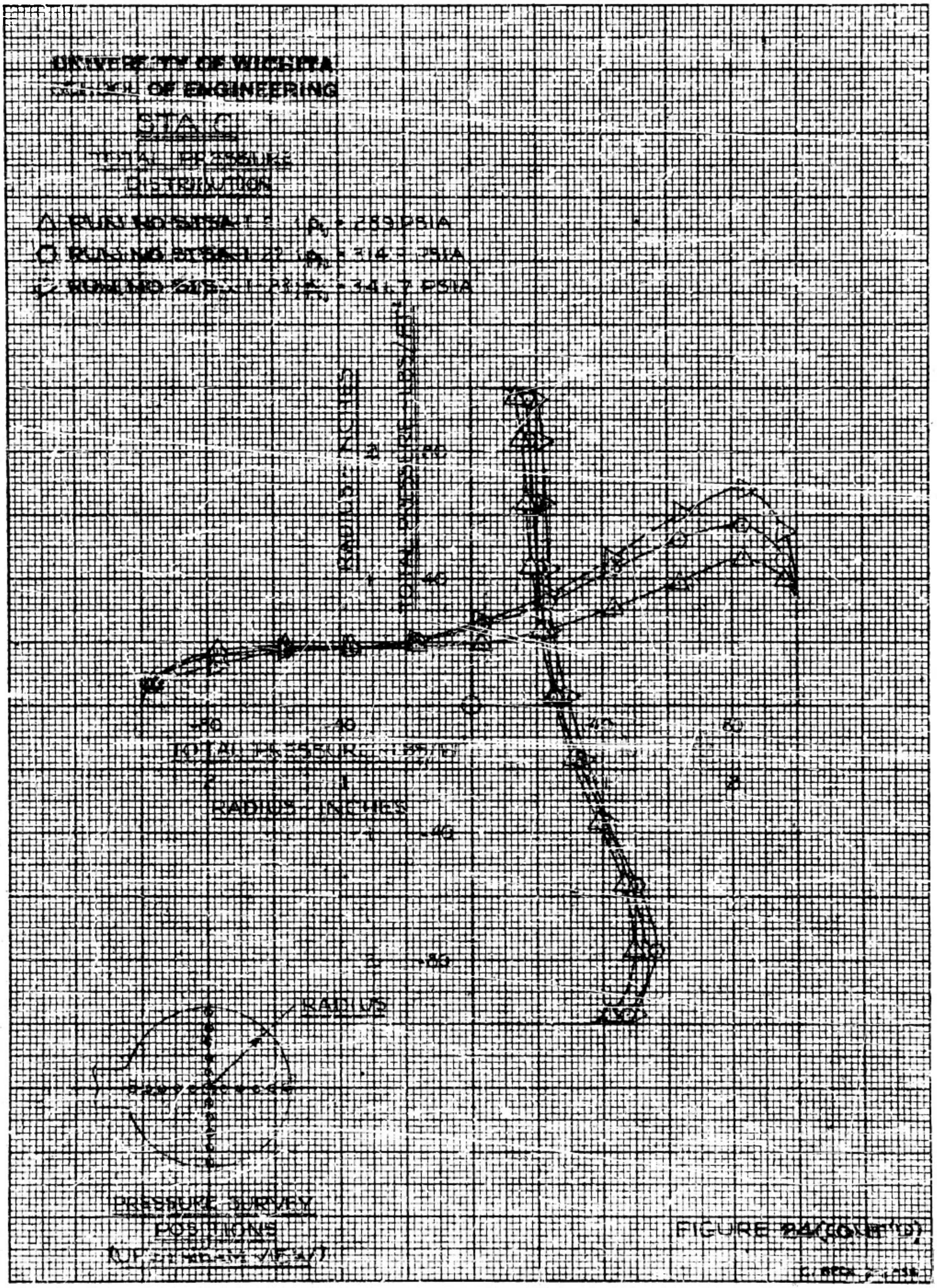

FIGURE 24(CONT'D)

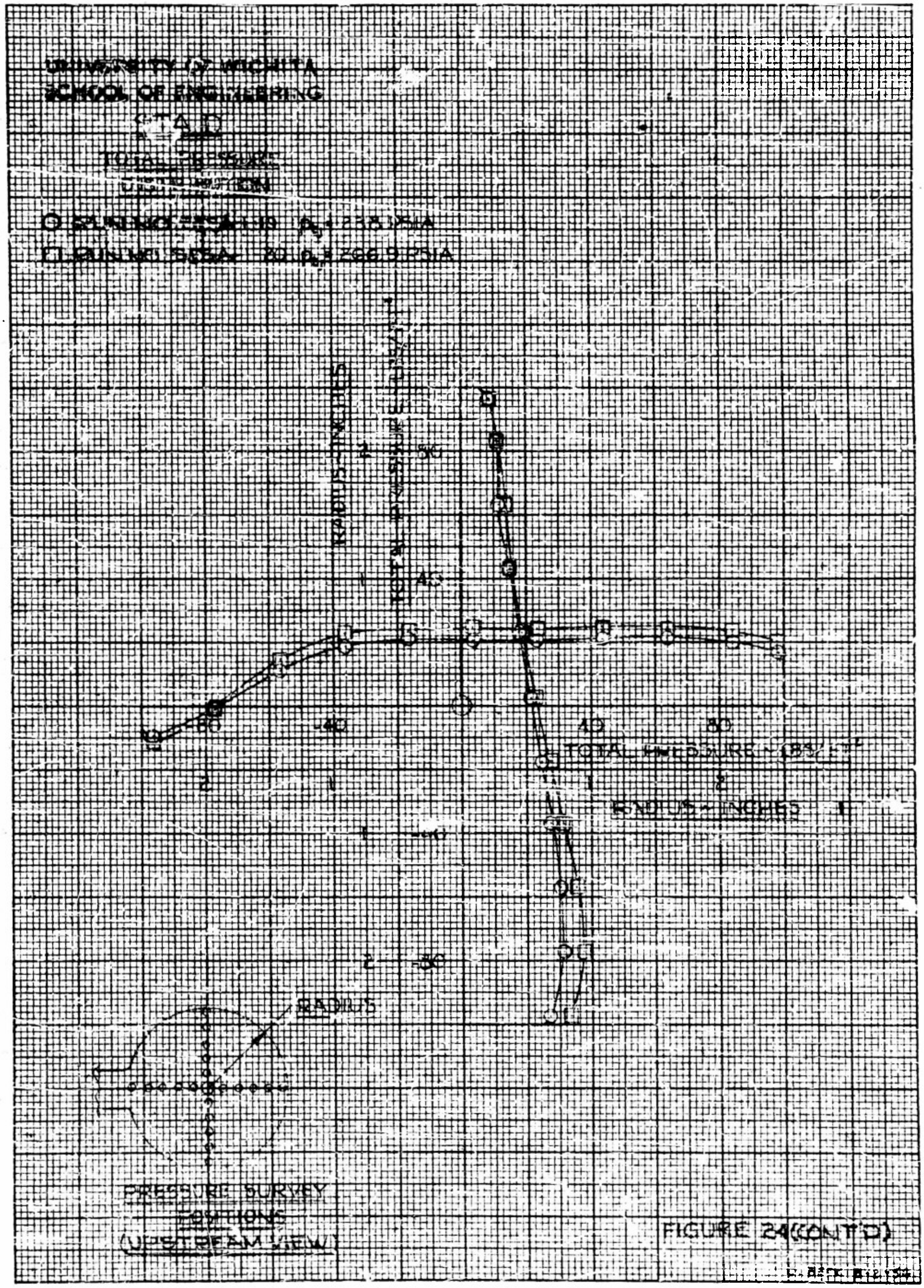

FIGURE 24 (CONT'D)

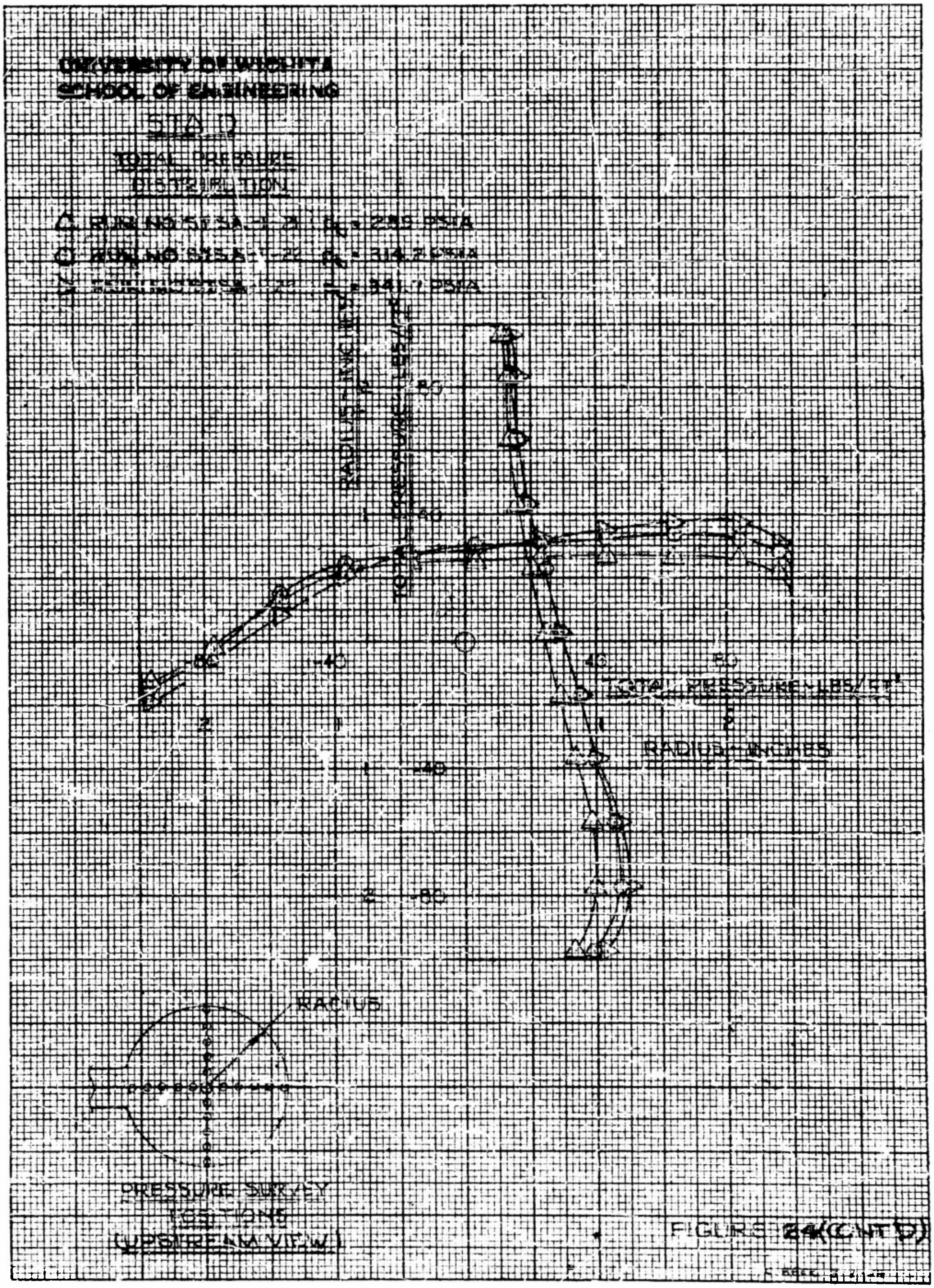

FIGURE 24(CONT'D)

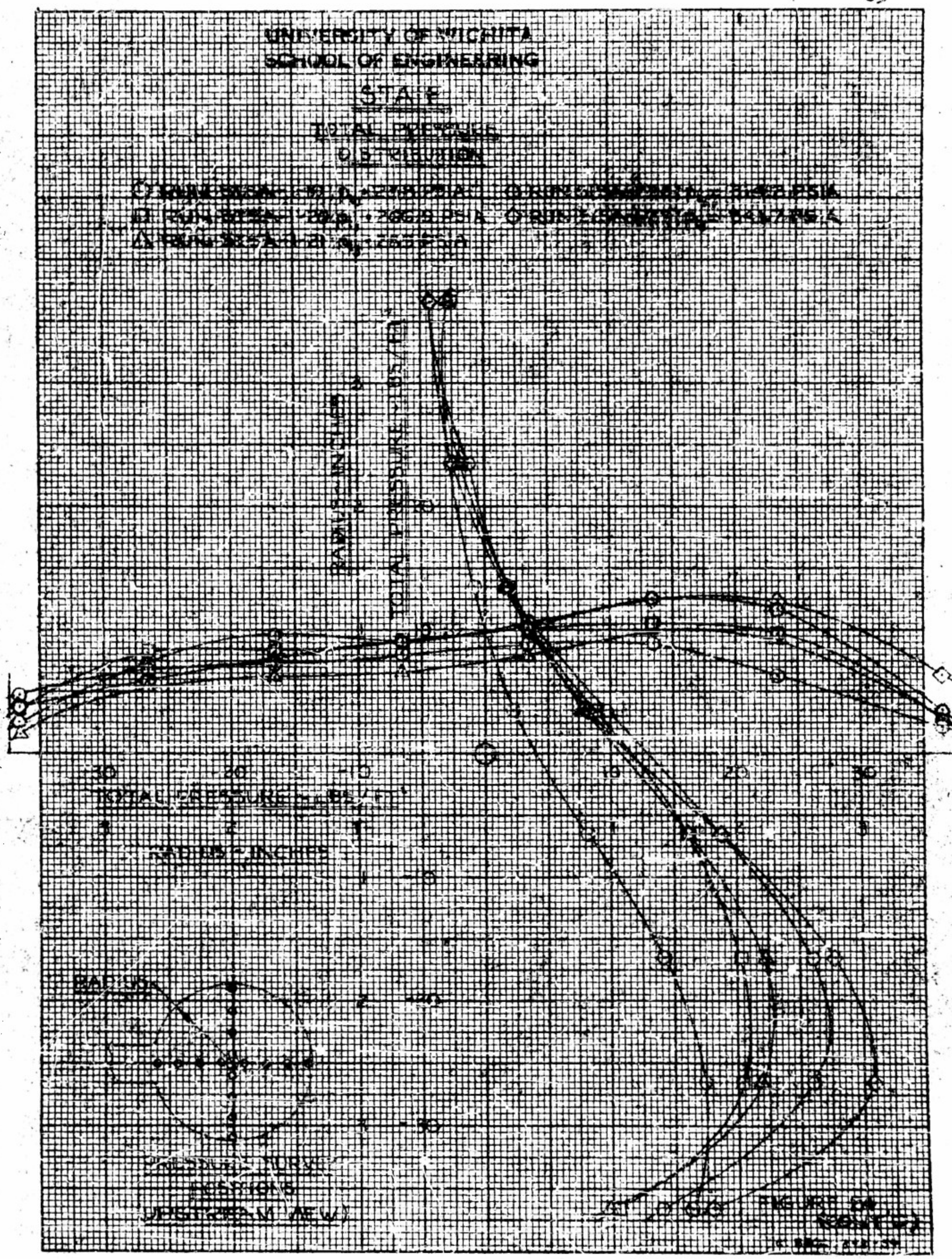
UNIVERSITY OF WICHITA
SCHOOL OF ENGINEERING
STATE
TOTAL PRESSURE
DISTRIBUTION
TOTAL PRESSURE ~ LBS./FT.²
RADIUS ~ INCHES
-30
-20
-10
10
20
30
RADIUS
PRESSURE SURVEY
POSITIONS
UPSTREAM VIEW
FIGURE

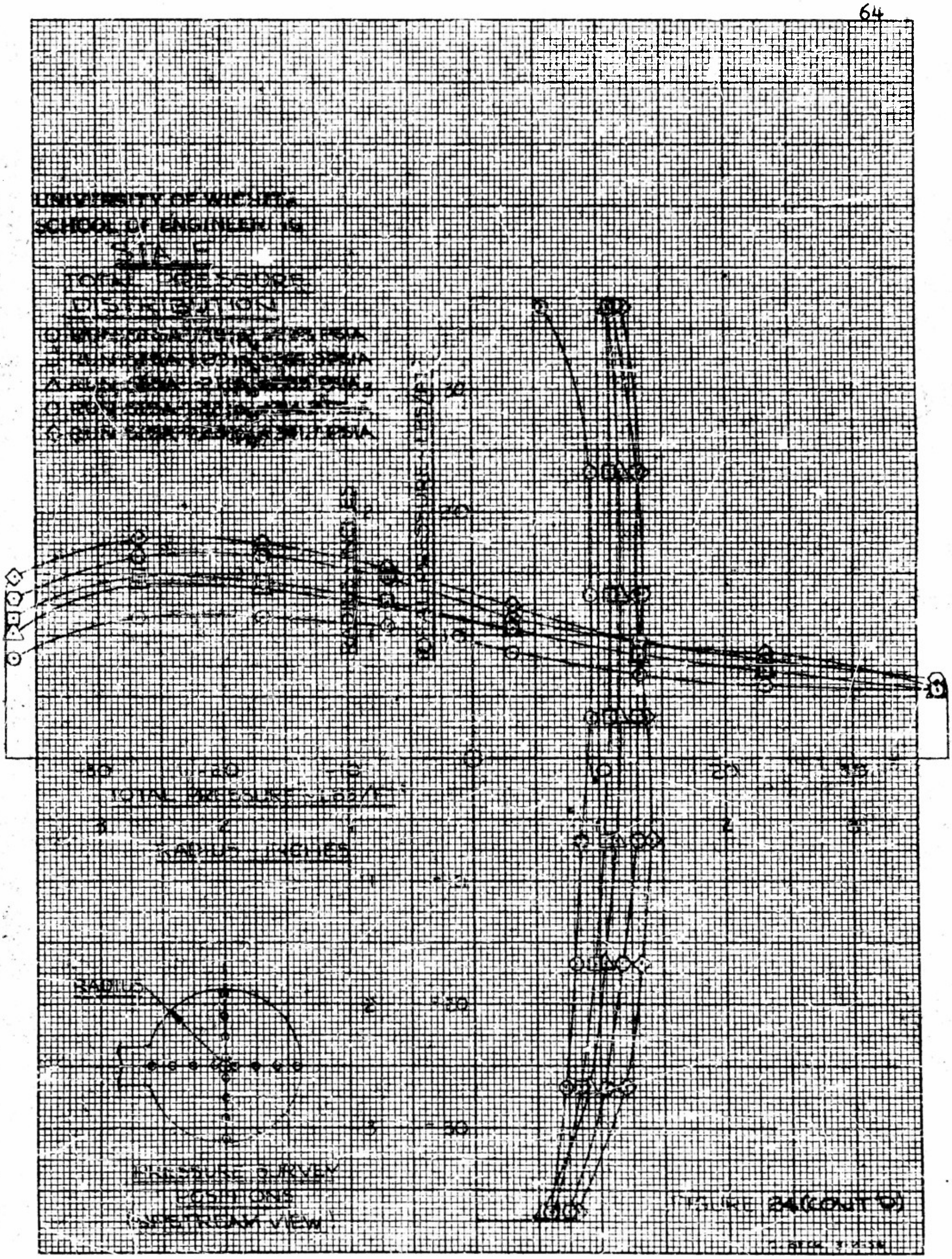

FIGURE 34 (CONT'D)

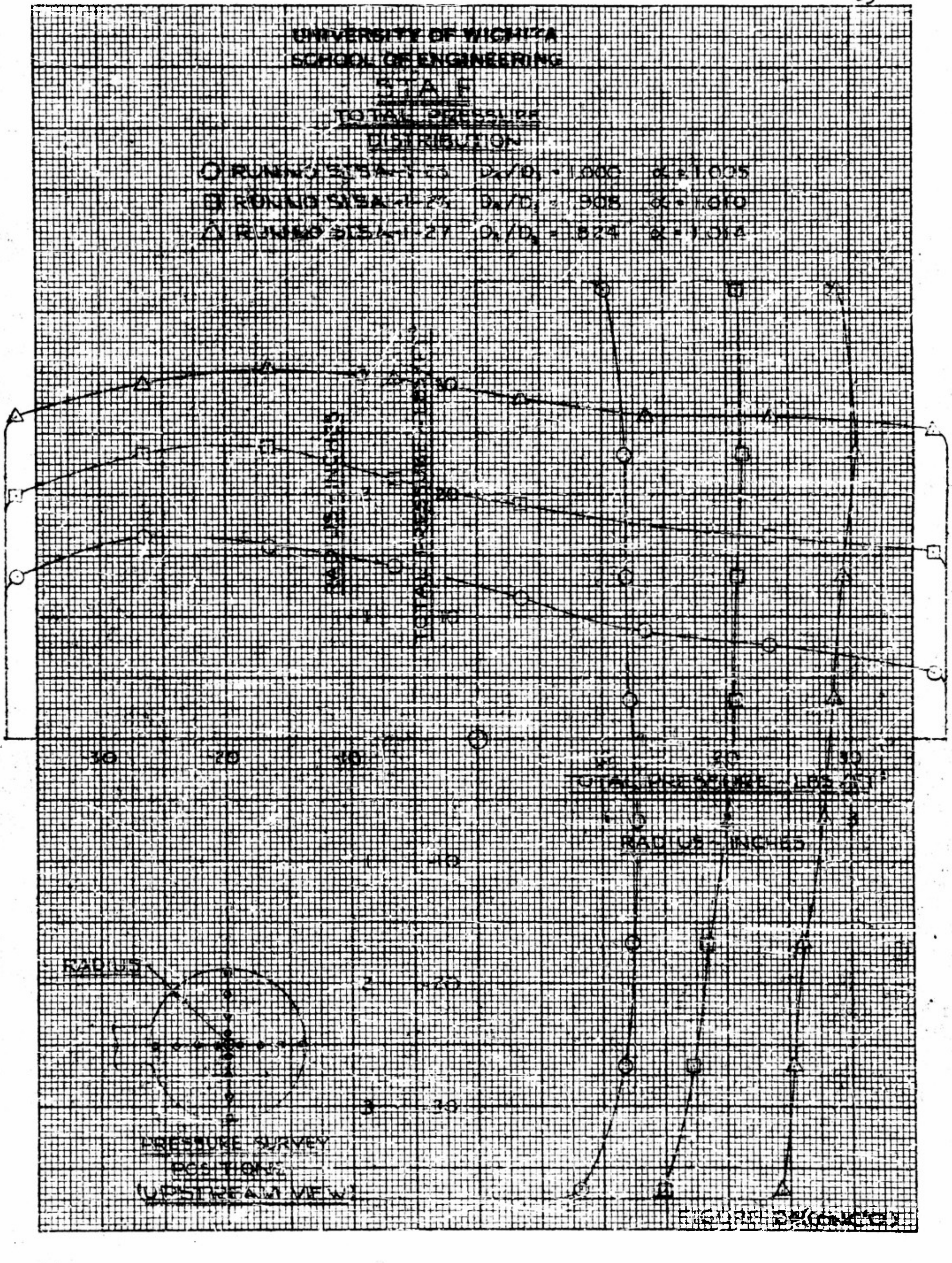

FIGURE 2 (CONT'D)

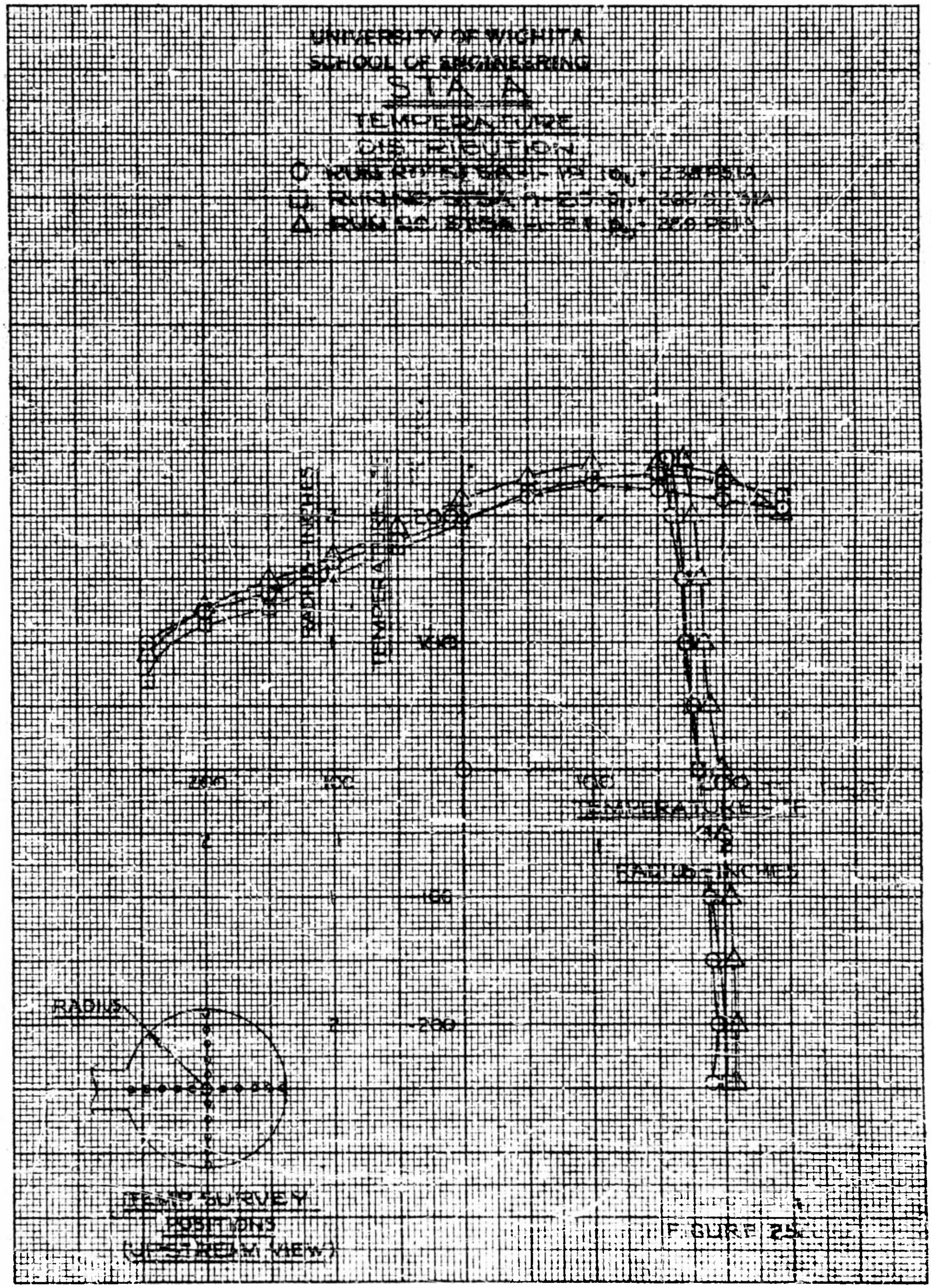
UNIVERSITY OF WICHITA
SCHOOL OF ENGINEERING
STA. A
TEMPERATURE
DISTRIBUTION
RADIUS - INCHES
TEMPERATURE - °F
200
100
100
200
TEMPERATURE - °F
RADIUS - INCHES
100
200
RADIUS
TEMP SURVEY
POSITIONS
(UPSTREAM VIEW)

FIGURE 25

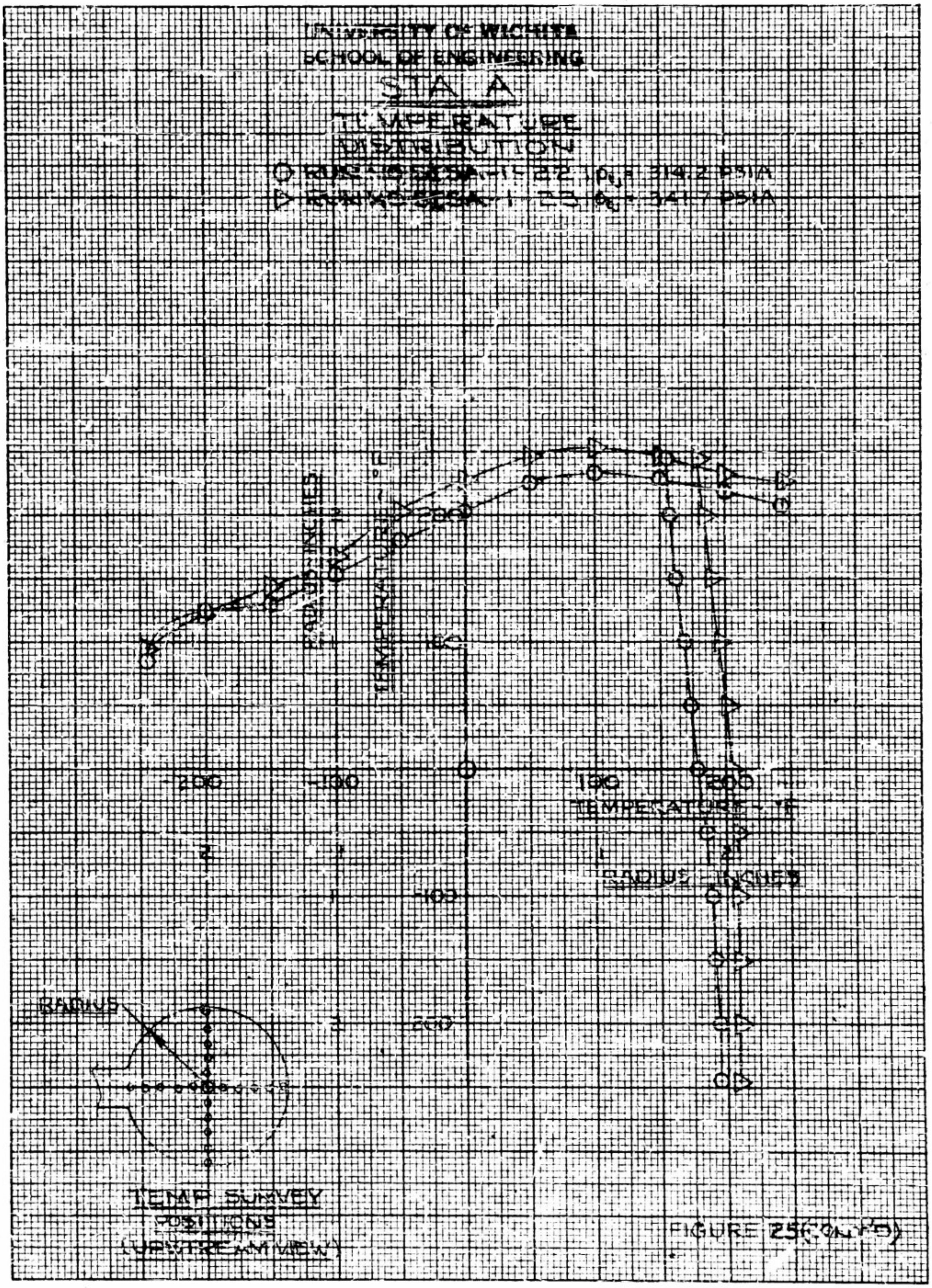

FIGURE 25(CONT'D)

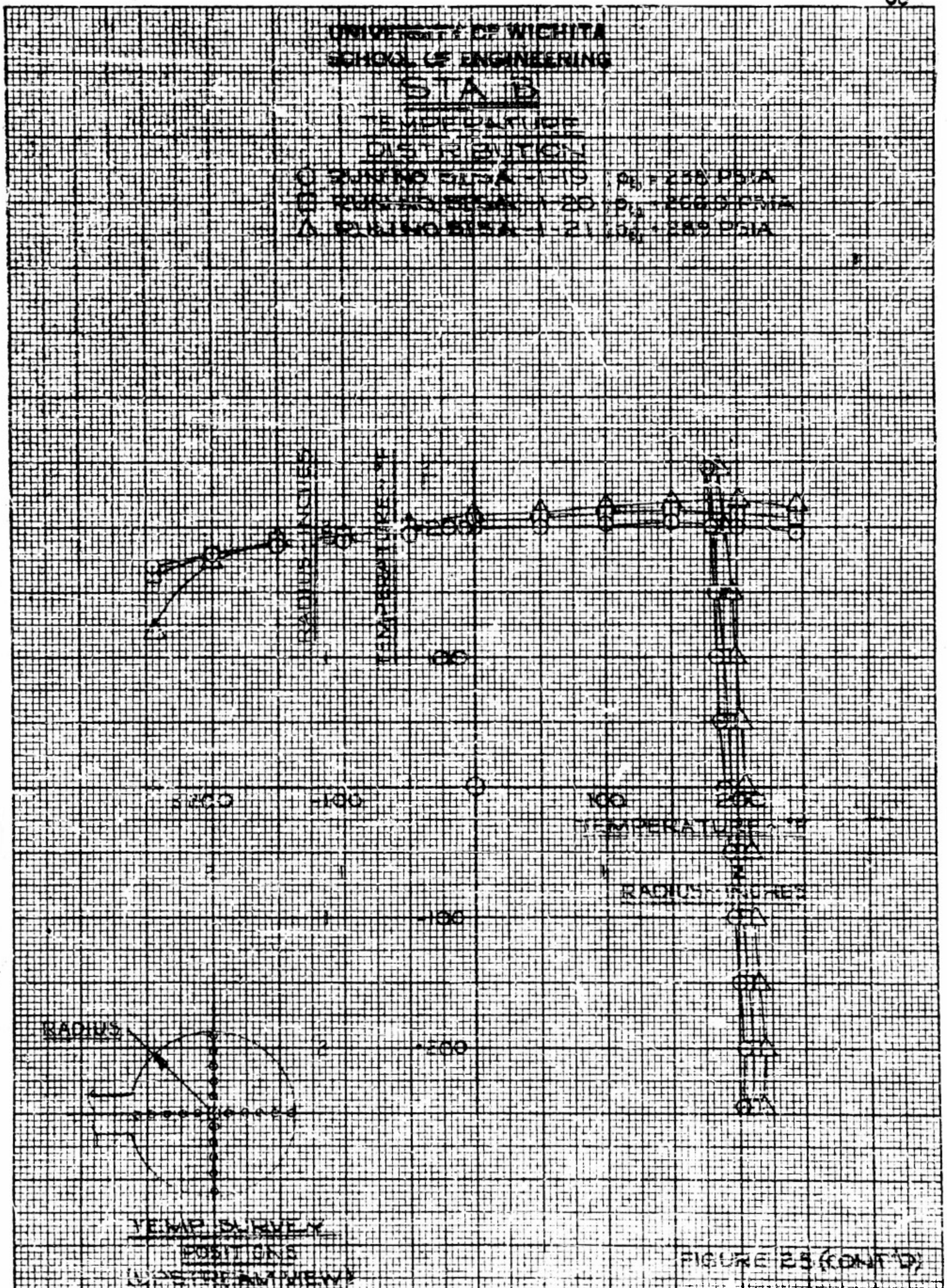

FIGURE 25 (CONT'D)

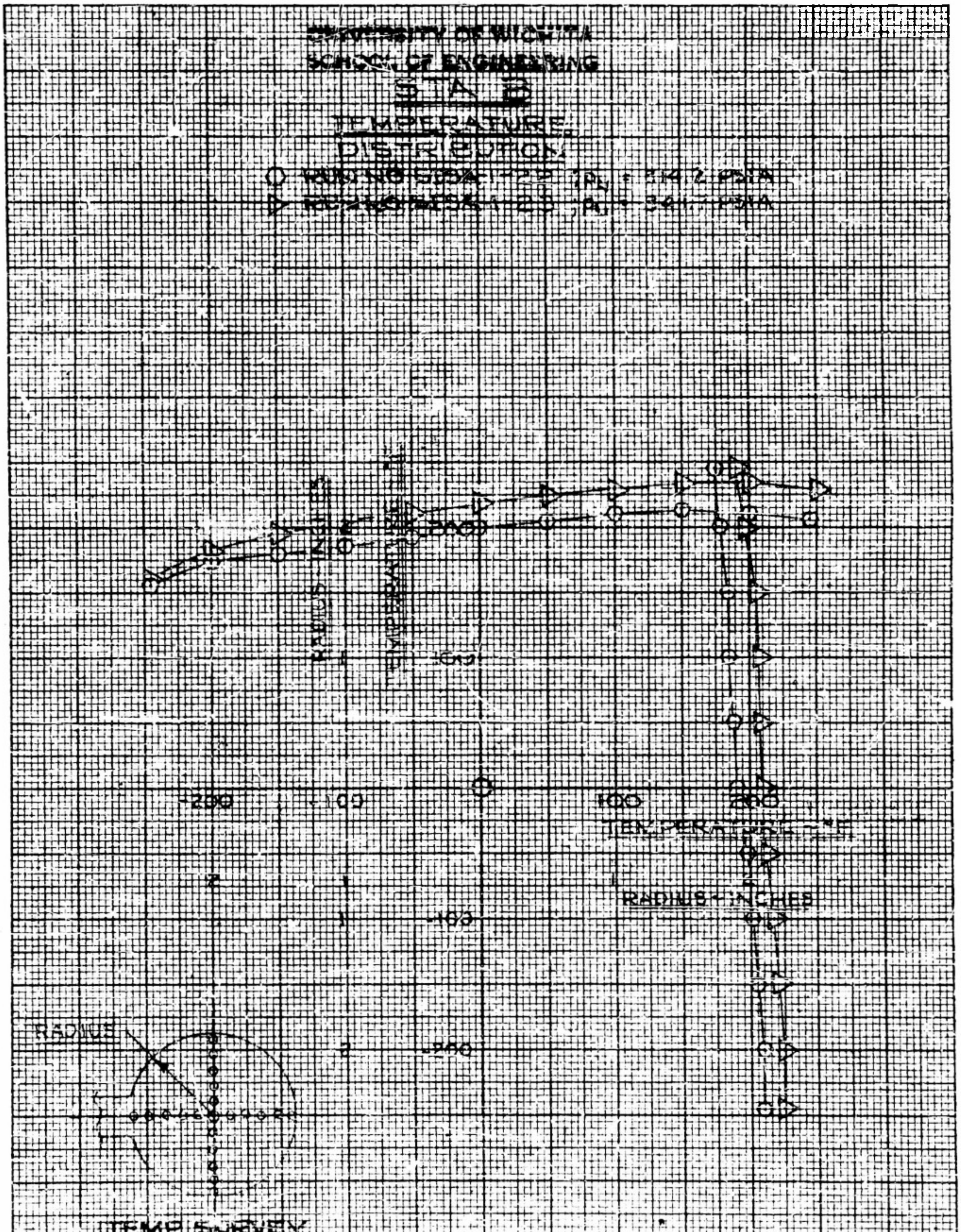

FIGURE 25 (CONT'D)

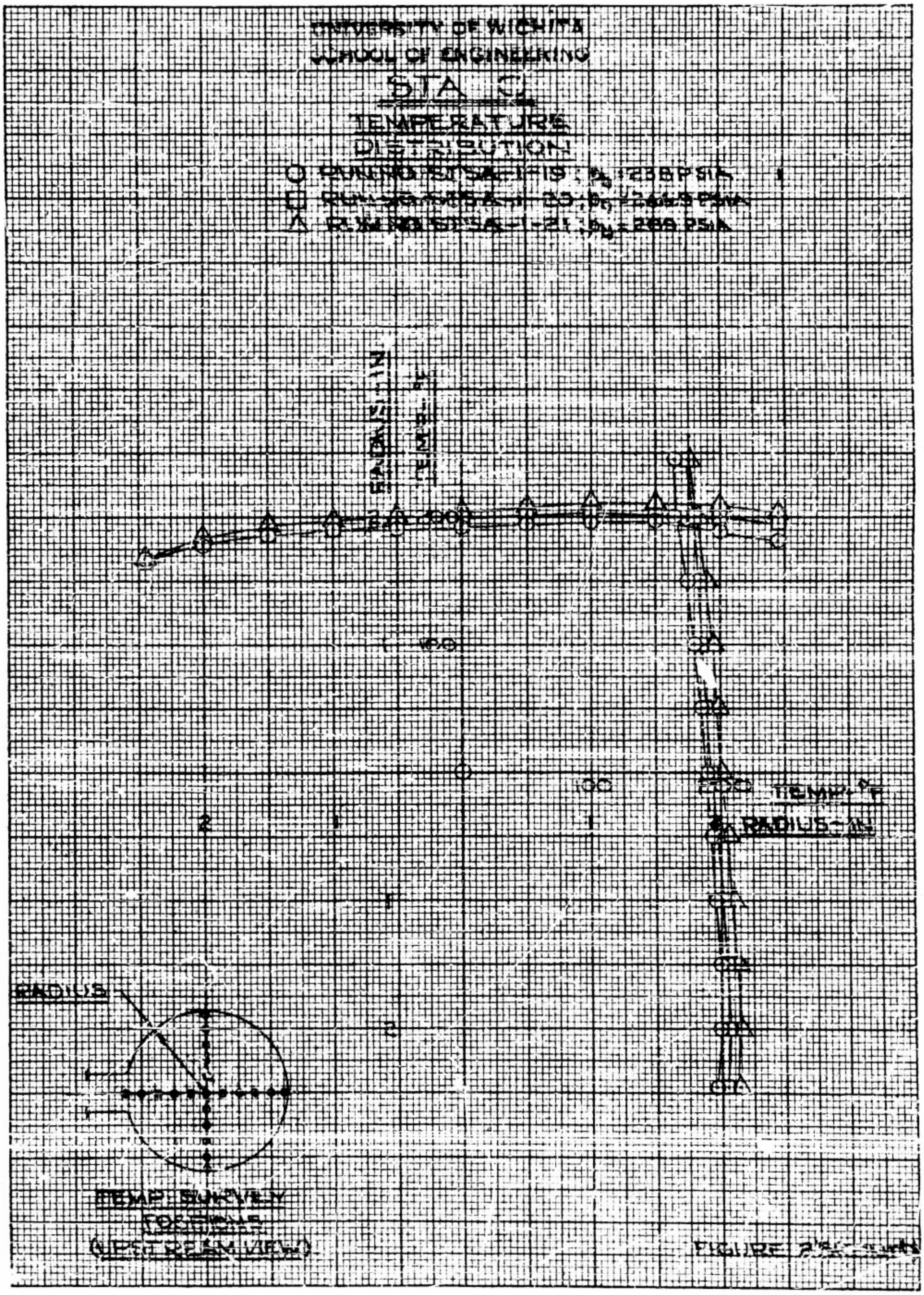
UNIVERSITY OF WICHITA
SCHOOL OF ENGINEERING
STA C
TEMPERATURE
DISTRIBUTION
TEMP. °F
RADIUS - IN
RADIUS
TEMP. SURVEY
(UPSTREAM VIEW)

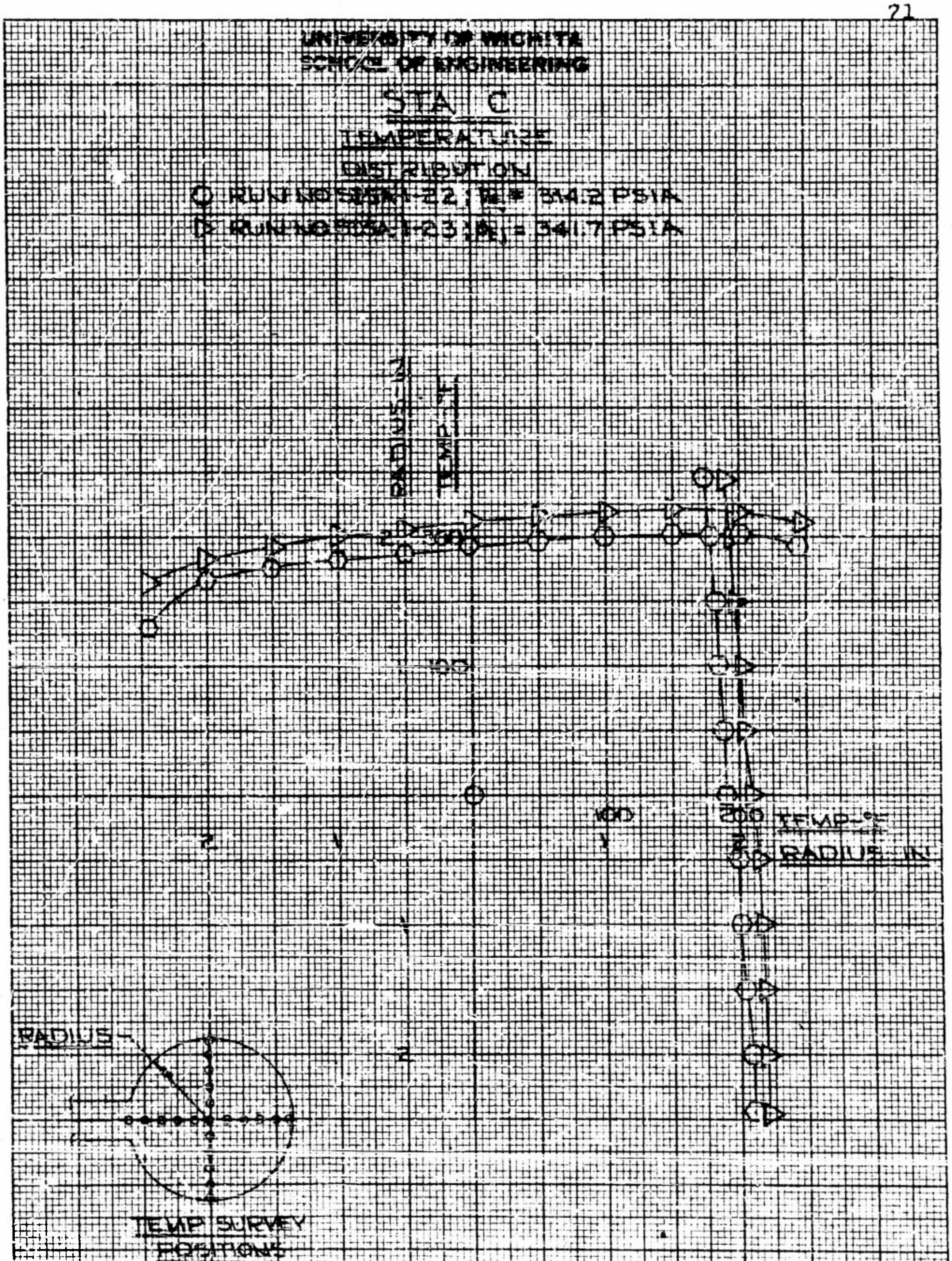

FIGURE 25(CONT'D)

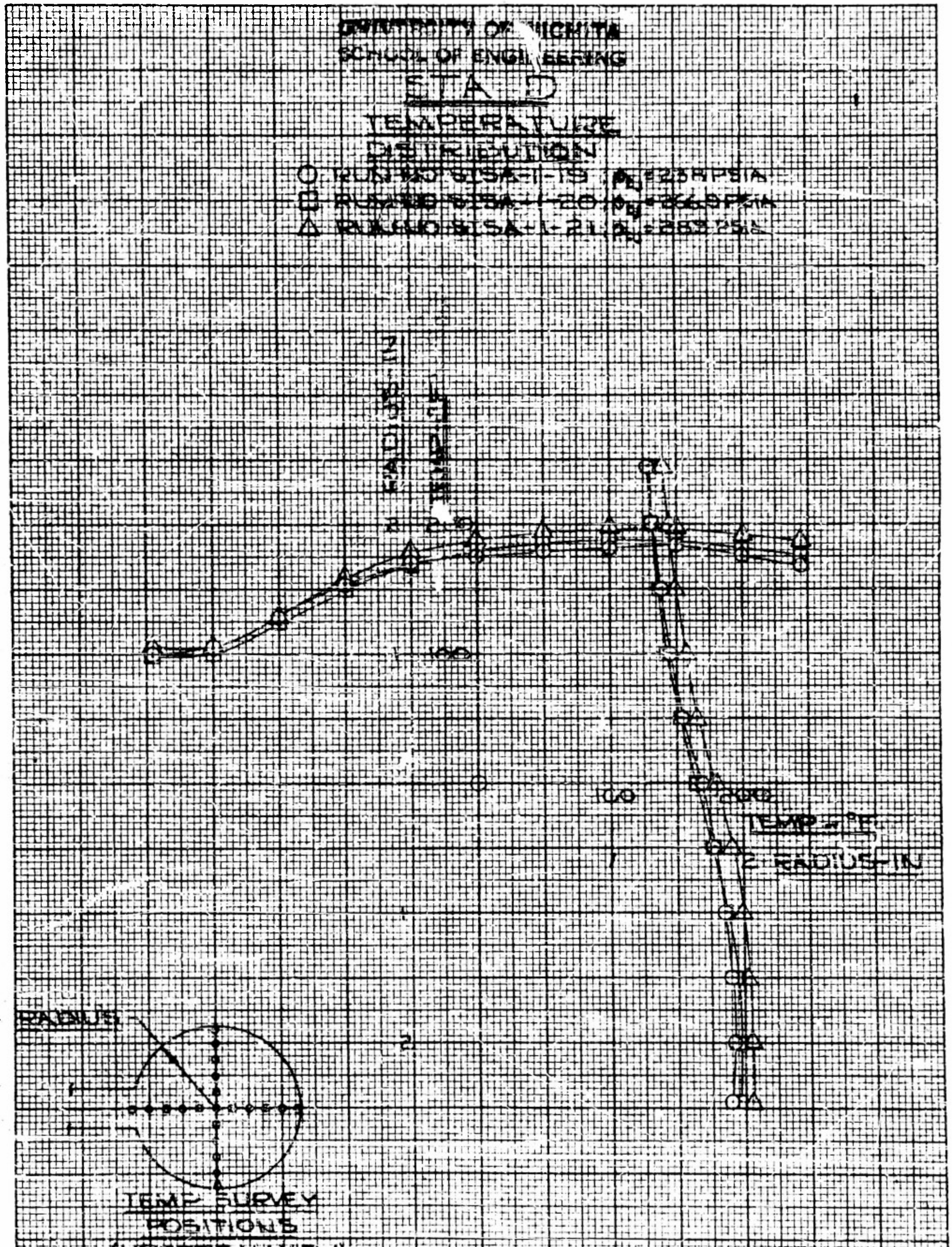

FIGURE 25 (CONT'D)

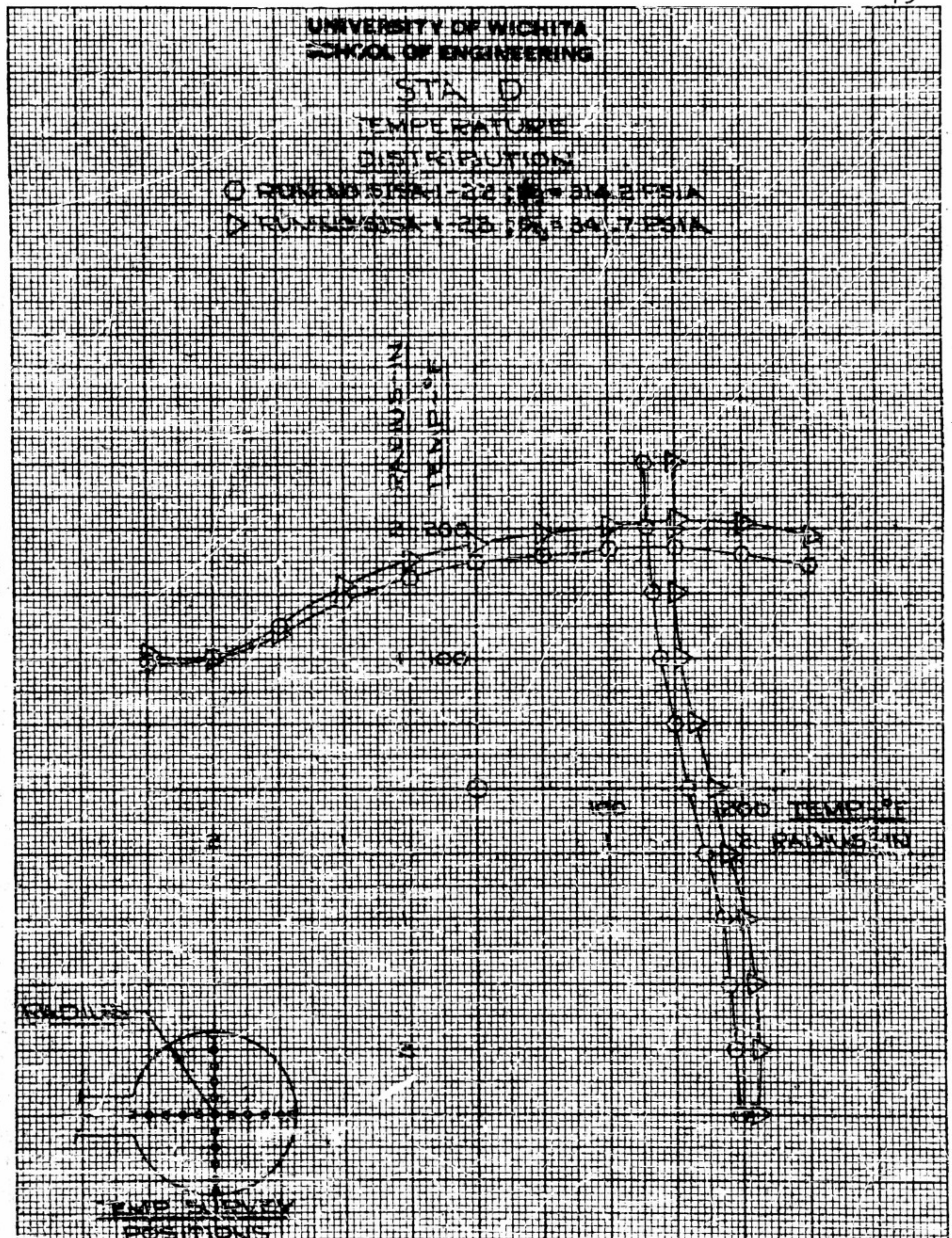
UNIVERSITY OF WICHITA
SCHOOL OF ENGINEERING
STA D
TEMPERATURE
DISTRIBUTION
RADIUS - IN
TEMP - °F
200
100
200 TEMP °F
RADIUS - IN
RADIUS
TEMP SURVEY
POSITIONS
(UPSTREAM VIEW)

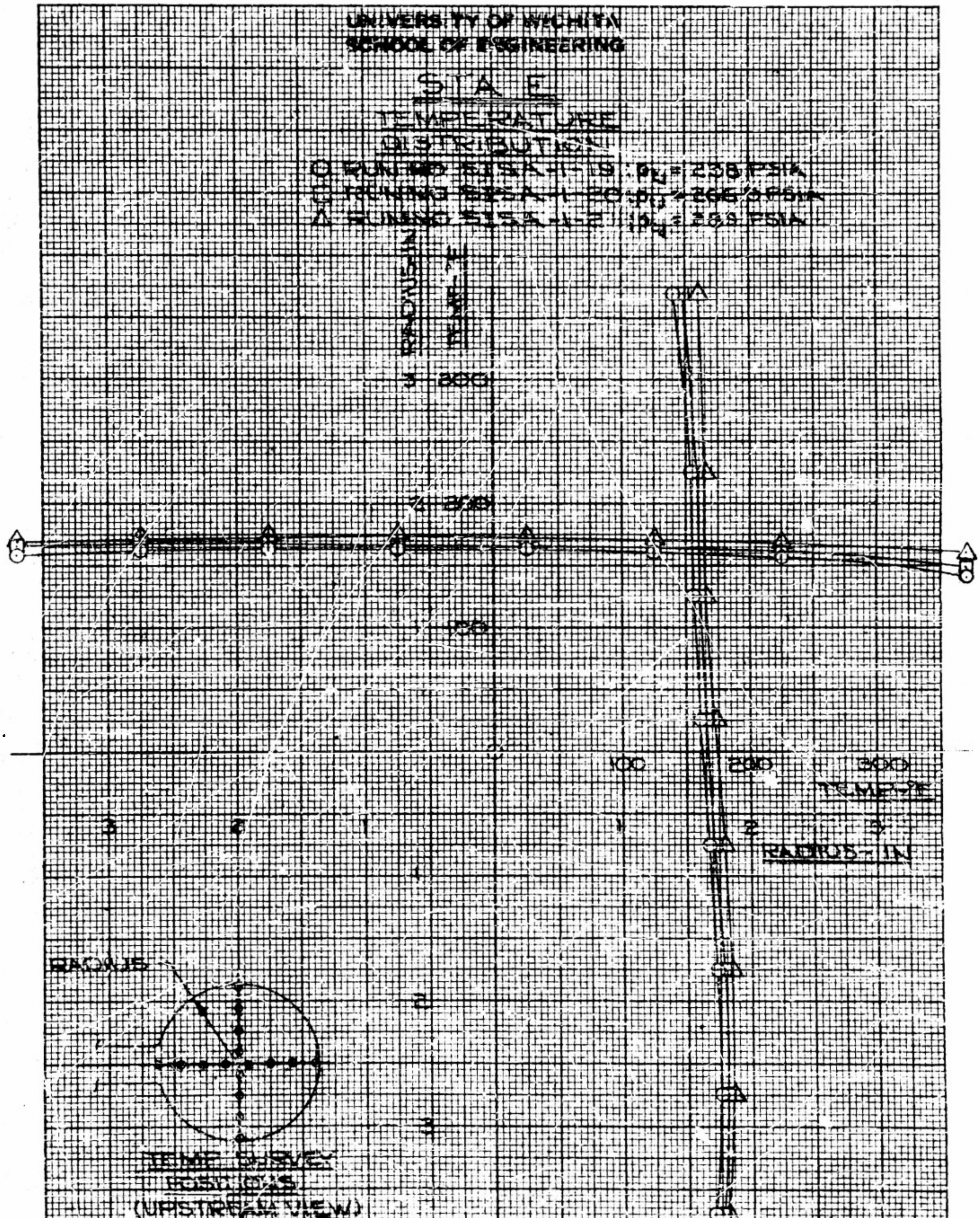

FIGURE 25 (CONT'D)

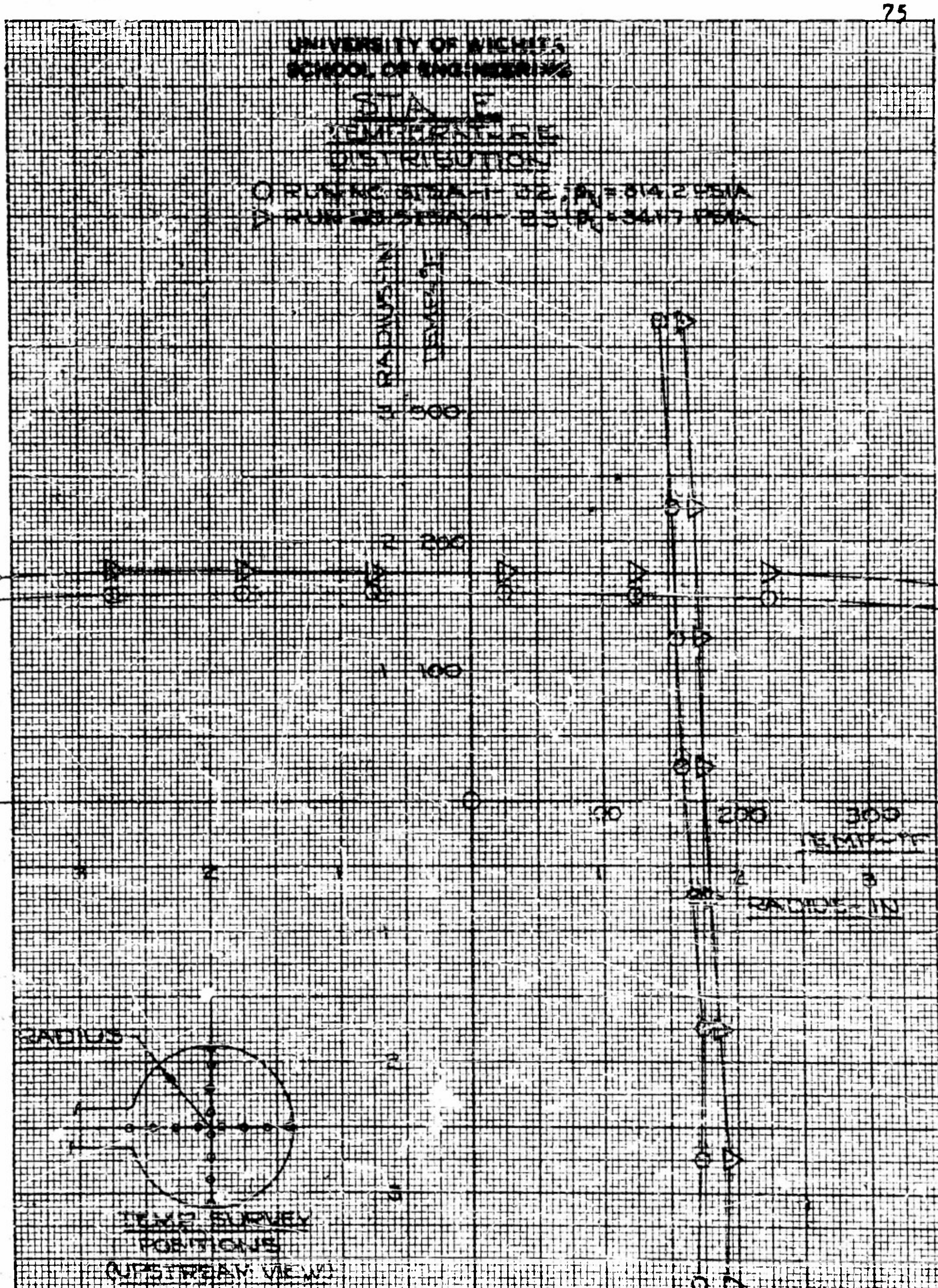

FIGURE 25(CONT'D)

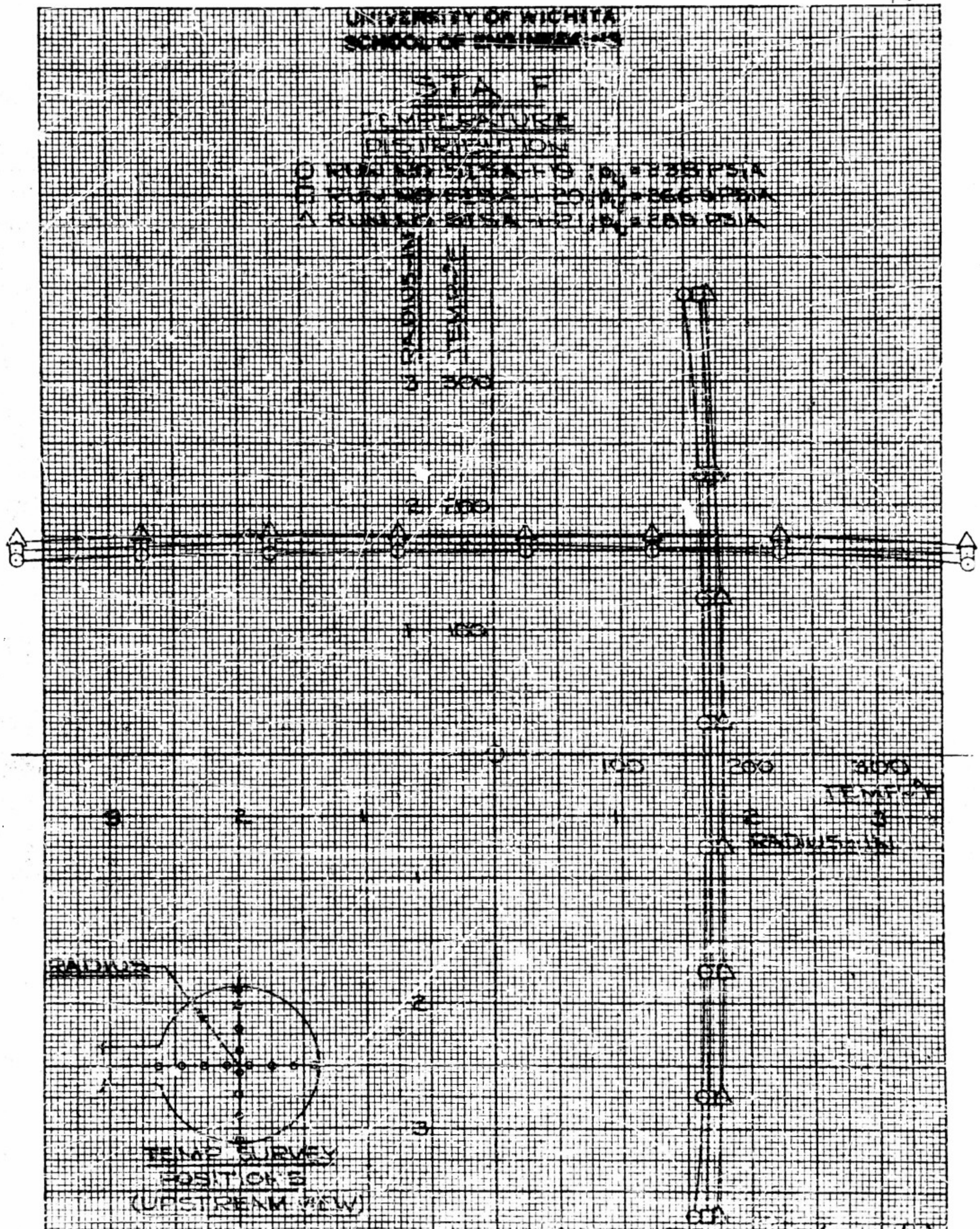

FIGURE 25 (CONT'D)

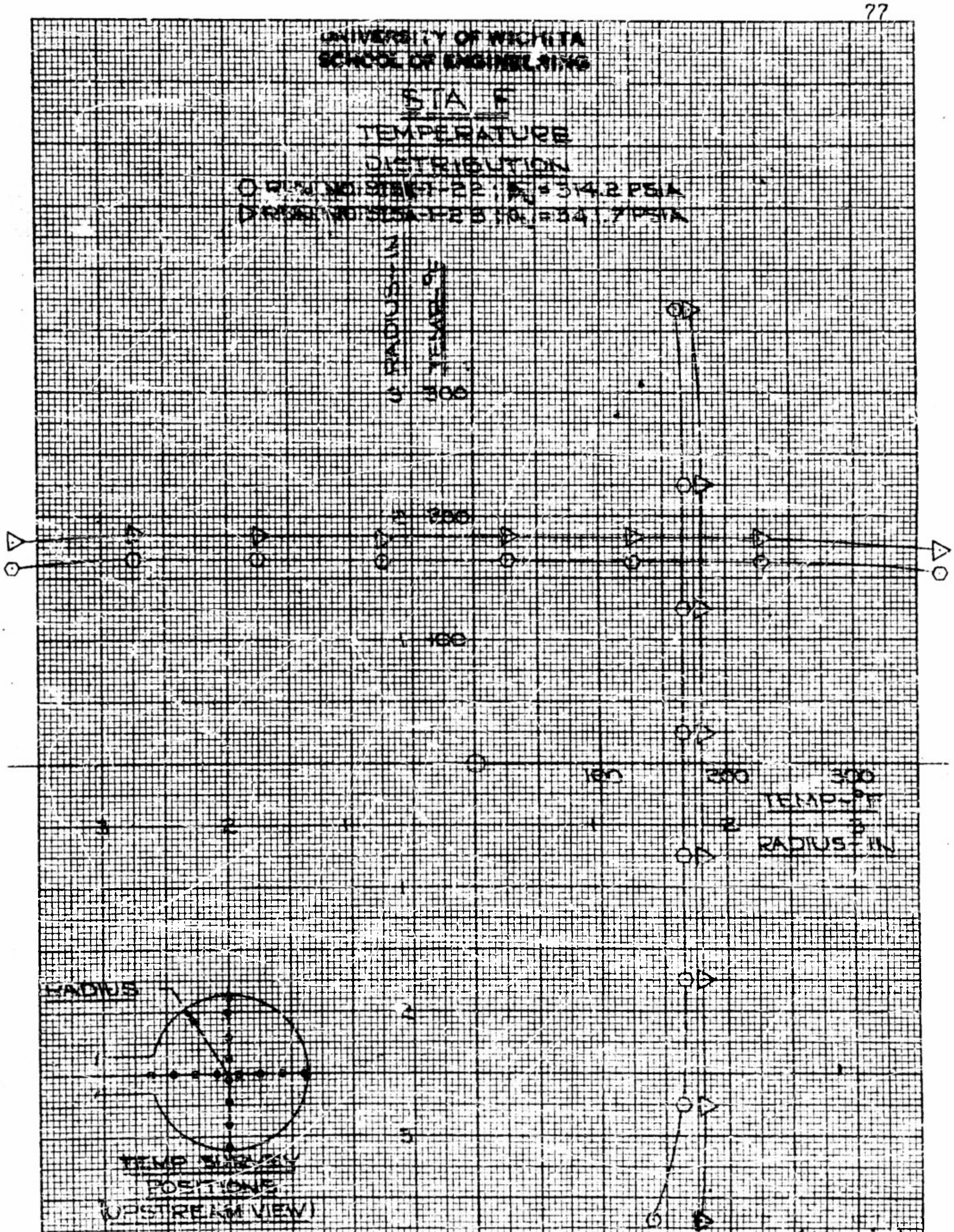

FIGURE 25 (CONT'D)

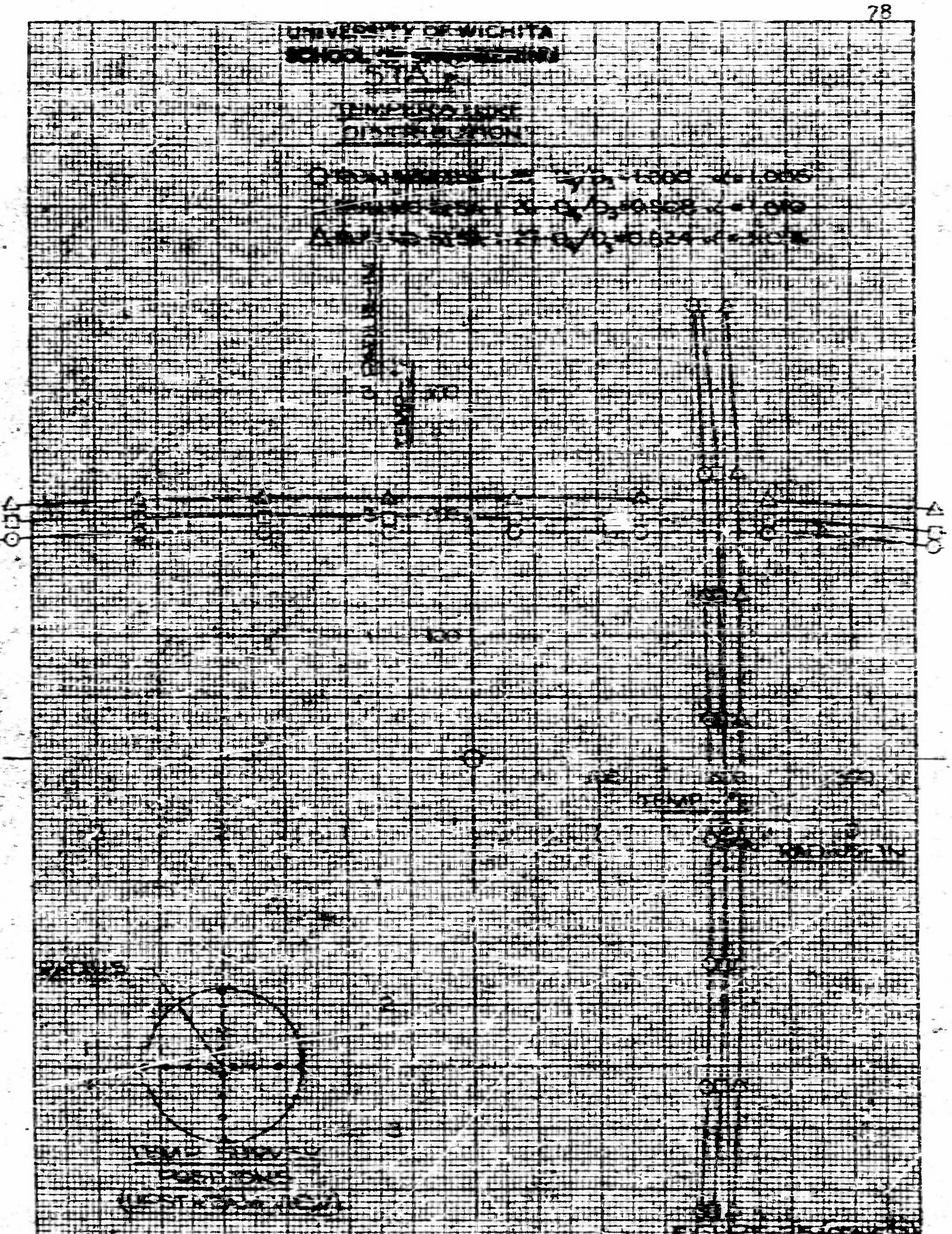
UNIVERSITY OF WICHITA
SCHOOL OF ENGINEERING
STA
TEMPERATURE
DISTRIBUTION
RADIUS-IN
TEMP
100
TEMP °F
RADIUS-IN
RADIUS
TEMP. SURVEY
POSITIONS
(LOOKING UPSTREAM)

FIGURE

UWER No. 131
University of Wichita, School of Engineering
PERFORMANCE TEST OF A SIDE-INLET, STEAM-TO-AIR JET PUMP WITH AN INBOARD NOZZLE: A.M. Heinrich.
February 1954. 78 pp., diagrs., photos., 5 refs.

An experimental investigation was conducted to determine the performance of a side-inlet, steam-to-air jet pump with an inboard nozzle. A jet pump with a cylindrical mixing tube was tested for mass ratio, pressure ratio, and efficiency. The transfer of the available energy in the primary flow to the secondary flow and the influence on performance of controlling the direction of secondary air flow into the mixing tube were also investigated.

Performance curves are presented together with curves showing mixing-tube, cross-sectional distributions of temperature and total pressure taken at several survey stations. This report is the first in a series on jet pumps with different taper ratio mixing tubes.

1.- Aerodynamics, Viscous Flow
2.- Jet Pumps
I.- Heinrich, A.M.
II.- UWER No. 131

UWER No. 131
University of Wichita, School of Engineering
PERFORMANCE TEST OF A SIDE-INLET, STEAM-TO-AIR JET PUMP WITH AN INBOARD NOZZLE: A.M. Heinrich.
February 1954. 78 pp., diagrs., photos., 5 refs.

An experimental investigation was conducted to determine the performance of a side-inlet, steam-to-air jet pump with an inboard nozzle. A jet pump with a cylindrical mixing tube was tested for mass ratio, pressure ratio, and efficiency. The transfer of the available energy in the primary flow to the secondary flow and the influence on performance of controlling the direction of secondary air flow into the mixing tube were also investigated.

Performance curves are presented together with curves showing mixing-tube, cross-sectional distributions of temperature and total pressure taken at several survey stations. This report is the first in a series on jet pumps with different taper ratio mixing tubes.

1.- Aerodynamics, Viscous Flow
2.- Jet Pumps
I.- Heinrich, A.M.
II.- UWER No. 131

UWER No. 131
University of Wichita, School of Engineering
PERFORMANCE TEST OF A SIDE-INLET, STEAM-TO-AIR JET PUMP WITH AN INBOARD NOZZLE: A.M. Heinrich.
February 1954. 78 pp., diagrs., photos., 5 refs.

An experimental investigation was conducted to determine the performance of a side-inlet, steam-to-air jet pump with an inboard nozzle. A jet pump with a cylindrical mixing tube was tested for mass ratio, pressure ratio, and efficiency. The transfer of the available energy in the primary flow to the secondary flow and the influence on performance of controlling the direction of secondary air flow into the mixing tube were also investigated.

Performance curves are presented together with curves showing mixing-tube, cross-sectional distributions of temperature and total pressure taken at several survey stations. This report is the first in a series on jet pumps with different taper ratio mixing tubes.

1.- Aerodynamics, Viscous Flow
2.- Jet Pumps
I.- Heinrich, A.M.
II.- UWER No. 131

UWER No. 131
University of Wichita, School of Engineering
PERFORMANCE TEST OF A SIDE-INLET, STEAM-TO-AIR JET PUMP WITH AN INBOARD NOZZLE: A.M. Heinrich.
February 1954. 78 pp., diagrs., photos., 5 refs.

An experimental investigation was conducted to determine the performance of a side-inlet, steam-to-air jet pump with an inboard nozzle. A jet pump with a cylindrical mixing tube was tested for mass ratio, pressure ratio, and efficiency. The transfer of the available energy in the primary flow to the secondary flow and the influence on performance of controlling the direction of secondary air flow into the mixing tube were also investigated.

Performance curves are presented together with curves showing mixing-tube, cross-sectional distributions of temperature and total pressure taken at several survey stations. This report is the first in a series on jet pumps with different taper ratio mixing tubes.

1.- Aerodynamics, Viscous Flow
2.- Jet Pumps
I.- Heinrich, A.M.
II.- UWER No. 131